

UNIVERSITY OF WARMIA AND MAZURY IN OLSZTYN

Technical Sciences

14(1)



PUBLISHER UWM

EDITORIAL BOARD

Stefan Cenkowski – University of Manitoba, Canada, Adam Chrzanowski – University of New Brunswick, Canada, Janusz Laskowski – University of Agriculture in Lublin, Lech Tadeusz Polkowski – University of Warmia and Mazury in Olsztyn, Vladimir Tilipalov – Kaliningrad State Technical University, Russia, Alojzy Wasilewski – University of Warmia and Mazury in Olsztyn

EDITORIAL COMMITTEE

Marek Markowski (Editor-in-Chief), Piotr Artiemjew, Ireneusz Białobrzewski, Tomasz Lipiński, Wojciech Sobieski

Executive Editor
Mariola Jezierska

The Technical Sciences is indexed and abstracted in BazTech (<http://baztech.icm.edu.pl>)

The Journal is also available (from volume 14) in electronic form on the web site <http://wydawnictwo.uwm.edu.pl> (subpage *Czytelnia*)

PL ISSN 1505-4675

© Copyright by Wydawnictwo UWM • Olsztyn 2011

Address
ul. Jana Heweliusza 14
10-718 Olsztyn-Kortowo, Poland
tel.: (48) (89) 523 36 61
fax: (48) (89) 523 34 38
e-mail: wydawca@uwm.edu.pl

Contents

Biosystems Engineering

| | |
|--|----|
| Z. Kaliniewicz – <i>The Effect of the Impurity Content of Buckwheat Nutlets on Product Purity after Cleaning in a Grader with Indented Pockets</i> | 5 |
| Z. Kaliniewicz, A. Grabowski, A. Liszewski, S. Fura – <i>Analysis of Correlations between Selected Physical Attributes of Scots Pine Seeds</i> | 13 |
| Z. Palkova, T. Rodny – <i>Analytical Model of the Optimal Capacity of an Irrigation System</i> | 23 |

Geodesy and Cartography

| | |
|--|----|
| A. Dumalski – <i>Evaluation of Possible Application of Terrestrial Laser Scanner – ScanStation in Vertical Displacement Measurements</i> | 33 |
| J. Rapiński, S. Cellmer – <i>Tests of Selected Automatic Positioning Systems in Post-Processing Mode</i> | 45 |

Information Technology

| | |
|---|----|
| P. Artiemjew – <i>Stability of Optimal Parameters for Classifier Based on Simple Granules of Knowledge</i> | 57 |
| M. Bednarczyk – <i>The Implementation of the Spatially Enabled Database with Open Source Software and Open Specifications Usage</i> | 71 |

Mechanical Engineering

| | |
|---|-----|
| A. Frączyk – <i>The Activation Energy of Primary Crystallization of $Fe_{95}Si_5$ Metallic Glass</i> | 93 |
| J. Napiórkowski, K. Kołakowski – <i>The Effect of the Surface Layer of a Plowshare Chisel on Plowshare Wear in Medium Loam</i> | 101 |
| P. Pasyniuk, W. Golimowski – <i>Work Indicators Test for Prototype John Deere 6830 Agricultural Tractor Fueled with Pure Vegetable Oil</i> | 109 |
| A. Rychlik, J. Napiórkowski – <i>The Use of Friction Parameters in Evaluating the Technical Condition of Rolling Bearings by the Quasi-Dynamic Method</i> | 119 |

Spis treści

Inżynieria rolnicza

| | |
|---|----|
| Z. Kaliniewicz – <i>Wpływ stopnia zanieczyszczenia surowca ziaren gryki na czystość produktu po czyszczeniu w tryjerze z wgłębieniami kieszonkowymi</i> | 5 |
| Z. Kaliniewicz, A. Grabowski, A. Liszewski, S. Fura – <i>Analiza współzależności wybranych cech fizycznych nasion sosny zwyczajnej</i> | 13 |
| Z. Palkova, T. Rodny – <i>Analityczny model optymalnej wydajności systemu nawadniania</i> | 23 |

Geodezja i kartografia

| | |
|---|----|
| A. Dumalski – <i>Ocena możliwości zastosowania skanera laserowego ScanStation do pomiaru przemieszczeń pionowych</i> | 33 |
| J. Rapiński, S. Cellmer – <i>Testowanie wybranych serwisów automatycznego pozycjonowania w trybie postprocessingu</i> | 45 |

Technologie informacyjne

| | |
|---|----|
| P. Artiemjew – <i>Badanie stabilności optymalnych parametrów klasyfikatora bazującego na prostych granulach wiedzy</i> | 57 |
| M. Bednarczyk – <i>Implementacja przestrzennie zorientowanej bazy danych z wykorzystaniem wybranego oprogramowania open source i otwartych specyfikacji</i> | 71 |

Inżynieria mechaniczna

| | |
|--|-----|
| A. Frączyk – <i>Energia aktywacji krystalizacji pierwotnej szkła metalicznego $Fe_{95}Si_5$</i> | 93 |
| J. Napiórkowski, K. Kołakowski – <i>Wpływ rodzaju warstwy wierzchniej dłuta lemieszka płuznego na zużycie w glinie średniej</i> | 101 |
| P. Pasyniuk, W. Golimowski — <i>Badania wskaźników pracy prototypowego silnika ciągnika rolniczego John Deer 6830 zasilanego nieprzetworzonym olejem roślinnym</i> | 109 |
| A. Rychlik, J. Napiórkowski – <i>Analiza wykorzystania parametrów tarcia w ocenie stanu technicznego łożysk tocznych metodą quasi-dynamiczną</i> | 119 |

**THE EFFECT OF THE IMPURITY CONTENT
OF BUCKWHEAT NUTLETS ON PRODUCT PURITY
AFTER CLEANING IN A GRADER WITH INDENTED
POCKETS**

Zdzisław Kaliniewicz

Department of Heavy Duty Machines and Separation Processes
University of Warmia and Mazury in Olsztyn

Key words: buckwheat, wild radish, impurity content, grader.

A b s t r a c t

This study analyzed four mixtures of buckwheat nutlets and wild radish siliques with impurity content (wild radish siliques) of 2.5, 5.0, 7.5 and 10.0%. Buckwheat nutlet yield, the efficiency of wild radish silique removal, the efficiency of mixture separation and product purity were determined at two depth settings of indented pockets (2.4 and 2.8 mm), three factors of static load of the cylinder with the mixture (0.1, 0.2 and 0.3 of full load) and five angles of the working edge of the trough (10, 20, 30, 40 and 50°). The obtained results indicate that the impurity content of raw material significantly affects the purity of the separated product.

**W PŁY W STOPNIA ZANIECZYSZCZENIA SUROWCA ZIAREN GRYKI NA CZYSTOŚĆ
PRODUKTU PO CZYSZCZENIU W TRYJERZE Z WGLĘBIENIAMI KIESZONKOWYMI**

Zdzisław Kaliniewicz

Katedra Maszyn Roboczych i Procesów Separacji
Uniwersytet Warmińsko-Mazurski w Olsztynie

Słowa kluczowe: gryka, rzodkiew świrzepa, stopień zanieczyszczenia, tryjer.

A b s t r a k t

Do badań wykorzystano cztery mieszaniny ziaren gryki i łuszczyn rzodkwi świrzepy o udziale: 2,5, 5,0, 7,5 i 10,0% składnika zanieczyszczającego – łuszczyn rzodkwi świrzepy. Wyznaczano uzysk ziarna gryki, skuteczność wydzielania łuszczyn rzodkwi świrzepy, skuteczność rozdzielania mieszaniny i czystość produktu na dwóch głębokościach wgłębień kieszonek (2,4 i 2,8 mm), przy trzech wskaźnikach statycznego obciążenia cylindra mieszaniną (0,1, 0,2 i 0,3 pełnego obciążenia) oraz pięciu kątach ustawienia roboczej krawędzi rynienki (10, 20, 30, 40 i 50°). Stwierdzono, że stopień zanieczyszczenia surowca wpływa istotnie na czystość produktu czyszczenia.

Symbols:

- c – purity of separated product,
- s – depth of indented pockets, mm,
- q_s – factor of static load of the cylinder with mixture,
- z – impurity content of raw material, %,
- α – setting angle of the working edge of the trough, °,
- ε – efficiency of mixture separation,
- ε_1 – buckwheat nutlet yield,
- ε_2 – efficiency of wild radish silique removal.

Introduction

Wild radish siliques constitute a group of impurities that are difficult to remove from buckwheat nutlet mixtures. The silique content of threshed buckwheat nutlets may be as high as 6% (SEM CZYSZYN, FORMAL 1990), accounting for 40% to 70% of total useless impurities. Under the repealed Polish Standard PN-R-65023:1999, which is yet to be replaced with an updated version, seed material was grouped into three quality classes (I – 98%, II – 98% and III – 96%). The admissible quantity of other plant seeds in the raw material was determined by the purity class. The number of other plant seeds in 1 kg of seed material was set at up to 50 seeds in super elite (SE) and elite (E) seed, up to 100 seeds in original (O) seed, up to 200 seeds in primary reproduction seed (I ods.) and certified seed (Okw), and up to 340 seeds in uncertified single-variety seed (No) and uncertified seed of unknown variety (N).

Wild radish siliques can be effectively removed from seed material in a grader with indented pockets (KALINIEWICZ 2000). To date, the grader's separation efficiency was analyzed at a constant impurity content of the purified material. The effect of impurity content on the purity of the separated mixture of buckwheat nutlets and wild radish siliques has not been investigated. According to the proposed hypothesis, the impurity content of buckwheat nutlets cleaned in a grader with indented pockets determines the purity of the resulting product.

The objective of this study was to determine the boundary content of impurities – wild radish siliques – in seed material purified in a grader with indented pockets which guarantees 95% buckwheat nutlet yield for a given product quality class.

Materials and Methods

The experimental material comprised nutlets of buckwheat cv. Luba and wild radish silique segments harvested in a farm estate near Olsztyn. The relative moisture content of the investigated mixture components was 12.3%

and 11.9%, respectively, with a corresponding thousand seed weight and thousand silique weight of 25.38 g and 21.43 g, respectively. The resulting mixture comprised buckwheat nutlets as the main component and wild radish siliques as the impurity. The percentage quantitative content of impurities in the mixture was 2.5%, 5.0%, 7.5% and 10.0% (percentage content by weight – 1.9%, 4.2%, 6.4% and 8.6%).

The study was conducted on a test stand presented in the work of KALINIEWICZ and RAWA (2004). It comprised a K-292 laboratory grader (Petkus), equipped with two cylinders with a length of 480 mm and an internal diameter of 240 mm, each with indented pockets of with different indentation depth. The experiment was conducted in three replications with the following parameters:

1) constants:

- horizontal inclination angle of cylinder axis – 2° ,
- distance from the working edge of the trough to cylinder surface – 6 mm,
- cylinder's kinematic indicator – 0.25,

2) variables:

- working depth of indented pockets $s = 2.4$ mm and 2.8 mm,
- factor of static load of the cylinder with mixture $q_s = 0.1, 0.2$ and 0.3,
- setting angle of the working edge of the trough $\alpha = 10^\circ, 20^\circ, 30^\circ, 40^\circ$ and 50° ,
- content of wild radish silique segments $z = 2.5\%, 5.0\%, 7.5\%$ and 10.0%,

3) results:

- buckwheat grain yield ε_1 ,
- efficiency ε_2 of wild radish silique removal,
- efficiency ε of mixture separation,
- purity c of the cleaned product.

Only two cylinders with a different depth of indented pockets recommended for buckwheat cleaning were used in the experiment (KALINIEWICZ 2000). The full load exerted by the mixture on the cylinder was determined on the assumption that all indented pockets can be filled with both buckwheat nutlets and wild radish siliques. Subject to the impurity content of the mixture, cylinder load varied from 175.4 to 177.7 kg h⁻¹ for indented pocket depth $s = 2.4$ mm and 156.1 to 158.1 kg h⁻¹ for indented pocket depth $s = 2.8$ mm.

The cylinder was filled with the mixture for around 60 s before every experiment. After the feeder and the grader were stopped, the trough and the waste container were removed and emptied. As the trough and the waste container were fitted back in place, the feeder and the grader were activated for 1 minute and the proper measurement was conducted. The waste which accumulated in the trough and in the waste container was separated into two fractions, buckwheat nutlets and wild radish siliques. Every fraction was weighed on AM 500 laboratory scales with a measuring precision of 0.01 g.

Buckwheat grain yield ε_1 was determined based on the ratio of the weight of nutlets removed to the trough and the total weight of nutlets in the trough and in the waste container. The efficiency ε_2 of wild radish silique removal was estimated based on the ratio of the weight of wild radish siliques removed to the waste container and the total weight of wild radish siliques in the trough and in the waste container. The efficiency ε of mixture separation was determined from the formula (GROCHOWICZ 1994):

$$\varepsilon = \varepsilon_1 - (1 - \varepsilon_2) \quad (1)$$

The purity c of the cleaned product was determined as the ratio of the weight of buckwheat nutlets removed to the trough and the total weight of buckwheat nutlets and wild radish siliques in the trough.

Experimental results were processed with the use of Winstat and Statistica software.

Results and Discussion

Linear correlation coefficients between variables are presented in Table 1, indicating that all independent variables are not correlated. The investigated qualitative indicators of the separation process (dependent variables) were significantly correlated with the setting angle of the grader trough. The efficiency of wild radish silique removal was highly correlated with the depth of indented pockets. The factor of static load of the cylinder with mixture was also significantly correlated with the efficiency of wild radish silique removal. It should be noted that the impurity content was significantly correlated only with the purity of the cleaned product.

Table 1

Coefficients of linear correlations between variables

| Variable (factor) | s | q_s | α | z |
|-------------------|---------------|--------------|---------------|---------------|
| s | 1.000 | 0.000 | 0.000 | 0.000 |
| q_s | 0.000 | 1.000 | -0.000 | -0.000 |
| α | 0.000 | -0.000 | 1.000 | 0.000 |
| z | 0.000 | -0.000 | 0.000 | 1.000 |
| ε_1 | 0.101 | -0.064 | -0.833 | 0.040 |
| ε_2 | -0.496 | 0.162 | 0.732 | -0.071 |
| ε | -0.108 | -0.002 | -0.675 | 0.016 |
| c | -0.411 | 0.079 | 0.200 | -0.552 |

Critical value of correlation coefficient – 0.103

Adopted level of significance – 0.05

Source: author's calculations

Table 2 presents the statistical parameters of the adopted indicators and the results of one-way analysis of variance verifying the statistical hypothesis that the mean values obtained in each treatment are equal. The presented data also suggest a drop in product purity with an increase in the impurity content of the separated material. The above seems to be a logical consequence of the observation that the impurity content of the raw material has no significant effect on buckwheat nutlet yield and the efficiency of wild radish silique removal.

Table 2
Statistical parameters of dependent variables grouped according to the impurity content of the mixture

| Variable | Impurity content | Mean | SD | Coefficient of variation | Test results |
|-----------------|------------------|-------|-------|--------------------------|---|
| ε_1 | $z_{2.5}$ | 0.734 | 0.343 | 46.67 | $F = 0.205$ $p(F) = 0.893$ no significant differences |
| | $z_{5.0}$ | 0.737 | 0.345 | 46.83 | |
| | $z_{7.5}$ | 0.755 | 0.340 | 45.03 | |
| | $z_{10.0}$ | 0.769 | 0.343 | 44.62 | |
| ε_2 | $z_{2.5}$ | 0.849 | 0.117 | 13.75 | $F = 1.280$ $p(F) = 0.28$ no significant differences |
| | $z_{5.0}$ | 0.865 | 0.121 | 13.96 | |
| | $z_{7.5}$ | 0.847 | 0.131 | 15.51 | |
| | $z_{10.0}$ | 0.827 | 0.148 | 17.96 | |
| ε | $z_{2.5}$ | 0.583 | 0.281 | 48.18 | $F = 0.092$ $p(F) = 0.965$ no significant differences |
| | $z_{5.0}$ | 0.601 | 0.288 | 47.90 | |
| | $z_{7.5}$ | 0.603 | 0.281 | 46.71 | |
| | $z_{10.0}$ | 0.596 | 0.276 | 46.36 | |
| c | $z_{2.5}$ | 0.995 | 0.003 | 0.33 | $F = 53.541$ $p(F) = 0.000$ $z_{2.5}, z_{5.0} > z_{7.5}, z_{10.0}^{**}$ $z_{2.5} > z_{5.0}^*$ $z_{7.5} > z_{10.0}^{**}$ |
| | $z_{5.0}$ | 0.992 | 0.005 | 0.49 | |
| | $z_{7.5}$ | 0.987 | 0.011 | 1.14 | |
| | $z_{10.0}$ | 0.980 | 0.012 | 1.22 | |

F – calculated value of the test statistic

$p(F)$ – probability that the calculated value of test statistic F is exceeded

* – statistically significant differences at $\alpha = 0.05$

** – statistically significant differences at $\alpha = 0.01$

Source: author's calculations

The next stage of the experiment involved a multivariate regression analysis using a second-order polynomial model with stepwise elimination of non-significant variables and polynomial degree for buckwheat nutlet yield and the purity of the cleaned product. The following functions were determined with the percentage of explained variability of 95.62 and 68.72, and the standard deviation of residuals of 0.072 and 0.006, respectively:

$$\varepsilon_1 = (24.993 \cdot \alpha - 1.016 \cdot \alpha^2 + 6.114 \cdot s \cdot \alpha + 693.800) \cdot 10^{-3} \quad (2)$$

$$c = (7.751 \cdot z - 2.127 \cdot s^2 - 0.137 \cdot z^2 - 0.019 \cdot \alpha^2 - 4.909 \cdot s \cdot z + 3.591 \cdot s \cdot z + 0.400 \cdot s \cdot \alpha + 0.041 \cdot z \cdot \alpha + 1001.339) \cdot 10^{-3} \quad (3)$$

It has been assumed that buckwheat nutlet loss cannot exceed 5%. In view of the above, equation (2) was used to determine the allowable range of trough setting angles for every indentation depth which was below 28° for $s = 2.4$ mm and below 32° for $s = 2.8$ mm.

Assuming that wild radish siliques are the only impurity in the mixture and that siliques, whose thousand segment weight is identical to that determined in raw material, have not been completely removed, product purity may reach the following boundary values for buckwheat nutlets of the following quality class:

- super elite (SE) and elite (E) seed – $c = 0.9989$,
- original (O) seed – $c = 0.9978$,
- primary reproduction (I ods.) seed and certified seed (Okw.) – $c = 0.9957$,
- uncertified single-variety seed (No) and uncertified seed of unknown variety (N) – $c = 0.9927$.

The above values and the determined setting angles of the working edge of the trough were input in equation (3) to calculate the admissible (boundary) impurity content of raw material which guarantees seed yield of a given quality class (disregarding the material's sowing value). The resulting data, shown in Figure 1, indicate that super elite and elite seed may be obtained when the angle of the working edge of the trough is higher than 14° for pocket depth $s = 2.4$ mm and higher than 19° for pocket depth $s = 2.8$ mm. The above parameters guarantee the lowest buckwheat nutlet loss during separation. At 5% buckwheat nutlet loss, the boundary content of wild radish siliques in the material is 5.1% and 1.8% for the above pocket depths, respectively. In seed material of the lowest quality class, the boundary impurity content of the mixture separated in a grader with indented pockets may be as high as 8.9% for pocket depth $s = 2.4$ mm and 5.0% for pocket depth $s = 2.8$ mm.

Conclusions

1. The results of a correlation analysis indicate that the content of wild radish silique impurities in buckwheat nutlets significantly affects the purity of seed material cleaned in a grader with indented pockets. The impurity content of seed material has no significant effect on buckwheat nutlet yield, the efficiency of wild radish silique removal and the efficiency of mixture separation.

2. Wild radish siliques are most effectively separated from buckwheat nutlets in a grader with indented pockets with a depth of 2.4 mm when the

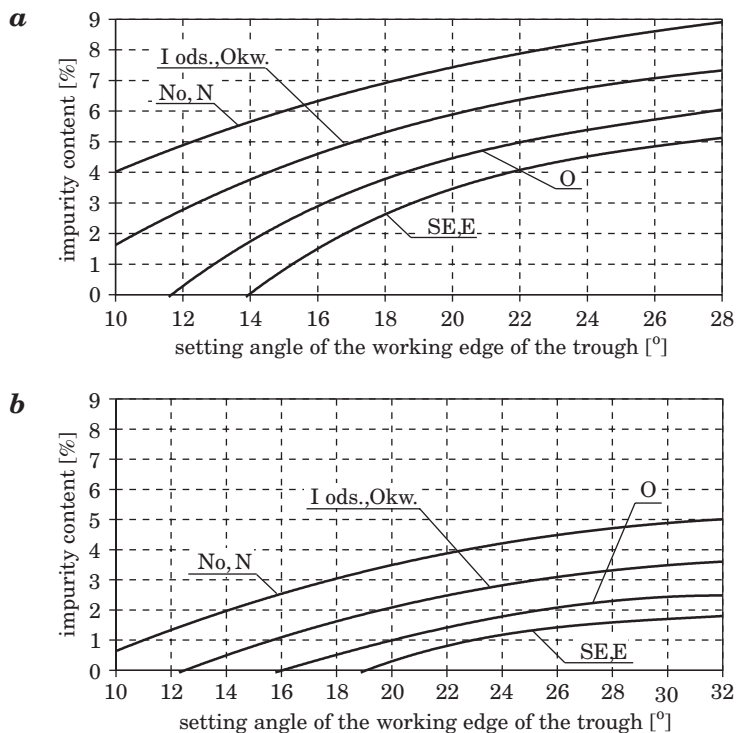


Fig. 1. Boundary content of wild radish silique impurities in buckwheat nutlets before cleaning in a grader with indented pockets that guarantees the production of seed material in the following quality classes: a – $s = 2.4$ mm, b – $s = 2.8$ mm; SE – super elite seed, E – elite seed, O – original seed, I ods. – primary reproduction seed, Okw. – certified seed, No – uncertified single-variety seed, N – uncertified seed of unknown variety

Source: developed by the author.

working edge of the trough is set at a maximum angle of 28° . The above parameters guarantee minimal buckwheat nutlet yield of 0.95 (buckwheat nutlet loss does not exceed 5%). The investigated grader may be applied to produce super elite seed provided that the impurity content of the material does not exceed 5.1% at the highest setting of the working edge of the trough.

References

- GROCHOWICZ J. 1994. *Maszyny do czyszczenia i sortowania nasion*. Wyd. Akademii Rolniczej. Lublin. ISBN 83-901612-9-X.
- KALINIEWICZ Z. 2000. *Modelowanie tryjerów z wgłębieniami kieszonkowymi w aspekcie poprawy skuteczności czyszczenia nasion gryki*. Rozprawa doktorska. Wydział Budownictwa, Mechaniki i Petrochemii Politechniki Warszawskiej w Płocku. Maszynopis.
- KALINIEWICZ Z., RAWA T. 2004. *Wyniki eksperymentalnej weryfikacji apriorycznego modelu matematycznego rozdzielczości tryjera do gryki*. Inżynieria Rolnicza, 3(58): 211–218.
- Materiał siewny, nasiona roślin rolniczych*. PN-R-65023:1999. Wydawnictwo Normalizacyjne, Warszawa.
- SEMCZYSZYN M., FORMAL Ł. 1990. *Analiza skuteczności pracy urządzeń czyszczących stosowanych w liniach technologicznych czyszczenia ziarna gryki. II. Wyniki badań jakości pracy urządzeń czyszczących*. Acta Acad. Agricult. Techn. Olst., Aedif. Mech., 21: 111–121.

ANALYSIS OF CORRELATIONS BETWEEN SELECTED PHYSICAL ATTRIBUTES OF SCOTS PINE SEEDS

***Zdzisław Kaliniewicz¹, Artur Grabowski¹,
Arkadiusz Liszewski¹, Sławomir Fura²***

¹ Faculty of Technical Sciences

University of Warmia and Mazury in Olsztyn

² Seed husking plant in Ruciane Nida, Maskulińskie Forest Inspectorate

Key words: Scots pine, seeds, separation properties, cleaning, sorting.

A b s t r a c t

Critical transport velocity, the thickness, width, length and the angle of sliding friction of Scots pine seeds harvested from three seed banks (conservation seed stand, commercial seed stand and seed plantation) were determined. The investigated attributes were compared by single classification analysis of variance, correlation, single-variable and multivariate regression analysis. The analyzed seed traits differed significantly between the specimens from the examined seed banks. The equations describing the correlations between the studied attributes were characterized by relatively low percentages of explained variation, which renders them unfit for designing seed and separation models.

ANALIZA WSPÓLZALEŻNOŚCI WYBRANYCH CECH FIZYCZNYCH NASION SOSNY ZWYCZAJNEJ

Zdzisław Kaliniewicz¹, Artur Grabowski¹, Arkadiusz Liszewski¹, Sławomir Fura²

¹ Wydział Nauk Technicznych

Uniwersytet Warmińsko-Mazurski w Olsztynie

² Wyłuszcarnia nasion w Rucianem Nidzie, Nadleśnictwo Maskulińskie

Słowa kluczowe: sosna zwyczajna, nasiona, cechy rozdzielcze, czyszczenie, sortowanie.

A b s t r a k t

Wyznaczono prędkość krytyczną unoszenia, grubość, szerokość, długość i kąt tarcia ślizgowego nasion sosny zwyczajnej, zebranych z trzech odmiennych baz nasiennych (wyłączony drzewostan

nasienny, gospodarczy drzewostan nasienny i plantacja nasienna). Porównywano te cechy, wykorzystując analizę wariancji z klasyfikacją pojedynczą, korelację oraz regresję jednej zmiennej i wielu zmiennych. Stwierdzono, że w większości przypadków analizowane cechy nasion z odmiennych baz nasiennych różnią się statystycznie. Równania współzależności między określonymi cechami charakteryzują się stosunkowo niskim procentem wyjaśnionej zmienności, co właściwie wyklucza ich zastosowanie do budowania modeli nasion i procesów rozdzielnicy.

Symbols:

F – seed cross-sectional area, mm²,

L – seed length, mm,

S – standard deviation of trait,

T – seed thickness, mm,

v – critical transport velocity of seeds, m s⁻¹,

V – seed volume, mm³,

W – seed width, mm,

x – average value of trait,

x_{\max} – maximum value of trait,

x_{\min} – minimal value of trait,

α, β – Donev's shape factors,

γ – angle of sliding friction, °,

χ^2_{cal} – calculated value of statistical parameter,

χ^2_{α} – value from statistical table at significance level $\alpha = 0.05$.

Introduction

The pine is a monoecious tree that begins to produce seeds at the estimated age of 15 years (isolated trees), generally around the age of 35 years. Large quantities of pine cones are produced every 3–4 years (MURAT 2002, *Nasiennictwo leśnych drzew...* 1995). Pine seeds are obtained from selected trees, conservation seed stands, commercial seed stands, seed plantations and farms. The largest quantity of seeds is harvested from commercial stands (around 72%) and conservation stands (around 14%) (MURAT 2002).

In principle, forest reproductive material is never mixed, and it is generally used only in the region of origin (MURAT 2005). Scots pine seeds are usually contaminated with organic pollutants only. Such impurities are produced in the process of husking and dewinging, and they are easily removed. Pollutants are separated into fractions using a mesh sieve, and they are cleaned in a pneumatic separator to remove empty and undeveloped seeds (SARNOWSKA, WIĘSIK 1998, *Nasiennictwo leśnych drzew...* 1995). Seed producers are often faced with a dilemma as to whether seeds of the same species harvested from different seed banks should be purified and sorted with the application of the same equipment settings or whether a different set of settings should be selected individually for every batch.

The aim of this study was to determine the key separation properties (critical transport velocity, dimensions, angle of sliding friction) of Scots pine

seeds and the correlations between the investigated attributes for the needs of the seed cleaning and sorting process.

Materials and Methods

The experimental material comprised Scots pine seeds harvested from cones supplied to the husking plant in Ruciane Nida. Cones were harvested from three seed banks:

a) conservation seed stand, 132 years, Maskulińskie Forest Inspectorate, Guzianka Forest District 28/16/045, forest site – fresh mixed coniferous forest, rusty soil (marked as WDN),

b) commercial seed stand, 137 years, Maskulińskie Forest Inspectorate, Śniardwy Forest District 28/16/025, forest site – fresh mixed coniferous forest, rusty soil (marked as GDN),

c) seed plantation, 11–15 years, Łomża Forest Inspectorate, Podgórze Forest District, forest site – fresh mixed broadleaved forest, brown soil (marked as PN).

Roughly 2 kg of pine cones were randomly selected from each batch of the harvested material. Seeds were husked by heating the cones repeatedly in a stream of air and cooling them at low temperature. The investigated samples were characterized by a low number of seeds which were dewinged by rubbing in a linen bag. After pollutant separation, the material was spread on a table and divided by halving (*Nasiennictwo leśnych drzew...* 1995) to produce research samples of around 300 seeds each. The selected method produced samples of uneven size: WDN – 291, GDN – 307, PN – 309.

Every sample was initially divided into fractions using the Petkus K-293 pneumatic classifier with the precision of 0.11 m/s, and critical transport velocity was determined for the mean of the class interval in each group. The seeds from every fraction were placed on a transparent plate, and their length and width was measured under an MWM 2325 workshop microscope. The third dimension (thickness) was determined using a dial indicator device with measurement precision of 0.01 mm. The angle of sliding friction was determined on an inclined plane with an adjustable angle of inclination and a friction plate of ST3S steel. Measurement precision was 1°. A slicing test was performed to determine seed fullness.

It was assumed that the shape of Scots pine seeds resembles an ellipsoid. The cross-sectional area F and volume V of individual seeds was calculated using the below formulas:

$$F = \frac{\pi \cdot W \cdot T}{4}$$

$$V = \frac{\pi \cdot L \cdot W \cdot T}{6}$$

Due to a distinctive axis of rotation, Donev's shape factors (FRĄCZEK, WRÓBEL 2006) were applied to determine the shape of the studied seeds. The axis of rotation and seed length overlap, therefore, Donev's shape factors took on the following form:

$$\alpha = \frac{L}{T}$$

$$\beta = \frac{W}{T}$$

The effectiveness of separation of undeveloped seeds was calculated based on the ratio of the number of seeds separated from the material to the total number of undeveloped seeds (5% seeds with the smallest volume). The loss of plump seeds was determined based on the ratio of developed seeds separated from the material to the total number of developed seeds (difference between the number of seeds in the sample and the number of undeveloped seeds).

The results were processed statistically using Winstat and Statistica applications with the involvement of the following procedures: determination of consistency between variable distribution and normal distribution, analysis of variance, correlation, single-variable and multivariate regression analysis and stepwise regression to eliminate non-significant factors.

Results and discussion

The results of the slicing test revealed that most of the analyzed pine seeds were full without any signs of spoilage. The statistical parameters describing the seeds' physical properties and the results of Pearson's χ^2 test are presented in Table 1. At the adopted level of significance ($\alpha = 0.05$), there were no grounds to refute the theory that empirical distribution is consistent with normal distribution. The least developed seeds were harvested from the commercial seed stand. They were characterized by the highest average critical transport velocity and the smallest angle of sliding friction. Seed dimensions were generally consistent with published data (BURACZYK 2010, GIL, KINELSKI 2003, TYLEK 1998).

Table 1
Statistical calculations of critical transport velocity, dimensions and angle of sliding friction of Scots pine seeds

| Parameter | x_{\min} | x_{\max} | x | S | χ^2_{cal} | χ^2_{α} |
|-------------------------------|------------|------------|--------------------|-------|-----------------------|-------------------|
| Conservation seed stand – WDN | | | | | | |
| v | 3.58 | 7.98 | 6.68 ^B | 0.787 | 6.321 | 7.815 |
| T | 1.03 | 1.84 | 1.45 ^B | 0.126 | 5.905 | 7.815 |
| W | 2.28 | 2.89 | 2.59 ^B | 0.083 | 7.542 | 7.815 |
| L | 3.99 | 5.67 | 4.92 ^A | 0.169 | 5.390 | 5.992 |
| γ | 27 | 40 | 33.55 | 2.235 | 5.628 | 5.992 |
| Commercial seed stand – GDN | | | | | | |
| v | 5.23 | 7.98 | 6.99 ^A | 0.513 | 5.841 | 5.992 |
| T | 1.05 | 1.68 | 1.40 ^C | 0.119 | 6.474 | 7.815 |
| W | 2.08 | 2.87 | 2.47 ^C | 0.145 | 2.063 | 9.488 |
| L | 3.40 | 5.36 | 4.59 ^C | 0.399 | 7.627 | 7.815 |
| γ | 25 | 40 | 33.28 ^B | 2.514 | 6.985 | 7.815 |
| Seed plantation – PN | | | | | | |
| v | 4.13 | 7.98 | 6.77 ^B | 0.774 | 7.744 | 7.815 |
| T | 1.20 | 1.92 | 1.54 ^A | 0.135 | 9.036 | 9.448 |
| W | 2.13 | 3.18 | 2.70 ^A | 0.159 | 2.859 | 5.992 |
| L | 3.29 | 5.63 | 4.79 ^B | 0.314 | 7.792 | 7.815 |
| γ | 27 | 41 | 33.92 ^A | 2.711 | 4.779 | 5.992 |

^{A, B, C} – uppercase letters in the superscript indicate significant variations at the level of 0.01

A single classification analysis of variance was performed to validate the significance of variations between the average values. A comparison of seeds harvested from the conservation stand (WDN) and the commercial stand (GDN) yielded interesting results since parent trees were almost even-aged and they grew in similar habitats. Insignificant differences between the above seed groups were reported only in respect of the angle of sliding friction. No significant variations were noted in a comparison of critical transport velocity and angle of sliding friction in WDN and PN seed groups. The above results indicate that in most cases, the physical attributes of seeds harvested from the investigated stands were marked by significant variations.

The following seed parameters are given in Table 2: Donev's shape factors, cross-sectional area and volume. The above parameters were subjected to a single classification analysis of variance, and the results are presented in Table 2. Significant variations were not reported only with regard to shape factor β of seeds harvested from the commercial stand and the seed plantation. The average values of cross-sectional area and seed volume indicate that the

plumpest seeds were harvested from the plantation, while the least developed seeds were obtained from the commercial stand. Conservation stand seeds were characterized by the highest value of shape factors α and β .

Table 2

Shape factors (α , β), cross-sectional area (F) and volume (V) of Scots pine seeds

| Parameter | x_{\min} | x_{\max} | x | S |
|-------------------------------|------------|------------|--------------------|-------|
| Conservation seed stand – WDN | | | | |
| α | 2.79 | 4.49 | 3.41 ^A | 0.269 |
| β | 1.46 | 2.38 | 1.80 ^{Aa} | 0.147 |
| F | 1.84 | 3.99 | 2.96 ^B | 0.303 |
| V | 4.91 | 15.02 | 9.72 ^B | 1.206 |
| Commercial seed stand – GDN | | | | |
| α | 2.32 | 4.50 | 3.29 ^B | 0.331 |
| β | 1.41 | 2.16 | 1.77 ^b | 0.126 |
| F | 1.72 | 3.76 | 2.73 ^C | 0.345 |
| V | 4.08 | 12.50 | 8.37 ^C | 1.433 |
| Seed plantation – PN | | | | |
| α | 2.15 | 4.02 | 3.12 ^C | 0.289 |
| β | 1.45 | 2.43 | 1.76 ^B | 0.156 |
| F | 2.26 | 4.52 | 3.28 ^A | 0.398 |
| V | 5.83 | 16.39 | 10.50 ^A | 1.649 |

^{A, B, C} – uppercase letters in the superscript indicate significant variations at the level of 0.01

^{a, b, c} – lowercase letters in the superscript indicate significant variations at the level of 0.05

The smallest and, presumably, the least developed seeds have to be eliminated from every population because their reserve nutrient substances do not support full seedling development (*Nasiennictwo leśnych drzew...* 1995). The allowable loss during seed sorting was adopted at 5%, and the sorting efficiency of undeveloped seeds and the loss of developed seeds, determined based on seed characteristics (critical transport velocity, length, width, thickness and angle of sliding friction), are given in Table 3. The analyzed seed batches were characterized by different classification limits, thus validating the principle that every seed batch should be processed individually, and the settings of seed sorting and cleaning equipment should be customized according to need (*Nasiennictwo leśnych drzew...* 1995). The above principle is further supported by the results of calculations performed after the separation of mixed seed batches. If separation efficiency were to be evaluated based on individual seed attributes, the GDN batch would yield a relatively high number of undeveloped seeds, whereas few such seeds would be produced by PN and WDN groups. The analyzed batch would also be marked by the highest loss of

plump seeds. The above indicates that the majority of seeds eliminated from the population would comprise the material harvested from the commercial stand, including both developed and undeveloped seeds. The noted results also suggest that if the smallest seeds were to be removed based on a single attribute, the separation process should be carried out with the involvement of graders (which separate seeds based on their length) that effectively remove undeveloped seeds, thus minimizing plump seed loss. The results of this study also validate the use of sieves in the process of cleaning and sorting Scots pine seeds. Pneumatic and friction separators should not be used as the only separating devices. Such equipment, in particular pneumatic separators, are applied to remove fine wing parts and empty seeds from husked material.

Table 3
Separation efficiency of undeveloped seeds extracted from Scots pine seed material

| Classification limit | Separation efficiency of undeveloped seeds [%] | Loss of plump seeds [%] |
|---------------------------|--|-----------------------------------|
| WDN | | |
| $v=5.23 \text{ m s}^{-1}$ | 0 | 5.43 |
| $L=4.67 \text{ mm}$ | 46.67 | 2.90 |
| $W=2.45 \text{ mm}$ | 26.67 | 3.98 |
| $T=1.26 \text{ mm}$ | 60.00 | 2.17 |
| $\gamma=30^\circ$ | 13.33 | 4.71 |
| GDN | | |
| $v=6.33 \text{ m s}^{-1}$ | 62.50 | 2.05 |
| $L=3.76 \text{ mm}$ | 68.75 | 1.71 |
| $W=2.26 \text{ mm}$ | 56.25 | 2.39 |
| $T=1.22 \text{ mm}$ | 43.75 | 3.07 |
| $\gamma=30^\circ$ | 6.25 | 5.12 |
| PN | | |
| $v=5.78 \text{ m s}^{-1}$ | 6.25 | 5.15 |
| $L=4.20 \text{ mm}$ | 62.50 | 2.06 |
| $W=2.49 \text{ mm}$ | 56.25 | 2.41 |
| $T=1.34 \text{ mm}$ | 37.50 | 3.44 |
| $\gamma=30^\circ$ | 18.75 | 4.46 |
| Total | | |
| $v=5.78 \text{ m s}^{-1}$ | WDN – 13.33; GDN – 0; PN – 6.25 | WDN – 7.97; GDN – 0.67; PN – 6.82 |
| $L=4.11 \text{ mm}$ | WDN – 6.67; GDN – 93.75; PN – 37.50 | WDN – 0; GDN – 7.90; PN – 0.68 |
| $W=2.31 \text{ mm}$ | WDN – 6.67; GDN – 75.00; PN – 12.50 | WDN – 0; GDN – 11.00; PN – 0 |
| $T=1.26 \text{ mm}$ | WDN – 46.67; GDN – 81.25; PN – 12.50 | WDN – 2.53; GDN – 6.52; PN – 0 |
| $\gamma=30^\circ$ | WDN – 13.33; GDN – 6.25; PN – 12.50 | WDN – 3.62; GDN – 6.87; PN – 4.10 |

The coefficients of linear correlation between the analyzed traits and the calculated parameters are presented in Table 4. The critical values of transport velocity, seed length, cross-sectional area, volume, angle of sliding friction and shape factors α and β were not exceeded. When the values of critical transport velocity and angle of sliding friction were compared against the remaining physical attributes and the calculated parameters, the resulting coefficients of correlation were very low. The highest correlation coefficient of 0.539 was observed between seed width and seed thickness. Nonetheless, the reported value is relatively low, as demonstrated by the spread of measurement points in Figure 1.

Table 4
Coefficients of linear correlation between the analyzed traits and statistical parameters of Scots pine seeds

| Parameter | v | L | W | T | γ | α | β | F | V |
|-----------|--------|--------|--------|--------|----------|----------|---------|-------|-------|
| v | 1.000 | | | | | | | | |
| L | -0.047 | 1.000 | | | | | | | |
| W | -0.069 | 0.372 | 1.000 | | | | | | |
| T | 0.094 | 0.342 | 0.539 | 1.000 | | | | | |
| γ | -0.070 | 0.101 | 0.096 | 0.072 | 1.000 | | | | |
| α | -0.117 | 0.411 | -0.237 | -0.711 | 0.004 | 1.000 | | | |
| β | -0.163 | -0.109 | 0.148 | -0.747 | -0.001 | 0.649 | 1.000 | | |
| F | 0.038 | 0.395 | 0.817 | 0.924 | 0.094 | -0.595 | -0.443 | 1.000 | |
| V | 0.011 | 0.684 | 0.783 | 0.857 | 0.120 | -0.318 | -0.391 | 0.937 | 1.000 |

Critical value of the correlation coefficient – 0.065

The correlation between separation properties has to be determined for the purpose of designing seed sorting and cleaning processes (GROCHOWICZ 1994). It supports the determination of adequate separation indicators without the need to measure all investigated traits. The equations describing the studied attributes, produced by the stepwise regression analysis, are presented in Table 5. Owing to generally low percentages of explained variation, the above table lists only correlations with the highest values. As demonstrated by the correlation analysis, the equations describing critical travel velocity and angle of sliding friction were characterized by very low goodness of fit. The above applies to both single-variable and multivariate equations. The equations describing the width and thickness of Scots pine seeds produced correlations with the highest percentage of explained variation. The noted values did not exceed 34, indicating that those equations should not be applied to convert parameters.

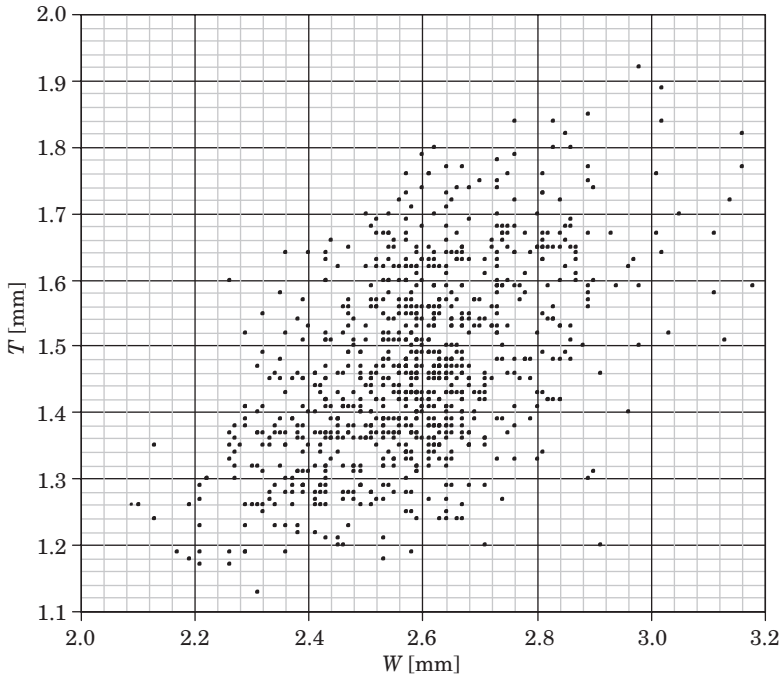


Fig. 1. Correlation between thickness T and width W of Scots pine seeds

Table 5
Single-variable and multivariate equations describing critical transport velocity, dimensions and angle of sliding friction of Scots pine seeds

| Equation | Percentage of explained variation | Standard deviation of residuals |
|--|-----------------------------------|---------------------------------|
| $v = -0.08\beta^3 + 7.29$ | 2.71 | 0.703 |
| $T = 0.46W + 0.28$ | 29.09 | 0.118 |
| $W = 0.63T + 1.66$ | 29.09 | 0.138 |
| $L = 50.66W - 17.67W^2 + 2.06W^3 - 43.67$ | 18.62 | 0.306 |
| $\gamma = 6.36 \cdot 10^{-4} V^3 + 32.98$ | 1.73 | 2.488 |
| $T = 0.41W + 0.1L^2 + 0.24$ | 31.37 | 0.116 |
| $W = 0.24L + 1.00T - 0.10L \cdot T + 0.64$ | 33.48 | 0.134 |
| $L = 7.97W - 1.47W^2 + 0.17W \cdot T - 6.64$ | 20.33 | 0.303 |

Level of significance – 0.05

Conclusions

1. The correlations between the separation properties of Scots pine seeds harvested from three seed banks were characterized by high variability, and the resulting equations showed a relatively low percentage of explained

variation. For this reason, the noted correlations should not be used for the purpose of designing seed cleaning and sorting processes.

2. Seed thickness and width were the most correlated attributes of Scots pine seeds, whereas critical travel velocity and length were the least correlated traits.

3. Due to statistical variations between seed populations from different seed banks, every seed batch should be processed individually, and the settings of seed sorting and cleaning equipment should be customized according to need.

Translated by ALEKSANDRA POPRAWKA

Accepted for print 15.04.2011

References

- BURACZYK W. 2010. *Właściwości nasion a cechy morfologiczne siewek sosny zwyczajnej (Pinus Sylvestris L.)*. Leśne Prace Badawcze, 71(1): 13–20.
- FRĄCZEK J., WRÓBEL M. 2006. *Metodyczne aspekty oceny kształtu nasion*. Inżynieria Rolnicza, 12: 155–163.
- GIL W., KINELSKI S. 2003. *Nasiona i siewki drzew*. MULTICO Oficyna Wydawnicza, Warszawa.
- GROCHOWICZ J. 1994. *Maszyny do czyszczenia i sortowania nasion*. Wydawnictwo Akademii Rolniczej, Lublin.
- MURAT E. 2002. *Szczegółowa hodowla lasu*. Oficyna Edytorska „Wydawnictwo Świat”, Warszawa.
- MURAT E. 2005. *Poradnik hodowcy lasu*. Oficyna Edytorska „Wydawnictwo Świat”, Warszawa.
- SARNOWSKA G., WIĘSIK J. 1998. *Wyluszczeniarka w Czarnej Białostockiej. Część III. Czyszczenie i separacja nasion*. Przegląd Techniki Rolniczej i Leśnej, 1: 19–21.
- TYLEK P. 1998. *Cechy planimetryczne nasion drzew liściastych*. Przegląd Techniki Rolniczej i Leśnej, 1: 22–24.
- Nasiennictwo leśnych drzew i krzewów iglastych*. 1995. Red. A. Załęski. Oficyna Edytorska „Wydawnictwo Świat”, Warszawa.

ANALYTICAL MODEL OF THE OPTIMAL CAPACITY OF AN IRRIGATION SYSTEM

Zuzana Palkova, Tomas Rodny

Slovak University of Agriculture in Nitra

Key words: irrigation system, queuing theory application, analytical model, process optimization.

A b s t r a c t

The size and stability of yield per hectare of agricultural crops are greatly affected by climatic conditions, temperature, solar radiation, but especially the quantity and quality of rainfall, which for most agricultural crops is insufficient. Building large-scale irrigation systems is difficult in terms of investment, as well as operating costs. Claimed agricultural yields often do not emanate from a set of certain claims for each of the crops, but are only an estimate based upon empirical experience. Precise determination of these data is very difficult and without the use of exact mathematical methods and information technology would be virtually impossible. Goal of this project is dedicated to enhance of an irrigation system analytical model usability, which would allow the determination of the optimal capacity of the irrigation system in response to microclimate and soil conditions with respect to the crops and irrigation facilities. Developing new methods of precise irrigation is the way of higher and ecological productivity in agricultural production subsystem.

ANALITYCZNY MODEL OPTYMALNEJ WYDAJNOŚCI SYSTEMU NAWADNIANIA

Zuzana Palkova, Tomas Rodny

Słowacki Uniwersytet Agrotechniczny w Nitrze

Słowa kluczowe: system nawadniania, zastosowanie teorii kolejowania, model analityczny, optymalizacja procesu.

A b s t r a k t

Wielkość oraz stabilność plonu z hektara uprawianego pola w dużej mierze zależy od warunków klimatycznych, temperatury, promieniowania słonecznego, ale w szczególności sposób od jakości oraz ilości opadów deszczowych. Opady te dla większości upraw rolniczych są niewystarczające. Oszacowanie wydajności systemu nawadniania nie wynika zatem jedynie z zapotrzebowania na wodę uprawianych roślin, lecz także zależy od czynników losowych – mikroklimatycznych. Aktualnie wydajność systemu nawadniania, wielkości jedynie przybliżonej, szacuje się często na podstawie

doświadczeń empirycznych. Dokładne określenie wydajności systemu nawadniania jest bardzo trudne i praktycznie niemożliwe bez zastosowania dokładnych metod matematycznych oraz technologii informatycznych. Celem pracy było zwiększenie użyteczności matematycznego modelu systemu nawadniania, co powinno pozwolić na określenie optymalnej wydajności systemu nawadniania w zależności od mikroklimatu i warunków gruntowych, z uwzględnieniem upraw oraz urządzeń nawadniających.

Prepositions of project solution

Irrigation system remains the weakest part of soil management. Ignoring water regime of soil and various crops from the beginning to the end of vegetation is large obstacle to economic and ecological irrigation. Research in the irrigation sector has accumulated enough theoretical and practical knowledge and needs only to look for ways and methods as soon as possible to get it into irrigation practice (HENNYEYOVÁ, PALKOVÁ 2006).

Goal of process observation in the irrigation system is the monitoring and analysis of various factors affecting the growth of crops, depending on the optimum moisture requirements of individual crops, and achieve higher productivity per area unit.

Precise irrigation as an aspect of agriculture is just the start of the research and represents application of water to exact location and exact dose. Using precise agricultural irrigation management is still in a state development and needs a lot of research and experimental work to define its realization case study and applicability (SOURELL 2003).

We try to integrate the accumulated knowledge into complex unit and then apply existing models and simulations in the experimental conditions, where we compare the efficiency of various algorithms and models of irrigation. Analyzing model and its behaviors we expand existing models with new optimization features and compare their results with the original models.

Description of irrigation process method

Irrigation is part of wide structure of agricultural production processes. Contains very specific conditions like product resources in an open environment that fully interacts with surrounding. Irrigation system process, in our case, we consider as isolated part of the overall process. We monitor its impact on the overall output with markers like yield per hectare.

Description of the processes can be statistically manageable through mathematical models. Mathematical model is a simplified view of real objects by using mathematical description, usually in order to solve the problem. The

problem can be solved if we have the appropriate methods. Methods and models of individual processes are classified as:

a) Deterministic models and methods, where values and relations between them are not random. These models are applied when examining the operations of production, distribution and production scheduling.

b) Stochastic models and methods, where values and relations between them have a probability character. These models are used in examining particular handling operations, supply and recovery. These includes models of processes in agriculture, in irrigation management too.

Individual factors and associated sub-processes entering the irrigation system are fully stochastic in nature. Solving problems in this area requires to use of methods of statistical analysis and mathematical probability. Application discipline for the monitoring and optimization of the irrigation system is the queuing theory (QT).

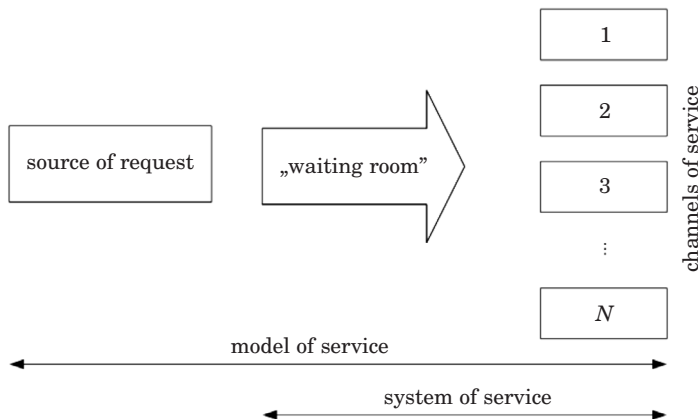


Fig. 1. The scheme of system of queuing theory

In our research based on existing mathematical models of irrigation systems are created on theoretical principles of queuing theory.

In agricultural practice are realised various combinations of systems based on queuing theory depending on the solution process. Standard QT process in irrigation system is defined as N-channel system, limited resource requirements, with a priority system in operation. Where the number of channels the system is defined as the available pool of technical device of irrigation, source of requirements as exact determined number of segment area units of agricultural crops, and priorities as currently requirements of individual segments on moisture in the soil.

In the case of irrigation system, the queuing system consists of service channels, which serve the requirements of current plants to supply additional irrigation. If the existing channels are not able to immediately serve the incoming requirements, they leave the system without serving, or are in the waiting queue, where they are for the release of a channel selected according to criteria given previously. This priority is necessary in the event that water demand is appearing for those crops which are economically important, or non-delivery of irrigation with them causing great economic damage. Stochastic elements in the case of irrigation system are:

- Input queue of requirements.
- Time longitude of requirements service.

Processing current mathematical QT is a complex process that requires the use of computing technology. Optimization can rationalize that process and achieve desired results in agricultural practice.

We define several possibilities of computing object simplification:

- Using only one channel of service – in this case we simplify handling process as we eliminate some algorithms from solution definition like channel of service choice.
- Rejection of priority – there is an elimination of algorithm for determining the order of the waiting room, where the solution is limited to servicing the requirements of a random stream of a final number of heterogeneous irrigation schemes.
- Discretization of requirements for heterogeneous servicing channels – used to monitor and review the effectiveness of choosing the correct handling channel.

These simplifications create separate groups of algorithms in the decision process:

- Algorithms for prioritizing requirements of different sectors of irrigation.
- Algorithms for efficient selection of technical equipment in the process of irrigation.
- Algorithms for modification of final order in the waiting room.

Described mechanisms determine individual factors of irrigation process. Each of element is based on unique inputs (database inputs). In fact, the algorithm outputs are counted in the overall impact on the effectiveness of decision-making. The overall process of irrigation using queuing theory is shown in the Figure 2.

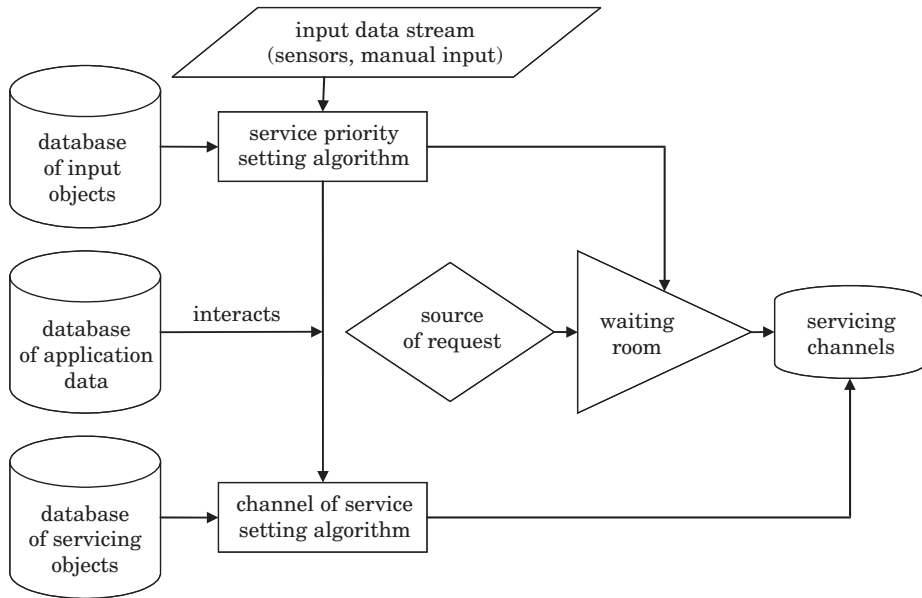


Fig. 2. The scheme of process of analytical model

Analytical model description

The basic idea of modeling real process, which include irrigation is possible in the simulation of real processes. Using modern CASE tools we can design a database model that corresponds to each element of the process operations of irrigation. The elements of the model between create relational links according to the reporting process steps. Particularity of this model is the use of hierarchical links between records, and implementing the potential of object databases. Then we can effectively manage data realtime, we can react quickly and data would be efficiently processed.

Input data stream represents data entering into the system from outside. That are inputs from measurements of soil moisture, temperature, plant life cycle, period and manual input about service device operators and others factors. The database of input objects, which consists of object-hierarchical database of product plants, database moisture requirements of plants and priorities of the rules table, creating input to decision-making algorithm for assigning priorities of requests and its enlistment in the waiting room. Database of servicing objects includes object-hierarchical database of service channels, their properties and methods from which we can determine the deployment of various devices to specific requirements.

The next section will present an algorithm based on a sample of database entry objects.

Alorithms determining priority of requests entering “waiting room”

We choose the model with one channel of service with priority of requirements, where the requirements do not leave the waiting room in the time interval. This process model considers an isolated instance, the weight of decision-making is based on a single algorithm that determines the priority of requests entering the system. By isolation of algorithms in the right combinations can objectively evaluate the effectiveness of algorithms. Evaluation of the results in this case is judged on the basis of the total time needed for the quantity served exactly the requirements of channel operation (in this case, the technical equipment of mobile irrigation system). Requirements entering the system are Poisson stream.

The probability of k number of requirements to time interval t is then determined by:

$$P_k(t) = \frac{(\lambda \cdot t)^k}{k!} \cdot e^{-\lambda \cdot t},$$

where λ is the parameter of arrival of requirements.

Requirements are random generated for the simulation. Real requirements entering the system on condition of achievement of critical levels of soil moisture measured by soil sensors. Any requirement in the stream carries the basic information that is stored (Input data stream buffer):

- Location of measured sector requirement by the sector ID,
- Requirement time of creation,
- Unique identification of plants according to the code of plant input DB,
- Current value of sensor measurement: current humidity, current temperature.

In this case, data from the sensor data stream pass throught filter, which decides whether it is a legitimate request. The filter has several factors:

- Current soil moisture,
- The time interval from the last irrigation time,
- Coefficient of decline of soil moisture.

Coefficient of moisture loss in the soil determines the relative value of measurement for adding to list of requirements:

$$R_{koef} = \frac{\Delta t_{int}}{L},$$

where Δt_{int} is the time interval since the last irrigation in hours, L is the ratio of intensity of crop moisture.

Each sensor records are stored in a database for need of algorithm analysis, especially for comparing current values with historical measurements.

Optimization algorithm for priority requirements determination compares the current entry requirements and information. Then the algorithm enters into a database application data, where information on measurements taken from sector and there are the values of other environmental variables.

Each incoming request gets to waiting room as the output value of the priority algorithm in the range of 1–100 points, which is the sum of the individual factors assessed. The value of 100 means the highest priority. The request in waiting room is placed in order according to its priority. In the waiting room is scheduled control mechanism that controls the duration requirement in a waiting room and this time changing the current priority of requirements depending on the complexity, the importance of technical crops, etc.

Analysis of the priority of each requirement monitors and compares the following parameters:

- The time interval from the last irrigation,
- The ratio of crop water demand balance in sector and current moisture,
- Compare the current value of moisture to the process of water balance during the crop vegetative life,
- The economic importance of crop,
- Progress of current environmental temperature vs. history with regard to the temperature requirements of plants,
- Inclusion of global climate variables: the probability of precipitation in the hours, service coefficient (you can manually adjust the priority according to the contingencies) and others.

Input data stream database record example:

| ID_Request | ID_Sector | ID_Plant | Time [dd.MM.yyyy] | Moisture [%] | Temp. [°C] |
|------------|-------------|----------|-------------------|--------------|------------|
| 103243200 | 2010-R-0013 | 808-003 | 12.06.2010 14:33 | 15 | 18 |
| 103245601 | 2010-R-0126 | 808-002 | 13.06.2010 10:28 | 30 | 22 |

Algorithm procedure fragment for time interval between different irrigation priority processing:

```
function SetTimeIntervalPriority(parID_Request,parInputValues:TstringList); // procedure input
var // variables definition
    DS: TappDataSet // Data stream data set
    Filter: string;
Priority,Interval:Integer;
begin // core
    // parID-Reguest – ID of request
    // parInputValues – set of global
    // variables selected from
    // application database by SQL query
```

```

try
DS := TappDataSet.Create; // instance constructor
Filter := 'DS.Value("ID_Request") = parID-Request';
DS.SetDSParams("10020,10203",filter); // opens data set of concrete data stream
DS.Open; DS.First;
If DS.RecordCount = 1 then // if record found
  Interval := DateDiff(day,DS.Value(Time), ParInputValues.strings[TimeLast]); // interval of last irrigation
  CASE // condition of priority
  ((Interval - ParInputValues.strings[water_need]) <= 0) : Priority := 10;
  ((Interval - ParInputValues.strings[water_need]) > 0) : Priority := 10 - ParInputValues.strings
  Else Priority:= 1; [water_need];
  END
finally
Result := Priority;
DS.Free;
end;
end;

```

Conclusion

The project currently in phase of additional algorithm tuning on virtual data, where we try to adjust the decision process and designed model approximately to real conditions. The main difficulty in our testing of solution is availability of databases with real input data, so we use data obtained primarily by internal measurements of our institution experiments.

The definitive effect of process optimization is getting in importance, depending on the size of irrigated area in the number of sectors and the number of technical resources. In small agricultural units we do not expect a visible effect of applying this method of process optimization.

The expected trend in near future is a significant turnover in irrigation look, as possibility how to solve the current problems. Some intensification tools have achieved an roof effect and therefore producers are looking for sub-options.

Wide cause of this state is extreme environment behavior, which can not guarantee an adequate supply of moisture during the vegetation period. Finally, it begins socio-political pressure to support the idea of organic agriculture, to which irrigation belongs too.

Accepted for print 19.01.2011

References

BISWAS A. 1980. *The Application of systems analysis to problems of irrigation, drainage and flood control*. Pergamon Press, ICID, Oxford, ISBN 0-08-023425-9.

-
- HENNEYOVÁ K., PALKOVÁ Z. 2006. *Využitie informačných technológií a simulačných modelov v závlahovom hospodárstve*. 1. vyd. Nitra: Slovenská poľnohospodárska univerzita, s. 108. ISBN 80-8069-715-9.
- KUMAR V., SINGH J., BHAKAR S.R. 2005. *Drainage and Irrigation Water Management*, Udaipur, Himanshu, XII: 315, ISBN 81-7906-099-3.
- RATAJ V. 2005. *Projektovanie výrobných systémov – Výpoty a analýzy*. Monografia. Nitra: SPU. s. 120. ISBN 80-8069-609-8.
- SOURELL H., AL-KARADSHEH E. 2003. *Precision Irrigation Toward Improving Irrigation Water Management*. ICID-CIID 2003 – 54th Executive Council of ICID 20th European Regional Conference Montpellier. 14–19 September 2003 [CD-ROM]. Montpellier, France.

**EVALUATION OF POSSIBLE APPLICATION
OF TERRESTRIAL LASER SCANNER – SCANSTATION
IN VERTICAL DISPLACEMENT MEASUREMENTS**

Andrzej Dumalski

Institute of Geodesy
University of Warmia and Mazury in Olsztyn

Key words: terrestrial laser scanner, vertical displacement.

Abstract

Author of the article conducted empirical studies to show the usefulness of the laser scanner in displacement measurements. Vertical displacements were measured on a tester that was specially contracted for that purpose. The test measurements were carried out by applying different methods and different instruments, i.e., the precise leveler, the total station applied with the reflector of without it and ScanStation laser scanner. The test results show great potential for laser scanning in determining the vertical displacements even of millimeter values. The paper also presents briefly how to use laser scanning in surveying measurements and a special attention was paid to some of the parameters characterizing accuracy of the laser scanning.

**OCENA MOŻLIWOŚCI ZASTOSOWANIA SKANERA LASEROWEGO SCANSTATION
DO POMIARU PRZEMIESZCZEŃ PIONOWYCH**

Andrzej Dumalski

Institut Geodezji
Uniwersytet Warmińsko-Mazurski w Olsztynie

Słowa kluczowe: skaner laserowy, przemieszczenia pionowe.

Abstract

Autor artykułu przeprowadził badania empiryczne mające na celu pokazanie przydatności skanera laserowego w pomiarach przemieszczeń obiektów inżynierskich. Na specjalnie do tego celu skonstruowanym przyrządzie pomiarowym dokonano pomiaru przemieszczenia pionowego. Wykorzystano różne instrumenty i techniki pomiarowe. Do wyznaczenia przemieszczenia pionowego zastosowano niwelator precyzyjny, tachimetr elektroniczny z funkcją pomiaru z reflektorem i bez oraz skaner laserowy ScanStation. Wyniki testu wskazują na duże możliwości skanowania laserowego w wyznaczaniu przemieszczeń pionowych i pozwalają na wychwycenie ich milimetrowych wartości. W pracy przedstawiono sposoby zastosowań skanowania laserowego w pomiarach oraz zwrócono uwagę na niektóre parametry dokładnościowe charakteryzujące skaner laserowy.

Introduction

Laser scanning was introduced in Poland in 2003. Since this time it became a subject of research for many specialists, especially for surveyors. Until then, the only way to measure inaccessible places was based on photogrammetric methods. This method was accurate, however, its range was rather small. Another disadvantage was, and still is, a long time of elaboration of the data. The advantage of the laser scanning is that we get 3D coordinates during the measurements at once. It is also possible to analyze results just after the measurements. The result, namely the point cloud is a set of vectors and all the measured points have 3D coordinates. Thus, it is possible to compute distances, angles or azimuths between them. From the practical point of view, it is important to know the accuracy of the measurements. Such accuracy depends on the instrument applied among others. It also shows the possible application of the laser scanner, namely the surveying problems where scanning accuracy is sufficient. One of such problems is analysis of deformation or displacement of engineering structures. Such displacements may have different sources and properties, and also different absolute values, which influence the choice of proper surveying instruments. The accuracies that are given by the scanner producers, encourage to apply laser scanners to measure even very small, millimeter displacements, Therefore, it seems important to test such accuracy in practice, especially that results of similar analyses are very promising (TOURNAS, TSAKIRI 2008, LOVAS et al. 2008). The present paper shows possible surveying applications of laser scanning and presents practical tests of use of the laser scanner in vertical displacement analysis.

Application of laser scanning

Laser scanning can be regarded as a new technique of inventory of engineering structures or measurement of ground surface. It can be use, for example, in architectural inventory of historical objects (WONG 2009), a single buildings (HEJBUDZKA et. al. 2009), group of engineering structures (GORDON et al. 2003), steel constructions (ĆMIEŁOWSKI et al. 2009) or water structures (ALBA et al. 2006). Laser scanning is used in mining areas where it is applied to measure outcrops, mine waste dumps and other by-products of mining activities (GEOFF 2008). It is also applied in archeology to inventory excavations (MOORE, FORSYTHE). It is often applied to measure equipment of refinery where direct measurements are usually impossible. Due to this technique one can measure all the points that are visible from the station of the scanner (FLOYD, SANDERS 2001). Laser scanner can also be a source of data for numeric model of terrain (BOJAROWSKI et al. 2008a).

There are two kinds of software that are necessary to work with a laser scanner. The first one controls the scanner during measurements, and the second one is applied to do basic operations on point clouds. One can obtain 3D models of complex structures, generate 2D pictures, model different shapes (pipes, lines or architectural elements) and fit them in a point cloud, find collisions, visualize objects, prepare animations etc. Laser scanner is therefore a good source of data for necessary documentation of buildings before renovation, and also in shape analyses of damaged buildings. Wide application of the method in question is due to its accuracy. Some applications require a centimeter, while the others a millimeter accuracy. Therefore, it seems reasonable to develop this technique, especially in analyses of displacements and deformations. The angle and distance accuracies of laser scanners make possible of their application in surveying.

Lasers scanners are the next step in development of electronic tachimeters. Similarly to tachimeters, they compute 3D coordinates (X , Y , Z) of measured points on the basis of directly measured distances, vertical and horizontal angles. It is so-called reflectorless measurement, and the accuracies of both kinds of the instruments are also similar. However, laser scanner is much more quicker than traditional total stations. The impulse technique of measurements enable us to measure few thousands of points per second, while the phase one even up to 500 000. The disadvantage of laser scanner is its relatively smaller range (for the impulse scanner it is several hundred meters). Only few scanner have range about one kilometer. It is worth noting that the scanner range depends on a kind and color of a reflecting surface. The darker it is, the smaller range is. It follows strength of a reflected light ray, which is sometimes called the fourth coordinate. Beside accuracy and fastness of scanner measurements, there are several other properties that are important and required by the users. All such properties can be divided into three main areas. The first area, namely reliability refers mainly to accuracy and resolution. The second one consists of measurement speed, range and field of vision. The third area, functionality refers to size of a scanner, simplicity of running, and especially to the software (PUDŁO 2006, 2008). It is hard to decide which properties are the most significant. However, it is obvious that it depends on a kind of surveying problem or task that the scanner is applied for. For example, if a large area is measured then it is better to choose a scanner of longer range and lower accuracy. On the other hand, if a small details are measured then one needs a scanner of high resolution and accuracy. The speed of measurements seems to be less significant in such problems, however, this could change over time. Most of new potential scanner users would choose an „optimal” and most useful type of scanner, namely a scanner of relatively high accuracy and average (several hundred meters) range.

Accuracy of Laser Scanner

As it was already mentioned, the accuracy of a laser scanner is a very important parameter that determines usefulness of a scanner to certain surveying tasks. Boehler and Marbs (BOEHLER et al. 2003) presented some more significant factors that influence such accuracy. Now, let us remind them briefly.

Angle accuracy

These errors stem from the fact that a laser beam is deflected in two perpendicular directions by operating with high precision reflecting mirrors. Rotations of the mirrors cause some errors in the reading of horizontal and vertical angles, which results directly in errors of 3D coordinates. These errors are especially evident in the plane perpendicular to the direction of measurements.

Distance accuracy

Distance accuracy is very significant for general accuracy of the scanner. It can be described by two components: determination of the time of propagation of electromagnetic wave from the deflector to the target and back, and determination of the refractive index of electromagnetic wave in the air. Thus, it can be describe by the mean error in the following formula

$$m_D = D \sqrt{\left(\frac{m_\tau}{\tau}\right)^2 + \left(\frac{m_n}{n}\right)^2},$$

where:

m_τ – mean error of time propagation,

m_n – mean error of the refractive index n .

The component m_τ describes the accuracy of time τ , thus it describes all instrumental errors as well as errors that stem from operating the scanner. On the other hand, the component m_n represents the accuracy of the refractive index, which depends on the air temperature, pressure and humidity. Thus it describes errors that stem from the physical facility (PŁATEK 1991).

Effects of surface color

Different colors of the reflecting surface are sources of some additional systematic errors. For the primary colors one can compute corrections, however, the color of the reflecting surface is generally a mixture of the primary colors. Thus, it is almost impossible to correct the measurement properly. Usually, these errors are not so significant and do not influence the accuracy of 3D model obtained. To protect measurement results from these errors one can apply markers of the same color at the measured points.

Scanner resolution

Resolution is an important property of the laser scanner that describes its ability to detect small objects. It depends on two main factors: the smallest change of the angle between two consecutive measurements and the size of a laser spot.

Edge effect

The edge effect occurs when the laser spot reaches the edge of the measured object. Then, only a part of the electromagnetic wave is reflected and return to the scanner. The rest can be reflected by adjacent surfaces and give incorrect measurements. Incorrectly measured points can be close to the real edge of the object but sometimes the differences may reach even decimeters. This effect is particularly evident when a spherical or cylindrical objects are measured.

Effect of reflectivity

Laser scanner records laser beams reflected from measuring surface. The strength of the returning signal depends mainly on reflective abilities of the surface. Such ability is described by the albedo. Bright surfaces give a stronger return signal than dark ones. If the surface is dark and glossy one can expect no return signal at all. Effects of different reflecting surfaces depend on the spectral characteristic of the laser. The surfaces of the different albedos may result in systematic errors that exceed the standard deviation of measurement by several times. Thus, if the object measured is built of some different materials one should expect such big errors. To protect results from these large systematic errors, one can cover the object with a uniform material of the constant albedo for the measurement time (if it is possible, of course).

Research project

The idea behind the research project was to compare results of a laser scanning with more conventional methods of vertical displacement determination. I used the laser scanner Leica SkanStation and for the comparison I chose the electronic tachimeter Leica TC 705 and the precise leveler Carl Zeiss Jena Ni 002. I analyzed differences in determination of vertical displacements that were simulated by a specially constructed equipment (Fig. 1).

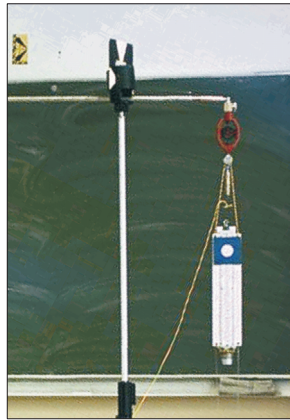


Fig. 1. Tester

Source: own development.

The tester was hung on an aluminum arm fastened to the wall just a few meters from the station. It consisted with a mini prism combined with a part of a precise leveling staff and a special shield HDS. During the tests, the tester was displaced in a vertical plane, and the values of displacements were measured by applying the instruments that were mentioned above. Thus, the displacements were measured using laser scanning, precise leveling or trigonometric method. The last method was carried out in two ways, namely with use of a prism and in reflectorless technique. In order to eliminate the vertical index error, the trigonometric method was carried out in two faces. The height differences dh were measured between the horizontal rotation axis of the telescope and the tester, which is a function of distance and a vertical angle. The displacements were also measured by precise leveling (accuracy of 0.2 mm/km of double leveling). These measurements were taken as a basis for comparison with laser scanning and the trigonometric method. The electronic tachimeter Leica TC705 has the following accuracy: angle accuracy $15''$, distance accuracy 2 mm + 2 ppm (measurements with a prism) and

3 mm + 2 ppm (reflectorless). While for the laser scanner ScanStation, it is respectively 35^{cc} for angle measurements and 4 mm for distances. The minimum change that can be measured vertically as well as horizontally is 1.2 mm.

The results of laser scanning were applied to model the shield HDS (Fig. 2) and to determine the center of the shield, namely a HDS vertex (dimensionless point) with 3D coordinates (X, Y, Z) (Fig. 3). The postprocessing was carried out by application of the software Cyclone v.5.6. I used only vertical component to determine the vertical displacements.

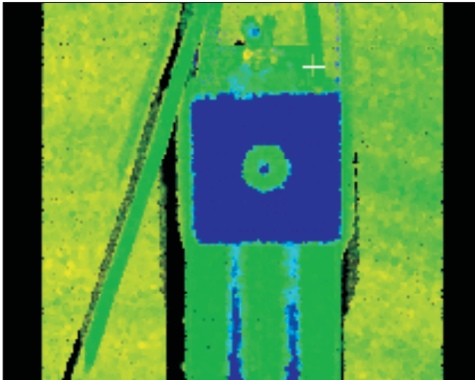


Fig. 2. Scan of the HDS target
Source: own development.

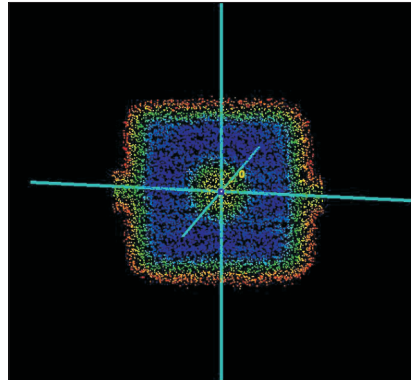


Fig. 3. Example of Vertex model upon the HDS target
Source: own development.

Table 1 presents the results of the measurements with the precise leveler, the electronic tchimeter (with a mirror and reflectorless) as well as the results of determination of the HDS shield vertexes.

Table 1

Measurement results

| Level | Precise leveler | | | Total station measurement with a mirror [mm] | | | Total station measurement without a mirror [mm] | | | Terrestrial laser scanner [mm] |
|-------|------------------|------------------|------------------|--|------------|---------|---|------------|---------|--------------------------------|
| | loc. I | loc. II | average | dh loc. I | dh loc. II | average | dh loc. I | dh loc. II | average | |
| A | 924509 317998 | 924343 317830 | 924426 317914 | 316 | 316 | 316 | -8 | -8 | -8 | 143 |
| B | 930234 323729 | 930071 323569 | 930153 323649 | 288 | 288 | 288 | -37 | -37 | -37 | 115 |
| C | 914095 307591 | 913940 307430 | 914018 307511 | 368 | 368 | 368 | 44 | 44 | 44 | 195 |

A, B, C - control levels

dh - height differences between the horizontal rotation axis of the telescope and the target

Table 2 presents the final values of the vertical displacements between the level A and both levels B and C.

Table 2

Value displacement

| Displacement | Precise leveler [mm] | Total station measurement with a mirror [mm] | Total station measurement without a mirror [mm] | Terrestrial laser scanner [mm] |
|--------------|----------------------|--|---|--------------------------------|
| A-B | 28.6 | 28.0 | 29.0 | 28.0 |
| A-C | -52.0 | -52.0 | -52.0 | -52.0 |

These results are also presented in Figure 4.

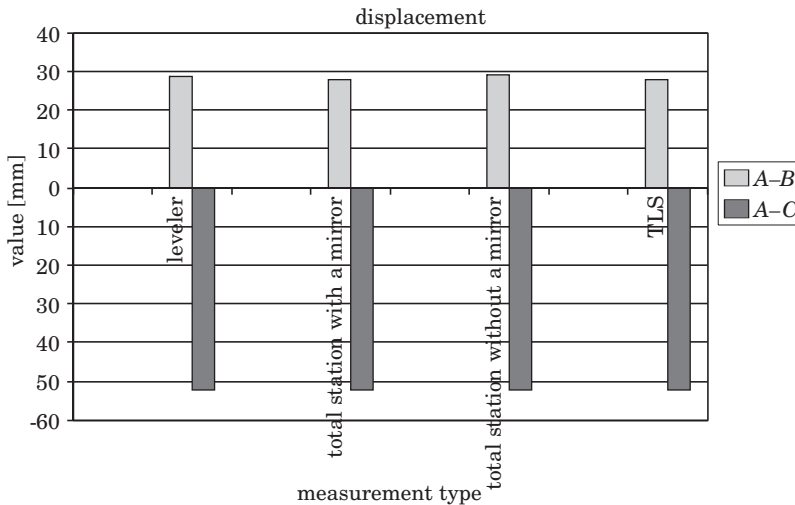


Fig. 4. Graphical Interpretation of measurement results

Source: own development.

Where displacements of an engineering structure are measured it is sometimes impossible to mark the objects with HDS shields. However, it is usually possible to find some distinct points that can be easily identified in the following measurement epochs. The tester that was applied in the research project also had such points. I chose one point, namely a clamp, which is pointed with the arrow in Figure 5. This characteristic point was scanned to determine its coordinates, which was the basis for computation of displacements. The results were compared with the precise leveling, and are presented in Table 3 and in Figure 6.

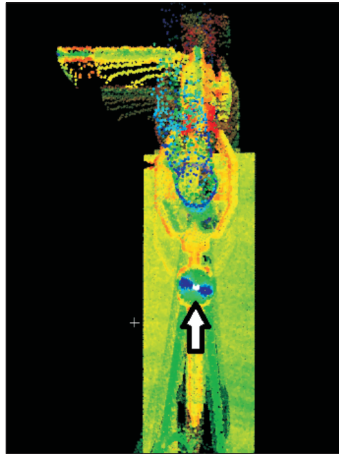


Fig. 5. Tester with measured point indicated (arrow)

Source: own development.

Table 3

Displacement Values

| Displacement | Precise leveler [mm] | Direct measurement [mm] |
|--------------|----------------------|-------------------------|
| A-B | 28.6 | 29.0 |
| A-C | -52.0 | -51.0 |

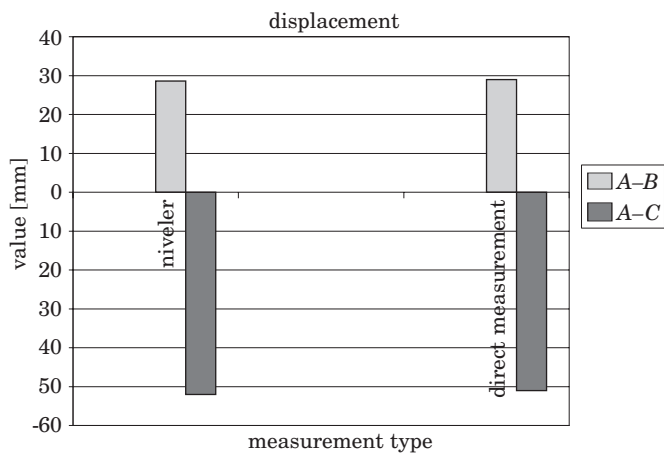


Fig. 6. Graphical Interpretation of the measurement results

Source: own development.

Conclusions

The results of the research project allow to formulate some general conclusions. The values of the displacements obtained by applying different methods are almost the same. The differences of 1 mm are within the accuracy of the measurements. Such good convergence results from rather small, few meters, distance between the measured object and the instruments. It is worth noting that a change of HDS shield for certain distinct point does not reduce the measurement accuracy. Thus, it is not necessary to mark object that are hard in access. However, one should choose only these points that are uniquely identifiable. In conclusion, the results of the laser scanning are very similar to the results of the trigonometric method (electronic tachimeter) as for the accuracy. Thus, the laser scanner can be an alternative to more conventional methods. The advantage of the laser scanning is large number of observations, which allows us not only to study displacements pointwise but also to do some spatial analyses (e.g., deformation)

Translated by ROBERT DUCHNOWSKI

Accepted for print 28.03.2011

References

- BOEHLER W., BORDAS VICENT M., MARBS A. 2003. *Investigating Laser Scanner Accuracy*. Proceedings of XIXth CIPA Symposium. Antalya, Turke. Sept. 30 – Oct. 4.
- BOJAROWSKI K., GOŚCIEWSKI D. 2008a. *Generowanie numerycznego modelu terenu na podstawie pomiaru skanerem laserowym*. Czasopismo Techniczne, 2-Ś.
- FALKOWSKI P. 2008. *Badanie skanera*. Geodeta, 4(155).
- GEOFF J. 2004. *High Definition Surveying-3D Laser Scanning: Understanding the “Useful Range” of Laser Scanners*. Professional Surveyor Magazine, 24(11). On line. <http://www.profsurv.com/magazine/article.aspx?i=1327> (dostęp: 10.03.2011)
- GEOFF J. 2008. *3D Scanning: Using Multiple Laser Scanners on Projects*. Professional Surveyor Magazine, 28(4). On line. <http://www.profsurv.com/magazine/issue.aspx?i=139> (dostęp: 10.03.2011).
- LOVAS T., BARSÍ A., DETREKOI A., DUNAI L., CSAK Z., POLGAR A., BERENYI A., KIBEDY Z., SZOCS K. 2008. *Terrestrial Laserscanning in Deformation Measurements of Structures*. The International Archives of the Photogrammetry, Remote Sensing and Spatial Information Sciences. XXXVII. (B5) 2008.
- MOORE P., FORSYTHE W. Ushet Port Complex, Rathlin. Island Rathlin Island Research Project, High Definition Building Survey, CAF HDBS 001h, on line: <http://www.qub.ac.uk/schools/CentreforArchaeologicalFieldworkCAF/Reports/HighDefinitionBuildingSurveys/Fileupload,64387,en.PDF> (dostęp: 10.03.2011).
- PLĄTEK A. 1991. *Geodezyjne dalmierze elektromagnetyczne i tachometry elektroniczne*. Cz. I. *Geodezyjne dalmierze elektromagnetyczne do pomiarów terenowych*. PPL, Warszawa-Wrocław.
- PUDŁO M. 2006. *Z prędkością światła*. Geodeta, 6(133): 52–53.
- PUDŁO M. 2008. *Skanuj w 3D*. Geodeta, 4(155): 22–27.

-
- SANDERS F.H.. 2001. *3-D laser scanning helps Chevron revamp platform*. Oil & Gas Journal, April 30, p. 92–94.
- TOURNAS E., TSAKIRI M. 2008. *Deformation Monitoring Based on Terrestrial Laser Scanner Point Cloud Registration*. 13th FIG Symposium on Deformation Measurement and Analysis. LNEC Lisbon 2008, may 12–15.
- WONG K. 2009. *A Surveyor's Norman Conquest*. Hight-definition scanning helps document historic Nenagh Castle. Cadalyst, 14–17, on line: <http://www.cadalyst.com/cad/civil-engineering/a-surveyor039s-norman-conquest-tech-trends-feature-3782> (dostep: 10.03.2011).

TESTS OF SELECTED AUTOMATIC POSITIONING SYSTEMS IN POST-PROCESSING MODE

Jacek Rapiński, Sławomir Cellmer

Institute of Geodesy
University of Warmia and Mazury in Olsztyn

Key words: GPS, on-line processing.

Abstract

GPS data post-processing is time consuming and sometimes difficult task, that must be performed after each static survey. To obtain good coordinates, one must perform baseline processing and adjustment of GPS vectors. This requires both time and dedicated software. To speed up the process and save some money, surveyors may use automated, on-line GPS data processing systems. In this paper, authors compare results obtained from three automatic on-line GPS processing systems (Polish ASG-Eupos, Australian AUSPOS and American APPS) with respect to accuracy, availability and performance.

TESTOWANIE WYBRANYCH SERWISÓW AUTOMATYCZNEGO POZYCJONOWANIA W TRYBIE POSTPROCESSINGU

Jacek Rapiński, Sławomir Cellmer

Instytut Geodezji
Uniwersytet Warmińsko-Mazurski w Olsztynie

Słowa kluczowe: GPS, serwisy automatycznego opracowania obserwacji GPS.

Abstrakt

Opracowanie obserwacji GPS w precyzyjnym pozycjonowaniu jest zadaniem złożonym i czasochłonnym. Musi być przeprowadzone po każdym pomiarze statycznym. Uzyskanie poprawnych współrzędnych wyznaczonego punktu jest możliwe po wyznaczeniu składowych wektorów GPS i wyrównaniu sieci tych wektorów. Zadanie to jest czasochłonne i wymaga odpowiedniego oprogramowania. Aby zaoszczędzić czas i pieniądze, geodeci mogą skorzystać z bezpłatnych serwisów opracowania obserwacji GPS. W artykule autorzy porównują wyniki uzyskane z trzech internetowych serwisów automatycznego opracowania obserwacji GPS (polskiego ASG-EUPOS, australijskiego AUSPOS i amerykańskiego APPS) pod względem ich dokładności, dostępności i działania.

Introduction

There is a wide variety of on-line GPS processing systems available in internet (TSAKIRI 2008). Many of these are commercial, which means that one has to pay for the data processing or maintaining the account. Web search for “free + online + GPS + baseline + processing” gave three results – AUSPOS, JPL’s APPS and ASG-EUPOS. This paper describes all three.

During a various GPS surveys, we got into situation, when most widely used GPS online processing system ASGEUPOS failed to process some base-lines. This was usually caused by insufficient number of observations (too short observation session, obstructions etc.). We have decided to check if other systems that does not use ASG-EUPOS reference stations can provide sufficient accuracy for certain surveying tasks. The online GPS processing systems are gaining attention all over the world.

Listing those of major importance in Poland:

- ASG-EUPOS of GUGiK
- JPL’s APPS (AUTO-GIPSY) of NASA
- AUSPOS of the National Mapping Division of GeoScience Australia
- CSRS-PPP of Natural Resources Canada
- SCOUT of SOPAC

We have compared three of those that use different positioning strategies.

Short description of the systems

For the convenience, the description of each system was put into tables.

Table 1

AUSPOS

| Parameter | Description |
|------------------------------|---|
| Web adress | http://www.auslig.gov.au/geodesy/sgc/wwwgps/ |
| GNSS systems and frequencies | GPS L1/L2 (requires both frequencies) |
| Send/receive data protocols | www, ftp, e-mail |
| Reference frame | GDA94 for Australia, ITRF 2005 at current epoch for the rest of the world. |
| Owner | The Australian Surveying and Land Information Group |
| Registration required | no |
| “Under the hood” | MicroCosm |
| Working time | 24/7 |
| Nominal results quality | σhorizontal <10 mm and σvertical <20 mm with 6 hours of data |

Source: DAWSON et. al. (2001)

Table 2

APPS

| Parameter | Description |
|------------------------------|---|
| Web address | http://apps.gdgps.net/index.php |
| GNSS systems and frequencies | GPS L1/L2 (requires both frequencies) |
| Send/receive data protocols | www, ftp, e-mail |
| Reference frame | GDA94 for Australia, ITRF 2005 at current epoch for the rest of the world. |
| Owner | Jet Propulsion Laboratory (NASA, California Institute of Technology). |
| Registration required | no for basic usability / yes for advanced options |
| “Under the hood” | GIPSY-OASIS v.5 |
| Working time | 24/7 |
| Nominal results quality | 10 cm |

Source: ZUMBERGE (1998)

Table 3

ASG-EUPOS

| Parameter | Description |
|------------------------------|---|
| Web address | http://www.asgeupos.pl/ |
| GNSS systems and frequencies | GPS L1/L2 (requires both frequencies), GLONASS at some reference stations |
| Send/receive data protocols | www, e-mail |
| Reference frame | European ETRF89, Polish 2000, 1992 and 1965 |
| Owner | GUGiK (Polish government) |
| Registration required | yes |
| “Under the hood” | no data |
| Working time | 24/7 |
| Nominal results quality | 0.01 m – 0.10 m depending on survey conditions |

Source: BOSY et al. (2007)

Comparison of the algorithms used by each system

Since each service uses different positioning approach, we provide a brief description of each systems positioning algorithm.

JPL APPS

This service uses the PPP (precise point positioning) method (ZUMBERGE 1999). It uses precisely estimated satellite transmitter parameters, such as satellite position and clock. These parameters are obtained from organizations

such as NASA or IGS instantly. The method is well described in ZUMBERGE et al. (1997). In the processing the JPL final products were used.

AUSPOS

Auspos has a dual frequency geodetic GPS data processing capability. It uses double differenced phase observations positioning algorithm. Pseudo-range observations are used for receiver clocks only. The detailed description of the system can be found in (DAWSON et al. 2001). The system used the following nearby IGS GPS stations: bor1, joz2 and joze. The distance from the receiver to the reference stations were about 250 km.

ASG-EUPOS

Modern approach named BETA was used in polish system ASG-Eupos. It uses triple differenced phase observations with Schreiber differencing scheme (KADAJ, SWIETON 2009). As a control, standard double differenced solution is used. This algorithm is described in KADAJ, SWIETON (2009). The system used six reference stations (distances to each station in parentheses): GDAN (0.3 km), STRG (44 km), KOSC (50 km), WLAD (51 km), (ELBL 54 km), GRUD (97 km).

Baselines used in processing are depicted in Figure 1.

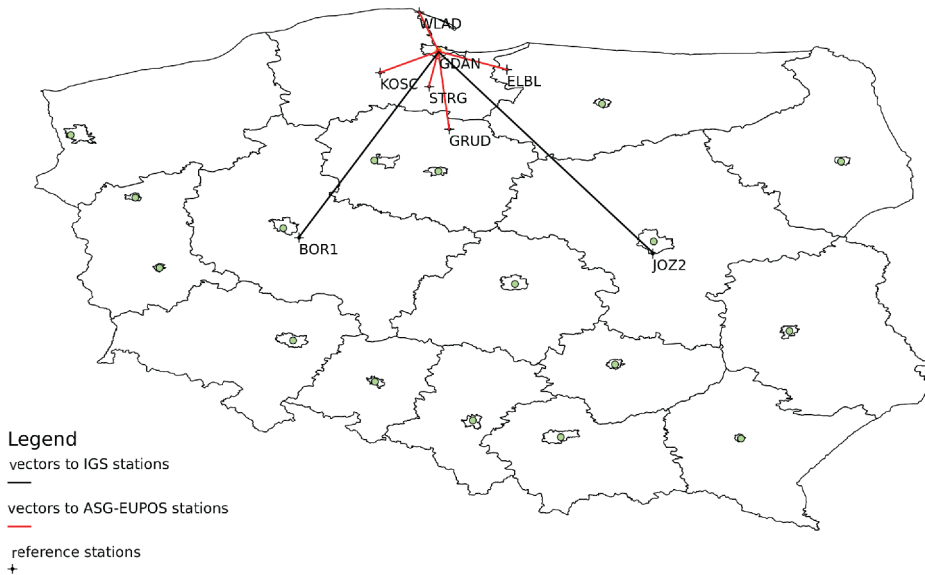


Fig. 1. ASG-EUPOS and IGS stations and the baselines analyzed in the experiment

Reference systems

AUSPOS returns coordinates in GDA94 reference frame for Australia and ITRF 2005 (current epoch) for the rest of the World, JPL's APPS works in ITRF 2005 (current epoch) and ASG-EUPOS works in ETRF89 (as it is a main system for Europe). For the purpose of comparison the coordinates must be transformed to one common reference system. Since all of the tests were performed in Poland we chose ETRF89. To obtain coordinates in ETRF89 all of the results from AUSPOS and JPL's APPS were transformed using the following scheme (NØRBECH et al. 2007):

1. Transformation from ITRF2005 epoch 2007.0 to ITRF2000 epoch 2007.0.
2. Apply the ITRF2000 Euler rotation velocities for Eurasia from epoch 2007.0 to epoch 1994.665.
3. Transformation from ITRF2000 epoch 1994.665 to ETRF2000.

Table 4
Transformation parameters at epoch 2000.0 and their rates from ITRF2005 to ITRF2000 (ITRF2000 minus ITRF2005)

| Parameters | T_1 | T_2 | T_3 | D | R_1 | R_2 | R_3 |
|-------------|-------|-------|-------|-----------|-------|-------|-------|
| Units | mm | mm | mm | 10^{-9} | mas | mas | mas |
| Parameters | 0.1 | -0.8 | -5.8 | 0.40 | 0.000 | 0.000 | 0.000 |
| Rates /year | -0.2 | 0.1 | -1.8 | 0.08 | 0.000 | 0.000 | 0.000 |

Source: <http://itrf.ensg.ign.fr/>

Table 5
Estimation of \dot{R}_{YY}

| YY | \dot{R}_1 | \dot{R}_2 | \dot{R}_3 |
|-------|-------------|-------------|-------------|
| Rates | mas/y | mas/y | mas/y |
| 94 | 0.20 | 0.50 | -0.65 |
| Rates | ± 0.021 | ± 0.008 | ± 0.026 |

Source: <http://itrf.ensg.ign.fr/>

Table 6
Transformation parameters and their rates from ITRF2000 to ETRF2000

| Parameters | T_1 | T_2 | T_3 | D | R_1 | R_2 | R_3 |
|------------|-------|-------|-------|-----------|-------|-------|--------|
| Units | mm | mm | mm | 10^{-9} | mas | mas | mas |
| Values | 54.1 | 50.2 | -53.8 | 0.40 | 0.891 | 5.390 | -8.712 |
| Rates/year | -0.2 | 0.1 | -1.8 | 0.08 | 0.081 | 0.490 | -0.792 |

Basic transformation formula is:

$$\begin{bmatrix} X \\ Y \\ Z \end{bmatrix}^{\text{sec ondary}} = \begin{bmatrix} X \\ Y \\ Z \end{bmatrix}^{\text{primary}} + \begin{bmatrix} T_1 \\ T_2 \\ T_3 \end{bmatrix} + \begin{bmatrix} D & -R_3 & R_2 \\ R_3 & D & -R_1 \\ -R_2 & R_1 & D \end{bmatrix} \cdot \begin{bmatrix} X \\ Y \\ Z \end{bmatrix}^{\text{primary}} \quad (1)$$

In the formula (1) each parameter for epoch EP:

$$P(t) = P(EP) + P \cdot (t - EP) \quad (2)$$

and Euler rotation formula:

$$\begin{bmatrix} X \\ Y \\ Z \end{bmatrix}^{\text{ITRF 2005}}_{2007} = \begin{bmatrix} X \\ Y \\ Z \end{bmatrix}^{\text{ITRF 2005}}_{t_c} + (t_c - 2007.0) \cdot \begin{bmatrix} 0 & -\dot{R}_3 & \dot{R}_2 \\ \dot{R}_3 & 0 & -\dot{R}_1 \\ -\dot{R}_2 & \dot{R}_1 & 0 \end{bmatrix} \cdot \begin{bmatrix} X \\ Y \\ Z \end{bmatrix}^{\text{ITRF 2005}}_{t_c} \quad (3)$$

In the above formulas T_1, T_2, T_3 are translation parameters, D is scale factor, R_1, R_2, R_3 are rotation parameters and $\dot{R}_1, \dot{R}_2, \dot{R}_3$ are rotation velocities. All of the required parameters were obtained from ITRF website (http://itrf.ensg.ign.fr/trans_para.php).

Tests

The test procedure was performed in the following steps for each system:

1. Split the data from 8 h session into 4, 2 and 1 h long sessions.
2. Uploading the data to the online system.
3. Receiving the results.
4. Transformation of the results to ETRF2000.
5. Comparison of the results to the results obtained from Bernese v5.0.

Three features were considered:

2. Availability
3. Performance
4. Accuracy

All of the services were available for all the test time. Since the speed of network connection depends on the distance from one computer to another, Australian page was slightly slower than American and European (trace route showed much more steps to connect to server). Time that was needed to receive the results is presented in Table 8.

Table 7

Waiting time

| System | Time [minutes] |
|------------|----------------|
| AUSPOS | 8 to 12 |
| JPL's APPS | 3 to 8 |
| ASG-EUPOS | 5 to 15 |

In order to test the performance and the accuracy, a sample of data was sent to each system. The test data consisted of 15 GPS data files in RINEX format. One eight hour long observation file was divided into 2, into 4 and into 8 files using teqc software. As a result 15 files were processed.

The survey conditions were good, there were not many obstacles and there was no problem with tracking satellites. Figure 2 depicts the satellite distribution during entire survey session.

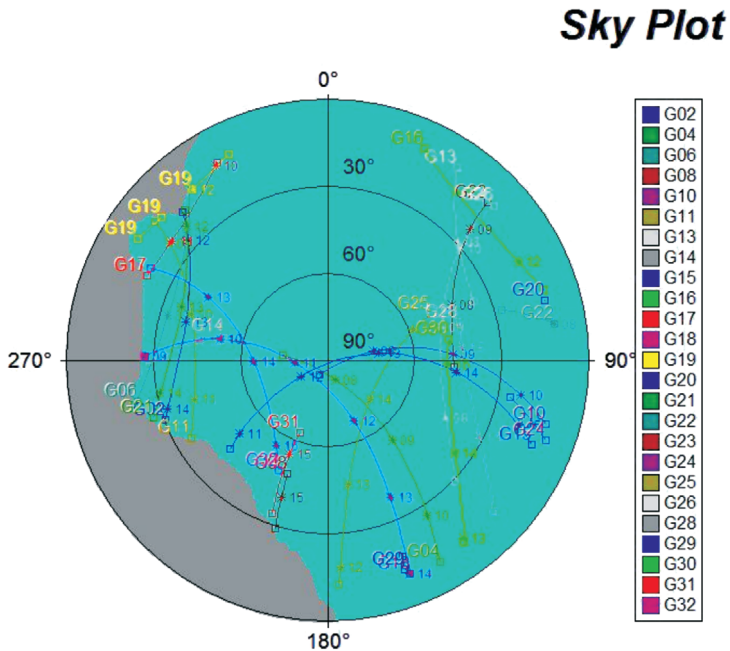


Fig. 2. Sky plot for 8h of observations

The Tables (8–10) below present which session was successfully processed by which system. Each cell in the table represents one session, the size of the cell represents its length. If the session was processed successfully the cell is

marked “fixed” if not “failed”. The case where system processed the data but the results were significantly different from good coordinates (more than 20 cm) is marked “float”.

Table 8

Processed sessions for AUSPOS

| | | | | | | | |
|-------------|-------------|-------------|-------------|-------------|-------------|--------------|--------------|
| 1 h (fixed) | 1 h (fixed) | 1 h (fixed) | 1 h (fixed) | 1 h (fixed) | 1 h (fixed) | 1 h (float) | 1 h (failed) |
| 2 h (fixed) | | 2 h (fixed) | | 2 h (fixed) | | 2 h (failed) | |
| 4 h (fixed) | | | | 4 h (fixed) | | | |
| 8 h (fixed) | | | | | | | |

Table 9

Processed sessions for JPL's APPS

| | | | | | | | |
|-------------|-------------|-------------|-------------|-------------|-------------|-------------|-------------|
| 1 h (fixed) | 1 h (fixed) | 1 h (fixed) | 1 h (fixed) | 1 h (fixed) | 1 h (fixed) | 1 h (fixed) | 1 h (fixed) |
| 2 h (fixed) | | 2 h (fixed) | | 2 h (fixed) | | 2 h (fixed) | |
| 4 h (fixed) | | | | 4 h (fixed) | | | |
| 8 h (fixed) | | | | | | | |

Table 10

Processed sessions for EUPOS

| | | | | | | | |
|--------------|--------------|--------------|--------------|--------------|--------------|--------------|--------------|
| 1 h (failed) | 1 h (failed) | 1 h (failed) | 1 h (failed) | 1 h (failed) | 1 h (failed) | 1 h (failed) | 1 h (failed) |
| 2 h (fixed) | | 2 h (fixed) | | 2 h (fixed) | | 2 h (fixed) | |
| 4 h (fixed) | | | | 4 h (fixed) | | | |
| 8 h (fixed) | | | | | | | |

JPL's APPS was able to process all of the data files with no outliers. AUSPOS failed in 2 sessions and results from one of the sessions were significantly different from the real coordinates.

Distribution of the satellites (Fig. 3 – DOP's) during last hour is also good – nothing indicates why last two sessions, calculated by two services, failed.

ASG EUPOS failed in all 8 one-hour sessions and in one two-hour session. Strict limitation of minimum 720 GPS observation epochs caused that all of the one hour long data was neglected by the system. Last two hour long session was not computed by two systems which may indicate worse satellite distribution in that time.

Sky Plot

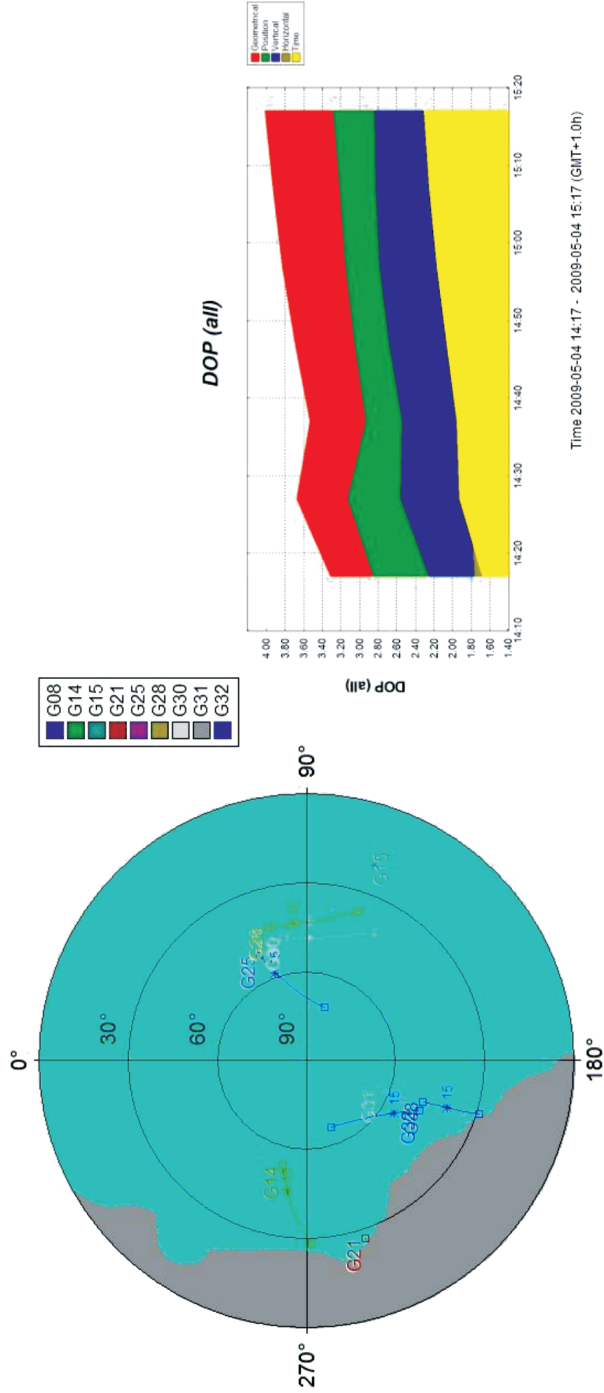


Fig. 3. Satellite distribution and DOP during last 1 hour session

Accuracy:

Coordinates calculated with Bernese v.5.0, from eight hour long session was considered to be “true” coordinates of the receiver. The differences in horizontal and vertical coordinates between “true” coordinates and results from each system are depicted in Figures 4 and 5. Table 11 presents standard deviations for each coordinate computed by these three systems.

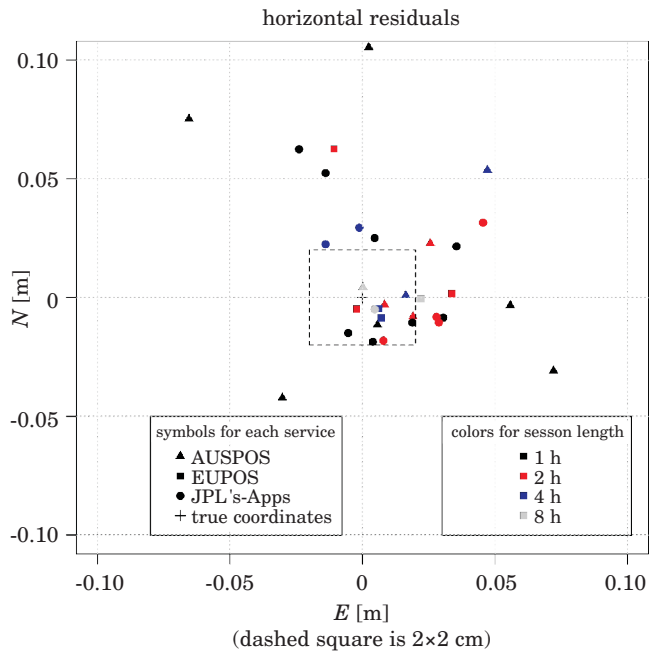


Fig. 4. Horizontal accuracy [in m]

Table 11

Standard deviations

| Session length | 1 h | | | 2 h | | | 4 h | | |
|--------------------|-------|-------|-------|-------|-------|-------|-------|-------|-------|
| Standard deviation | sd N | sd E | sd H | sd N | sd E | sd H | sd N | Sd E | sd H |
| Eupos | - | - | - | 0.003 | 0.015 | 0.014 | 0.074 | 0.018 | 0.022 |
| AUSPOS | 0.051 | 0.060 | 0.075 | 0.009 | 0.016 | 0.037 | 0.022 | 0.037 | 0.050 |
| JPL's APPS | 0.021 | 0.032 | 0.028 | 0.015 | 0.022 | 0.041 | 0.009 | 0.005 | 0.040 |

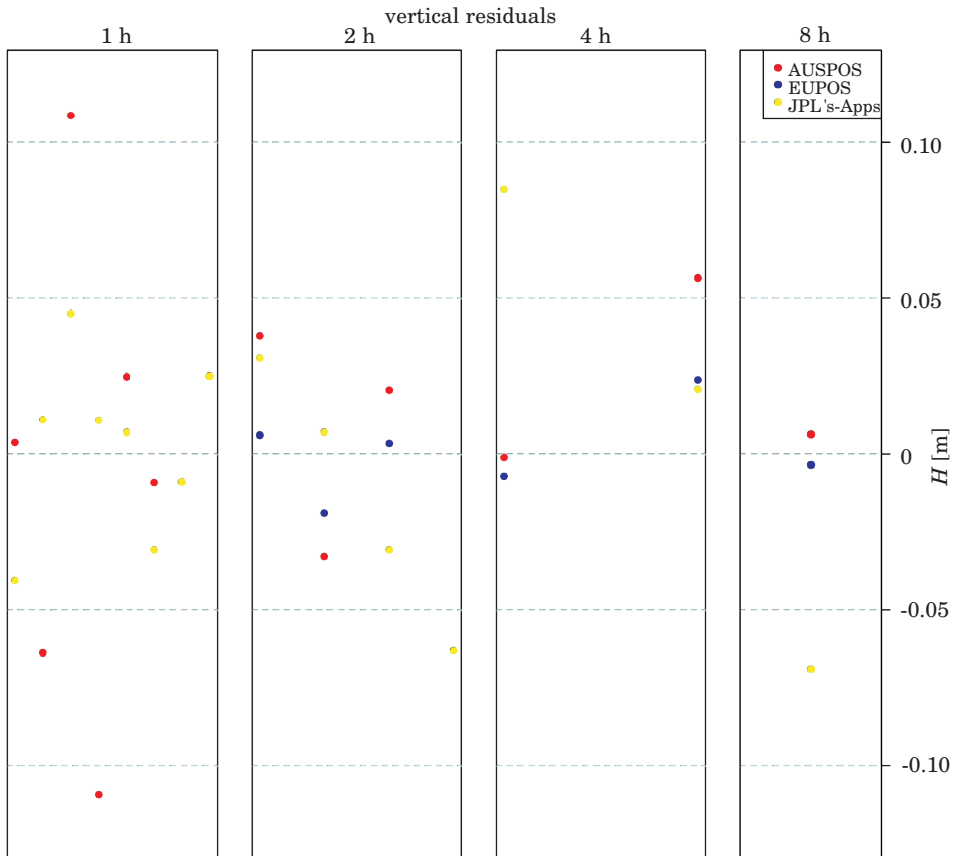


Fig. 5. Vertical accuracy [in m]

Conclusions

– ASG-EUPOS gave good accuracy using it's own reference stations. The main disadvantage is the necessity to provide long observation session (more than 720 epoch).

– JPL's APPS and AUSPOS give also good results using IGS reference stations. If for some reason survey sessions are shorter than 720 epochs, AUSPOS or JPL's APPS may be used, but in order to obtain results in ETRF89 the separate transformation procedure is necessary.

– Each of described systems may be used to process data from static GPS sessions. The resulting accuracy is in 10 cm level, which is satisfying for certain tasks.

References

- BOSY J., GRASZKA W., LEONCZYK M. 2007. *ASG-EUPOS – A Multifunctional Precise Satellite System in Poland*. European Journal of Navigation, 5(4): 2–6.
- DAWSON J., GOVIND R., MANNING J. 2001. *The AUSLIG on-line GPS processing system (AUSPOS)*. Proceedings of Satnav2001, Canberra, July.
- KADAJ R., ŚWIETON T. 2009. *Algorithm and software of automatic postprocessing module (apps) in polish precise satellite positioning system ASG-EUPOS*. Zeszyty Naukowe Politechniki Rzeszowskiej. Budownictwo i Inżynieria Środowiska, 51(262): 37.
- KRISTIANSEN O., HARSSON B.G. 1998. *The New Norwegian National Geodetic Network EUREF 89*. In: *Proceedings of the General Assembly of the Nordic Geodetic Commission*, Ed. B. Jonsson. LMV-rapport 1999.12: 162–195.
- NØRBECH T., KIERULF H. 2007. *An Approximate Transformation from ITRF2005 Current Epoch to EUREF89*. geoforum.no. 2007. http://www.geoforum.no/kurs-og-konferanser/publiserte-foredrag/2007/foredrag-fra-geodesi-og-hydrografidagene/norbech-transform_itrf2005_euref89-artikkel.pdf (Available 8 July 2010).
- TSAKIRI M. 2008. *GPS Processing Using Online Services*. Journal of Surveying Engineering, 134(4): 115–125.
- ZUMBERGE J.F., HEIN M.B., JEFFERSON D.C., WATKINS M.M., WEBB F.H. 1997. *Precise Point Positioning for the Efficient and Robust Analysis of GPS Data from Large Networks*. Journal of Geophysical Research, 102(B3): 5005.
- ZUMBERGE J.F. 1999. *Automated GPS Data Analysis Service*. GPS Solutions, 2(3): 76–78.

**STABILITY OF OPTIMAL PARAMETERS
FOR CLASSIFIER BASED ON SIMPLE GRANULES
OF KNOWLEDGE**

Piotr Artiemjew

Chair of Mathematical Methods in Computer Sciences
University of Warmia and Mazury in Olsztyn

Key words: rough sets, rough inclusions, granules of knowledge, classification of data, missing values, stability of optimal parameters.

A b s t r a c t

Searching for optimal parameters of a classifier based on simple granules of knowledge investigated recently by the author (ARTIEMJEW 2010) raises a question about stability of optimal parameters. In this article, we will check dependence of stability of the optimal radius of granulation on random damage of decision system. The results of experiments show the dependence of stability on size of damage and strategies of treating missing values. This kind of research aims at finding methods of protecting decision systems which are vulnerable to damage against decreasing their classification effectiveness, which means preserving classifying possibilities similar to undamaged decision systems.

**BADANIE STABILNOŚCI OPTYMALNYCH PARAMETRÓW KLASYFIKATORA
BAZUJĄCEGO NA PROSTYCH GRANULACH WIEDZY**

Piotr Artiemjew

Katedra Metod Matematycznych Informatyki
Uniwersytet Warmińsko-Mazurski w Olsztynie

Słowa kluczowe: zbiory przybliżone, inkluzje przybliżone, granule wiedzy, klasyfikacja danych, uszkodzenia systemu decyzyjnego, stabilność optymalnych parametrów.

A b s t r a c t

Przeprowadzone w ostatnim czasie badania (ARTIEMJEW 2010) zmierzające do wyszukiwania optymalnych parametrów klasyfikacji modułów decyzyjnych opartych na prostych granulach wiedzy zrodziły pytanie o stabilność optymalnych parametrów klasyfikacji. W pracy sprawdzono zależność stabilności optymalnych promieni granulacji od losowego uszkodzania systemu decyzyjnego. Wyniki badań wskazały jednoznacznie, że istnieje zależność między stabilnością a wielkością uszkodzenia

i strategiami traktowania wartości uszkodzonych. Tego typu badania mają na celu szukanie metod zabezpieczania systemów decyzyjnych, które są podatne na uszkodzenia, przed zmniejszeniem ich efektywności klasyfikacyjnej. Celem było zachowanie możliwości klasyfikacyjnych zbliżonych do efektywności nieuszkodzonych systemów decyzyjnych.

Introduction

Knowledge is understood here as ability to classify and as far as real phenomena are considered, the frame is that of information systems each of which is a pair $I = (U, A)$ where U is a set of objects, entities, and A is a set of attributes; decision system is a triple $DS = (U, A, d)$, where $d \notin A$. The basic form of granulation in decision and information systems consists in partitioning U into classes of the indiscernibility relation $IND(A)$ defined as $IND(A) = \{(u, v) : a(u) = a(v), \forall a \in A\}$. Each class $[u]_A = \{v \in U : IND_A(u, v)\}$ is interpreted as a elementary granule and unions of elementary granules are granules of knowledge. Another approach to granulation, proposed by (POLKOWSKI 2008), consists in using rough inclusions, cf. (POLKOWSKI 2008).

A rough inclusion is a relation $\mu \subseteq U \times U \times [0,1]$ which can be regarded as graded similarity relation extending the indiscernibility relation by relaxing restrictions on attribute values. We let $IND(u, v) = \{a \in A : a(u) = a(v)\}$.

In our approach we use rough inclusion proposed by (POLKOWSKI 2008), to classify test objects. Test object is classified by granules, which have been formed from training set as follows,

$$g_{r_{\text{gran}}}(u) = \{v \in U : \frac{|IND(u, v)|}{|A|} \geq r_{\text{gran}}\}$$

where $r_{\text{gran}} \in [0,1]$ is the granulation radius.

The most numerous decision class transfers decision to our testing object. If tie occurs, it is resolved by a random choice. This type of classification is the simplest among studied by the author cf. (ARTIEMJEW 2008, 2009, POLKOWSKI, ARTIEMJEW 2007). The results of research for optimal parameters for this method is available in (ARTIEMJEW 2010). In this work we continue this approach and our main purpose is to find the threshold of the optimal parameter stability for the random damage of the decision system.

In the work (ARTIEMJEW 2010) we have proposed a method for experimental detecting of the optimal radius value for a given data set, by means of multiple CV-5 and subsequent confirmation by means of Leave One Out method. Once the optimal value is found for the test data, it can be used for classifying incoming objects without any need for full granulation procedure. For the multiple damage of the decision system in fixed percentage, the

stability of optimal parameter is checked by Leave One Out Method. Optimal radius of classification is stable if despite the damage of the decision system it is still the same and fulfills the criterion of optimality, which is a maximal value of accuracy within coverage in the range of $[0.9, 1.0]$.

Classification by simple granules of knowledge theoretical background

Rough inclusion generally is a predicate of the form $\mu_\pi(x, y, r)$, where x, y are individual objects, $r \in [0,1]$, which satisfies the following requirements, relative to a given part relation π on a set U of individual objects, see (POLKOWSKI 2008),

- 1) $\mu_\pi(x, y, 1) \Leftrightarrow \text{ing}_\pi(x, y)$;
- 2) $\mu_\pi(x, y, 1) \Rightarrow [\mu_\pi(z, x, r) \Rightarrow \mu_\pi(z, y, r)]$
- 3) $\mu_\pi(x, y, r) \wedge s < r \Rightarrow \mu_\pi(x, y, s)$

Those requirements seem to be intuitively clear. 1) demands that the predicate μ_π is an extension to the relation ing_π of the underlying system of Mereology; 2) does express monotonicity of μ_π , and 3. assures the reading. “to degree at least r ”. We use here only one rough inclusion, albeit a fundamental one, viz., (POLKOWSKI 2008) for its derivation,

$$\mu_L(u, v, r) \Leftrightarrow \frac{|\text{IND}(u, v)|}{|A|} \geq r.$$

A granule $g_\mu(u, r)$ about $u \in U$ of the radius r , relative to μ , is defined by letting,

$$g_\mu(u, r) \text{ is ClsF}(u, r),$$

where the property $\text{F}(u, r)$ is satisfied with an object v if and only if $\mu(v, u, r)$ holds, and Cls is the class operator, see, e.g., (POLKOWSKI 2008). Practically, in case of μ_L the granule $g(u, r)$ collects all $v \in U$ such that $|\text{IND}(v, u)| \geq r \cdot |A|$.

Error evaluation

Classifiers are evaluated by error which is the ratio of the number of correctly classified objects to the number of recognized test objects (called also total accuracy) and total coverage, $\frac{\text{rec}}{\text{test}}$, where rec is the number of recognized test cases and test is the number of test cases.

The results by Leave One Out method should be modified. We build for Leave One Out method the confusion matrix, where testing objects from all

folds are treated as one test decision system, and we compute accuracy as percentage of correctly classified testing objects. Coverage is a percent of objects which have been classified. The motivation to use Leave One Out method is to be found, among other places in (MOLINARO, SIMON, PFEIFFER 2005). This paper proves the effectiveness and almost unbiased character of this method.

Voting by granules on decision values

Given a granule $g = g_{r_{\text{gran}}}(u)$ of test objects u in a training decision system (U_{trn}, A, d) , for each test object u , the value of decision assigned to u by the granule g is defined as, $d(u) = d'$ such that, for D as the set of granule's $g_{r_{\text{gran}}}(u)$ decision classes,

$$d' = \{d'' \in D : \max |\{v \in g_{r_{\text{gran}}}(u) : d(v) = d''\}|\}$$

in case of tie, random choice is applied.

The procedure of classification by means of Standard Granules (CSG algorithm)

1. The training decision system (U_{trn}, A, d) and the test system (U_{tst}, A, d) has been input, where $U_{\text{tst}}, U_{\text{trn}}$ is respectively universe of test and training objects, A is a set of attributes and d is a decision reflecting a partition of objects into classes.

2. The granular radius $r_{\text{gran}} \in \{\frac{0}{\text{card}\{A\}}, \frac{1}{\text{card}\{A\}}, \dots, \frac{\text{card}\{A\}}{\text{card}\{A\}}\}$ has been chosen.

3. For classified test object $u \in U_{\text{tst}}$, the classification granule $g_{r_{\text{gran}}}(u)$ has been found in the training set U_{trn} as follows, $g_{r_{\text{gran}}}(u) = \{v \in U_{\text{trn}} : \frac{|\text{IND}(u,v)|}{|A|} \geq r_{\text{gran}}\}$, where $r_{\text{gran}} \in [0,1]$.

4. The most numerous decision class of granule $g_{r_{\text{gran}}}(u)$ transfers decision to our test object. If tie occurs, it is resolved randomly.

Empirical method of checking the stability of the optimal parameters

By the x percent damage of the decision system (U, A, d) , we mean that we insert a number of $x\% * |A| * |U|$ random stars inside the system. Credit Approval (UCI Repository) contains a little bit of original missing values

marked as "?", but it doesn't matter for us, because we treat these missing values as additional descriptors. Only artificial damage created by stars is considered as missing values. As we can see in Figure 1, the stability of optimal parameter is checked by five times random damage of the original decision system and classified by the leave one out method, where finally we obtain an average result. Radius is stable when in spite of the damage is the same as original decision system optimal radius.

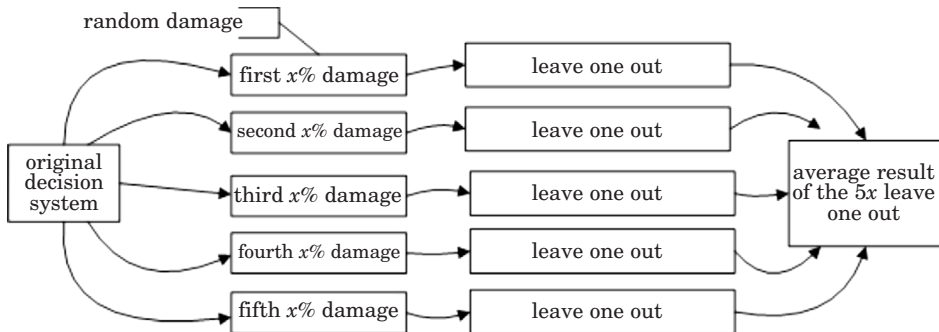


Fig. 1. Stability checking method of the optimal radius for the classifier based on simple granules of knowledge (CSG)

Methods for treating missing values

During the classification of the damaged decision system by simple granules of knowledge we are considering two ways of treating missing values. The first one is „*=*” and the second one is strategy „*=don't care”. For both strategies we are using the same damaged decision systems. For instance for Credit Approval (UCI Repository) decision system we are damaging $x\% \cdot 15 \cdot 690$ descriptors. Details of percentage damaged for the considered decision system are shown in Table 1.

Table 1
Detailed information regarding the percentage damage of Credit Approval (UCI Repository); Damper = Percentage damage of decision system, Starnum = Number of stars in damaged decision system

| Damper [%] | Starnum | Damper [%] | Starnum | Damper [%] | Starnum |
|------------|---------|------------|---------|------------|---------|
| 1 | 103 | 6 | 621 | 15 | 1552 |
| 2 | 207 | 7 | 724 | 20 | 2070 |
| 3 | 310 | 8 | 828 | 25 | 2587 |
| 4 | 414 | 9 | 931 | 30 | 3105 |
| 5 | 517 | 10 | 1035 | | |

Results of experiments for the strategy „* = *”

Results for Credit Approval at percentage damage from interval [1% to 10%]

At first we would like to show results in details for the first one-percentage-damage, see Table 2. Short description for all 1 percentage damage and average result we can see in Table 3 and finally, in Figure 2 we can see visualization of error for all 1 percentage damage. The results for damages from interval 2% to 10% will be shown in the short form only, see Table 4 and 5.

Table 2
 „* = *”; Leave One Out; First 1% damage; Credit Approval (UCI Repository); Classification by means of standard granules (CSG); r_{gran} = Granulation radius, T_{acc} = Total accuracy, T_{cov} = Total coverage, M_{gran} = The mean percentage size of classification granule in training system; The best results for:
 $r_{\text{gran}} = 0.6$, $T_{\text{acc}} = 0.846497$, $T_{\text{cov}} = 0.972464$, $M_{\text{gran}} = 24.3942$

| r_{gran} | T_{acc} | T_{cov} | M_{gran} |
|-------------------|------------------|------------------|-------------------|
| 0 | 0.555072 | 1 | 689 |
| 0.0666667 | 0.555072 | 1 | 687.104 |
| 0.1333333 | 0.555072 | 1 | 673.4 |
| 0.2 | 0.573913 | 1 | 633.51 |
| 0.266667 | 0.750725 | 1 | 559.814 |
| 0.3333333 | 0.826087 | 1 | 442.325 |
| 0.4 | 0.824638 | 1 | 296.896 |
| 0.466667 | 0.833091 | 0.998551 | 165.516 |
| 0.5333333 | 0.836972 | 0.995652 | 73.2928 |
| 0.6 | 0.846497 | 0.972464 | 24.3942 |
| 0.666667 | 0.837113 | 0.702899 | 5.53623 |
| 0.7333333 | 0.838093 | 0.304348 | 0.802899 |
| 0.8 | 0.8333333 | 0.0695652 | 0.110145 |
| 0.866667 | 0.750001 | 0.0173913 | 0.0376812 |
| 0.9333333 | 0.799999 | 0.00724638 | 0.0115942 |
| 1 | 0 | 0 | 0 |

Table 3
 „* = *”; Leave One Out; All results for 1% of the damage; Credit Approval (UCI Repository);
 Classification by means of standard granules (CSG); Optimal r_{gran} = Optimal granulation radius, T_{acc}
 = Total accuracy, T_{cov} = Total coverage, M_{gran} = The mean size of classification granule in training
 system, M_{trn} = Mean training table size

| | Optimal r_{gran} | T_{acc} | T_{cov} | M_{gran} | $\frac{M_{gran}}{M_{trn}} \cdot 100\%$ [%] |
|------------------|--------------------|-----------|-----------|------------|---|
| nil | 0.6 | 0.860327 | 0.975362 | 26.7913 | 3.89 |
| First 1% damage | 0.6 | 0.846497 | 0.972464 | 24.3942 | 3.54 |
| Second 1% damage | 0.6 | 0.856049 | 0.946377 | 23.8667 | 3.46 |
| Third 1% damage | 0.6 | 0.854572 | 0.966667 | 23.7594 | 3.45 |
| Fourth 1% damage | 0.6 | 0.861862 | 0.965217 | 23.7275 | 3.44 |
| Fifth 1% damage | 0.6 | 0.857576 | 0.956522 | 23.7768 | 3.45 |
| Average result | 0.6 | 0.855312 | 0.96145 | 23.905 | 3.47 |

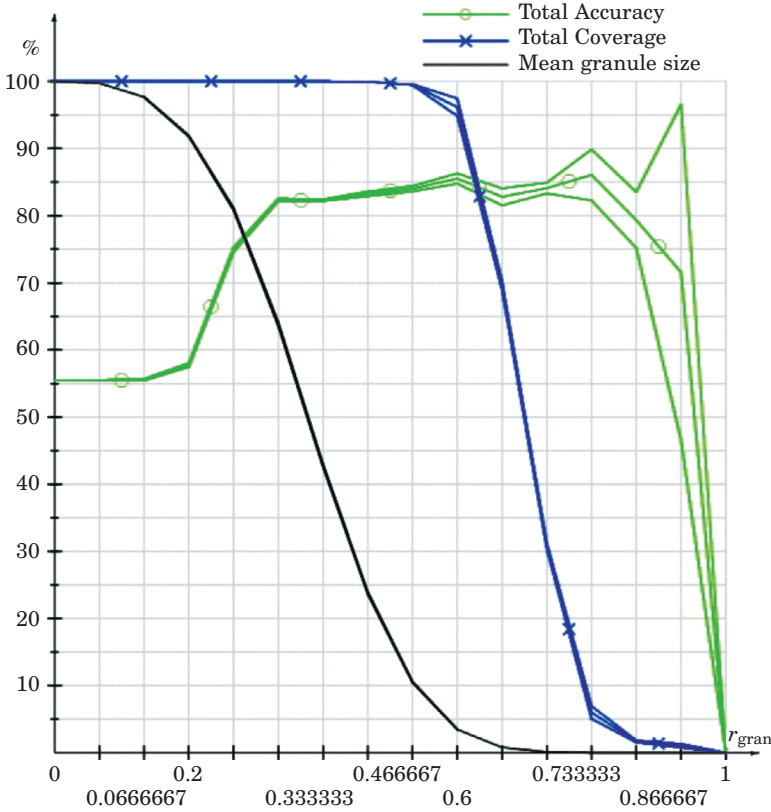


Fig. 2. „* = *”; Leave One Out; Average results of experiments and error visualization for all 1% of the damage; $\frac{(\max - \min)}{2}$; Credit Approval (UCI Repository); Classification by means of standard granules (CSG); r_{gran} = Granulation radius, T_{acc} = Total accuracy, T_{cov} = Total coverage, M_{gran} = The mean percentage size of classification granule in training system; The best results for: $r_{gran} = 0.6$, $T_{acc} = 0.855312$, $T_{cov} = 0.96145$, $M_{gran} = 23.905$

Table 4
 „* = *”; Leave One Out; Average results for all damage; Credit Approval (UCI Repository); Classification by means of standard granules (CSG); Damper = Percentage damage of decision system, $\text{Optimal}r_{\text{gran}}$ = Optimal granulation radius, T_{acc} = Total accuracy, T_{cov} = Total coverage, M_{gran} = The mean size of classification granule in training system, M_{trn} = Mean training table size

| Damper [%] | $\text{Optimal}r_{\text{gran}}$ | T_{acc} | T_{cov} | M_{gran} | $\frac{M_{\text{gran}}}{M_{\text{trn}}} \cdot 100\%$ [%] |
|------------|---------------------------------|------------------|------------------|-------------------|--|
| nil | 0.6 | 0.860327 | 0.975362 | 26.7913 | 3.89 |
| 1 | 0.6 | 0.855312 | 0.96145 | 23.905 | 3.47 |
| 2 | 0.6 | 0.850606 | 0.935074 | 20.5066 | 2.98 |
| 3 | 0.6 | 0.85161 | 0.92174 | 17.607 | 2.56 |
| 4 | 0.533333 | 0.84138 | 0.990436 | 52.3532 | 7.6 |
| 5 | 0.533333 | 0.844274 | 0.984638 | 46.987 | 6.82 |
| 6 | 0.533333 | 0.837318 | 0.98348 | 43.0766 | 6.25 |
| 7 | 0.533333 | 0.83784 | 0.975942 | 39.0534 | 5.67 |
| 8 | 0.533333 | 0.835582 | 0.973044 | 35.5524 | 5.16 |
| 9 | 0.533333 | 0.833924 | 0.97565 | 31.2922 | 4.54 |
| 10 | 0.466667 | 0.834204 | 0.99826 | 81.524 | 11.83 |

Table 5
 „* = *”; Leave One Out; Table of errors' percentage for all damage; $\frac{(\max - \min.)}{2}$; Credit Approval (UCI Repository); Classification by means of standard granules (CSG); Damper = Percentage damage of decision system, $\text{Optimal}r_{\text{gran}}$ = Optimal granulation radius, T_{acc} = Total accuracy, T_{cov} = Total coverage, M_{gran} = The mean size of classification granule in training system

| Damper [%] | $\text{Optimal}r_{\text{gran}}$ | T_{acc} [%] | T_{cov} [%] | M_{gran} [%] |
|------------|---------------------------------|----------------------|----------------------|-----------------------|
| 1 | 0.6 | 0.76 | (+)-1.3 | (+)-0.0483 |
| 2 | 0.6 | (+)-0.54 | (+)-0.94 | (+)-0.0538 |
| 3 | 0.6 | (+)-1.48 | (+)-0.79 | (+)-0.0961 |
| 4 | 0.533333 | (+)-0.69 | (+)-0.43 | (+)-0.2614 |
| 5 | 0.533333 | (+)-1.08 | (+)-0.43 | (+)-0.1962 |
| 6 | 0.533333 | (+)-0.67 | (+)-0.57 | (+)-0.2711 |
| 7 | 0.533333 | (+)-1.61 | (+)-0.65 | (+)-0.2097 |
| 8 | 0.533333 | (+)-1.15 | (+)-0.5 | (+)-0.2908 |
| 9 | 0.533333 | (+)-1.15 | (+)-0.28 | (+)-0.1079 |
| 10 | 0.466667 | (+)-0.73 | (+)-0.07 | (+)-0.3075 |

Additional result for Wisconsin Diagnostic Breast Cancer data set

In Table 6 additional results obtained from classification by means of simple granular structures, for the damage in range 1 to 7% are collected.

Table 6
„* = *”; Leave One Out; Average results for all damage; Wisconsin Diagnostic Breast Cancer (UCI Repository); Classification by means of standard granules (CSG); Damper = Percentage damage of decision system, $\text{Optimal}.r_{\text{gran}}$ = Optimal granulation radius, T_{acc} = Total accuracy, T_{cov} = Total coverage, M_{gran} = The mean size of classification granule in training system, M_{trn} = Mean training table size

| Damper [%] | $\text{Optimal}.r_{\text{gran}}$ | T_{acc} | T_{cov} | M_{gran} | $\frac{M_{\text{gran}}}{M_{\text{trn}}} \cdot 100\%$ [%] |
|------------|----------------------------------|------------------|------------------|-------------------|--|
| nil | 0.258065 | 0.870722 | 0.924429 | 33.7047 | 5.93 |
| 1 | 0.258065 | 0.874908 | 0.921616 | 30.8408 | 5.43 |
| 2 | 0.258065 | 0.875358 | 0.907908 | 28.6496 | 5.04 |
| 3 | 0.258065 | 0.879718 | 0.908964 | 26.168 | 4.61 |
| 4 | 0.258065 | 0.877342 | 0.902638 | 23.6408 | 4.16 |
| 5 | 0.258065 | 0.873384 | 0.902286 | 22.9652 | 3.9 |
| 6 | 0.258065 | 0.87183 | 0.902284 | 21.084 | 3.58 |
| 7 | 0.225806 | 0.855392 | 0.96485 | 46.9272 | 7.97 |

A summary for the strategy „* = *”

At the fixed optimality condition: $\text{Optimal}.r_{\text{gran}} = \{r_{\text{gran}} : \text{for maximal accuracy at coverage} \in [0.9, 1.0]\}$, within „* = *” strategy for Credit Approval (UCI Repository) the optimality of the radius during classification is stable for damages of 1, 2, 3%. Above three percent, beginning from 4% coverage for radius $r_{\text{gran}} = 0.6$ is becoming smaller than 0.9, hence, in spite of maximal accuracy, our radius ceases being optimal. For damages of 4–7% accuracy is still maximal for radius 0.6, but coverage $\in [0.8; 0.9]$. Starting from 8% to 10%, the best accuracy is for radius 0.533333. For 10% damage at $r_{\text{gran}} = 0.6$ coverage $\in [0.7, 0.8]$. Finally when we are applying the strategy „* = *” during the classification CSG, stability of the optimum is low and is kept for 1, 2 and 3% damage. However, the level of accuracy is high for this damage. Classification error resulting from randomization of damage is following. for 1–3% damage $T_{\text{acc.error}} \in [0.54\%, 1.48\%]$, $T_{\text{cov.error}} \in [0.79\%, 1.3\%]$, for 4–7% damage $T_{\text{acc.error}} \in [0.88\%, 1.29\%]$, $T_{\text{cov.error}} \in [0.86\%, 1.52\%]$ and finally for 8–10% damage $T_{\text{acc.error}} \in [1.21\%, 1.45\%]$, $T_{\text{cov.error}} \in [0.79\%, 2.17\%]$. Result shows that

there is no bigger dependency between the classification error resulting from randomization and the percentage of damage.

Preserving the radius' optimality is dependent on the classification granule size. The bigger the damage is, the coverage and M_{gran} for originally optimal radius becomes smaller. The optimum is moving to the direction of the radius 0.533333 for which classification granules have similar size to classification granules of the originally optimal radius. It is possible to predict that the optimum with the increase of the damage will fall down. The additional result for Wisconsin Diagnostic Breast Cancer (UCI Repository) see Table 6 confirm this hypothesis.

Results for the strategy „*=don't care”

Results for Credit Approval at percentage damage from interval [1 to 10%] and 15, 20, 25, 30%

The results for damages from interval 1 to 10% and 15, 20, 25, 30% will be shown in the short form only, see Table 7.

Table 7
„*=don't care”; Leave One Out; Average results for all damage; Credit Approval (UCI Repository); Classification by means of standard granules (CSG); Damper = Percentage damage of decision system, $\text{Optimal}.r_{\text{gran}}$ = Optimal granulation radius, T_{acc} = Total accuracy, T_{cov} = Total coverage, M_{gran} = The mean size of classification granule in training system, M_{trn} = Mean training table size

| Damper [%] | Optimal. r_{gran} | T_{acc} | T_{cov} | M_{gran} | $\frac{M_{\text{gran}}}{M_{\text{trn}}} \cdot 100\%$ [%] |
|------------|----------------------------|------------------|------------------|-------------------|--|
| nil | 0.6 | 0.860327 | 0.975362 | 26.7913 | 3.89 |
| 1 | 0.6 | 0.854102 | 0.977392 | 29.2134 | 4.24 |
| 2 | 0.6 | 0.843688 | 0.975362 | 30.5474 | 4.43 |
| 3 | 0.6 | 0.84391 | 0.97855 | 32.446 | 4.71 |
| 4 | 0.6 | 0.843138 | 0.98319 | 35.3892 | 5.14 |
| 5 | 0.6 | 0.84488 | 0.9829 | 36.4368 | 5.29 |
| 6 | 0.6 | 0.837492 | 0.988116 | 40.021 | 5.81 |
| 7 | 0.533333 | 0.836474 | 0.99971 | 109.477 | 15.89 |
| 8 | 0.6 | 0.834058 | 0.993912 | 45.1226 | 6.55 |
| 9 | 0.6 | 0.833386 | 0.993332 | 45.9836 | 6.67 |
| 10 | 0.533333 | 0.827828 | 1 | 121.15 | 17.58 |
| 15 | 0.6 | 0.822166 | 0.99913 | 67.351 | 9.78 |
| 20 | 0.6 | 0.807246 | 1 | 91.8064 | 13.3 |
| 25 | 0.533333 | 0.797104 | 1 | 234.658 | 34.06 |
| 30 | 0.666667 | 0.794494 | 1 | 70.849 | 10.28 |

Additional result for Wisconsin Diagnostic Breast Cancer data set

We include in Table 8 additional results obtained from classification by means of simple granular structures, for the damage in range 1 to 5%.

A summary for the strategy „*=don't care”

In considered strategy for Credit Approval (UCI Repository) stability of optimal radius is higher than in strategy „*=*”. Optimal radius is preserved for 1–6% damage. Granules are being extended in this strategy and at the moment when they have too large noise inside the optimum is being lost. Starting from 7% damage, optimal radius is instable and reaches values 0.6 or 0.533333. At this method at the increase of damage, the coverage is growing to 1 because of the classifying granules' extension. The optimum is moving to the direction of radius 0.666667.

It is possible to expect that the optimal radius with the increase of the damage will move up. The additional result for Wisconsin Diagnostic Breast Cancer (UCI Repository) see Table 8 confirm this hypothesis.

Table 8
„*=don't care”; Leave One Out; Average results for all damage; Wisconsin Diagnostic Breast Cancer (UCI REPOSITORY); Classification by means of standard granules (CSG); Damper = Percentage damage of decision system, $Optimal.r_{gran}$ = Optimal granulation radius, T_{acc} = Total accuracy, T_{cov} = Total coverage, M_{gran} = The mean size of classification granule in training system, M_{trn} = Mean training table size

| Damper [%] | $Optimal.r_{gran}$ | T_{acc} | T_{cov} | M_{gran} | $\frac{M_{gran}}{M_{trn}} \cdot 100\%$ [%] |
|------------|--------------------|-----------|-----------|------------|--|
| nil | 0.258065 | 0.870722 | 0.924429 | 33.7047 | 5.93 |
| 1 | 0.258065 | 0.862936 | 0.956766 | 41.5476 | 7.31 |
| 2 | 0.290323 | 0.869142 | 0.919506 | 23.9922 | 4.22 |
| 3 | 0.290323 | 0.837724 | 0.9529 | 29.8426 | 5.25 |
| 4 | 0.322581 | 0.844062 | 0.914938 | 15.7237 | 2.77 |
| 5 | 0.322581 | 0.79595 | 0.939192 | 20.22 | 3.43% |

Conclusions

It follows from experiments that for small damage of decision system in the range of few percent, optimal parameters for the classifier basing on simple granules of knowledge maintain optimality. Range of the optimality is depend-

ent on the strategy of treating missing values during classification and the decision system structure. For the exemplary Credit Approval (UCI Repository) system at the damage interval from 1 to 6% and strategy of treating missing values „*=don't care”, the decision system still contains the same optimal parameter. For the strategy „*=*” stability is saved only for 1 to 3% damage, but in this case we have obtained better accuracy of classification than in strategy „*=don't care”. For Wisconsin Diagnostic Breast Cancer (UCI Repository) at strategy „*=don't care” optimal radius is saved only for 1% damage and for the strategy „*=*” optimum is preserved for damage from interval 1 to 6%. Generally we can say that at „*=*” strategy optimal radius with the increase of the damage will move down and for „*=don't care” strategy it will move up. Finally the optimum of CSG is more stable for the strategy „*=*”.

From the engineering point of view, obtaining an answer to the question of how to preserve stable level of classification in the case of real software and hardware discrete decision systems is really important, particularly if these decision systems are susceptible to noise and to damage conditional information. Thanks to such knowledge it is possible to design decision modules which are damage-resistant and are automatically adaptable to new conditions. In the future work, we will check the relation between the amount of information and stability of optimal parameters of classification based on simple granules of knowledge.

Acknowledgements

The research has been supported by grant 1309-802 from Ministry of Science and Higher Education of the Republic of Poland.

Translated by EWA SIENKIEWICZ

Accepted for print 22.03.2011

References

- ARTIEMJEW P. 2009. *On strategies of knowledge granulation and applications to decision systems*. PhD Dissertation, Polish Japanese institute of Information Technology, L. Polkowski, Supervisor, Warsaw.
- ARTIEMJEW P. 2008. *Natural versus granular computing. Classifiers from granular structures*. Proceedings of 6th International Conference on Rough Sets and Current Trends in Computing RSCTC'08, Akron, Ohio, USA, vol. 5306, Springer Berlin / Heidelberg, pp. 150–159.
- ARTIEMJEW P. 2010. *In search of optimal parameters for classifier based on simple granules of knowledge*. III International Interdisciplinary Technical Conference of Young Scientists (Inter-Tech 2010), 3: 138–142, Poznan University Press.

-
- POLKOWSKI L. 2008. *A Unified Approach to Granulation of Knowledge and Granular Computing Based on Rough Mereology. A Survey*. In.: *Handbook of Granular Computing*. Eds. W. Pedrycz, A. Skowron, V. Kreinovich. John Wiley & Sons, New York, pp. 375–401.
- POLKOWSKI L., ARTIEMJEV P. 2008. *Rough mereology in classification of data. Voting by means of residual rough inclusions*. Proceedings of 6th International Conference on Rough Sets and Current Trends in Computing RSCTC'08, Akron, Ohio, USA.
- POLKOWSKI L., ARTIEMJEV P. 2007. *On granular rough computing. Factoring classifiers through granular structures*. In: *Rough Sets and Intelligent Systems Paradigms, International Conference, RSEISP*. Eds. M. Kryszkiewicz, J.F. Peters, H. Rybiński, A. Skowron. LNAI, 4585: 280–290. Springer, Berlin.
- POLKOWSKI L. 2007. *Granulation of knowledge in decision systems. The approach based on rough inclusions. The Method and its applications (plenary talk)*. Lecture Notes in Artificial Intelligence (Proceedings RSEiSP'07), 4585: 69–79.
- MOLINARO A.M., SIMON R., PFEIFFER R.M. 2005. *Prediction error estimation. A comparison of resampling methods*. *Bioinformatics*, 21(15): 3301–3307, Oxford University Press, Oxford, UK. UCI Repository: <http://www.ics.uci.edu/mllearn/databases/>

**THE IMPLEMENTATION OF THE SPATIALLY
ENABLED DATABASE WITH OPEN SOURCE
SOFTWARE AND OPEN SPECIFICATIONS USAGE**

Michał Bednarczyk

Chair of Surveying
University of Warmia and Mazury in Olsztyn

Key words: open source software, OpenGIS specifications, relational database, MySQL, spatial database.

A b s t r a c t

This article describes the design approach in the elaboration and implementation of spatial database. This solution consists of computer programs, algorithms and appropriately designed database schema. The primary objective was to use open source software, and assumptions contained in the OpenGIS open specifications.

**IMPLEMENTACJA PRZESTRZENNE ZORIENTOWANEJ BAZY DANYCH
Z WYKORZYSTANIEM WYBRANEGO OPROGRAMOWANIA OPEN SOURCE
I OTWARTYCH SPECYFIKACJI**

Michał Bednarczyk

Katedra Geodezji Szczegółowej
Uniwersytet Warmińsko-Mazurski w Olsztynie

S ł o w a k l u c z o w e: oprogramowanie open source, specyfikacje OpenGIS, relacyjna baza danych, MySQL, baza danych przestrzennych

A b s t r a k t

W artykule opisano autorskie podejście podczas opracowywania i implementacji bazy danych przestrzennych. Rozwiązanie to składa się z programów komputerowych, algorytmów i odpowiednio zaprojektowanego schematu bazy danych. Podstawowym założeniem było wykorzystanie oprogramowania open source oraz założeń zawartych w otwartych specyfikacjach OpenGIS.

Introduction

This article describes a way to develop a spatially-enabled database for GIS systems. The primary objective of the proposed solution was based on the assumptions contained in the OpenGIS specifications, developed by the Open Geospatial Consortium (OGC) and MySQL – an open source relational database management system. A database schema has been designed as a part of this objective, as well as algorithms and computer programs for converting data into a form suitable for the inclusion in the database schema, and an application which enables remote access to the data on the server. For the most part, the article describes the database itself, which, as the unitary data source, is the most important part of any GIS system. Although the applications needed for data conversion and loading are just as important, the paper will only mention them briefly, because a full description would take too much space.

Open source – means software developed with source code. It is possible to download it, use, make changes in source code and compile without any payment. It is mostly distributed under GNU/GPL license. The reason for addressing this subject was the increasing interest in open specifications and open source software, as well as its still growing quality and functionality. This creates a need for a closer look at the possibilities of its application in practice, because it often involves sizable financial savings.

OpenGIS specifications are rather extensive and have a wide range of applications. This paper discusses only the scope of the OpenGIS specification as implemented in the MySQL system and directly used in the approach described below. The reader will find here some general information about the OpenGIS specifications and a description of the scope of their implementation in the MySQL system. As the next step the author describes the spatially-enabled database he created. The proposed solution uses the capabilities of MySQL, resulting both from the work of its authors and the implementation of the OpenGIS specifications. The final section of the paper describes the practical use of the database created as a data source for Java application, developed by the author.

Open GIS Specifications

OpenGIS Specifications are technical documents, describing in detail interfaces or encoding. They are widely available, free of charge. They can be used by all the software developers wishing to use the proposed solutions in their products. Creation of these specifications is the basis of the Open Geospatial

Consortium to facilitate the interoperability of different computer programs. The ideal situation would be if the programs created by two different developers implementing the same specification worked without a problem.

These documents are created for GIS products, especially for web applications. OGC open standards are being largely taken over by International Organization for Standardization (ISO) to become ISO standards. The cooperation between OGC and International Organization for Standardization results in ISO standards and OGC specifications being identical. The difference is only in copyrights (GAŹDZICKI 2007). OGC specifications standardize many GIS issues such as: Catalogue Services, Coordinate Transformation Service, GML, Web Map Service, Web Feature Service, OpenLS Service, simple features implementation and many others. More information can be found on: <http://www.opengeospatial.org>.

For the purposes of this article the assumptions of OGC specification (*Implementation Specification for Geographic Information – Simple Feature Access*) were used. It describes interfaces for accessing spatial data, defines methods of publication, storage, retrieval and perform operations on vector graphical objects (simple features) comprising the digital map (points, lines, areas etc.). Assumptions of this OGC specification have been implemented in MySQL relational database management system.

MySQL Relational Database Management System

MySQL was created in the second half of 90's of the last century. MySQL's creator is Michael "Monty" Widenius from the Swedish company TeX DataKonsult AB (BEDNARCZYK 2005). The first open source version of MySQL was published in may 1995. The process of development and improvement has accelerated since that time. This happens because of the members of the Internet community who started to create MySQL together, who see in it an excellent database management system for web applications. Mainly because of its high performance.

Today MySQL is one of the most popular database management systems among the open source products (STONES, MATTHEW 2003). It is developed as an open source with an appropriate business model. It means that MySQL can be distributed under two different kinds of licenses: non-commercial free GNU/GPL or full paid commercial license. Commercial version is fully supported with additional services, such as 24 hours technical support (help in configuration, advices, increasing of functionality, use of advanced functions etc.), additional tools for better configuration, automatic updates. Commercial license is also recommended when MySQL source code is to be used as a part of another commercial system.

As the MySQL evolved, more abilities have become available. At first there were only basic functions, which are needed for data storage and distribution – table creation, data and table manipulation using SQL, safety mechanisms etc. MySQL ver.5 used by the author of this article has the following features (AXMARK, WIDENIUS 2007):

- transactions,
- replication
- cluster,
- spatial extensions (implemented according to Open GIS specifications),
- stored procedures and functions,
- triggers,
- views,
- information schema (system metadata).

In addition, extensive documentation and many tools for data administration and management are included. All these things make MySQL very similar to commercial systems such as Oracle for example. Due to spatial extensions included in MySQL and increase of functionality (compared to earlier versions used primarily for Websites), the possibility of using this system in the field of GIS is worth considering.

Spatial Extensions and Geometry Types in MySQL

As mentioned, spatial extensions in MySQL are implemented according to Open GIS specifications and based on the OpenGIS Geometry Model. They extend SQL language, available in MySQL, with new functions and geometry types for storing and managing spatial data. In MySQL 5 not all recommended by the OpenGIS functions are available yet – this applies mainly to spatial analyses. Spatial extensions appeared for the first time in MySQL version 4.1.

As mentioned earlier, the implementation of spatial extensions in MySQL is based on the considerations of OpenGIS Specifications. For this system, they are an extension of spatial SQL environment (geometric) data types (geometry types), together with the features to support them. Not all functions recommended by the OpenGIS are available in MySQL 5 – this applies mainly to spatial analyses. For the first time they appeared in MySQL version 4.1.

Geometry types are used to store information about feature geometry (point, line, area etc.). They can be divided into:

- types which store information about simple-geometry features, such as: POINT, LINestring, POLYGON, GEOMETRY – each of the above geometry types.

– Types which store information about complex-geometry features, which can contain many simple geometry features, such as: MULTIPOINT, MULTILINESTRING, MULTIPOLYGON, GEOMETRYCOLLECTION.

They can be used in the same way as the standard SQL data types (for example INTEGER, CHAR or REAL). Therefore, they can be used to create a column in table or define a variable of type, for example POLYGON. Class hierarchy of geometry types is presented in the diagram below (Fig. 1).

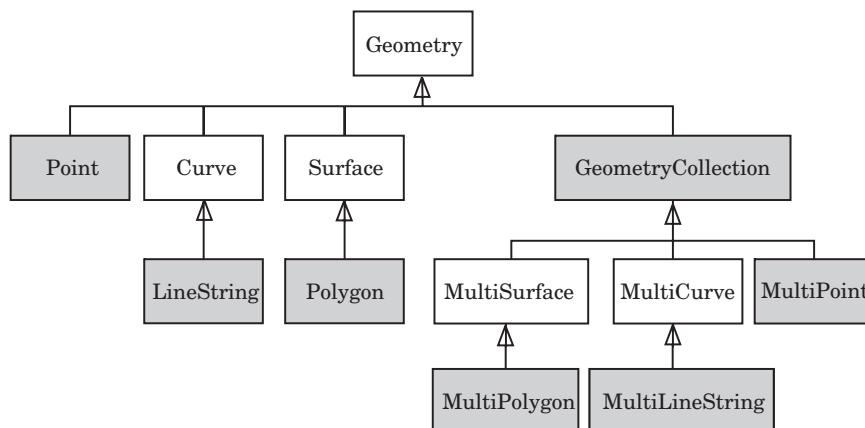


Fig. 1. Geometry types class hierarchy diagram, according to Open GIS specification

Source: OpenGIS Implementation Specification for Geographic information – Simple feature access – Part 2: SQL option. <http://www.opengeospatial.org>.

GEOMETRY class is the parent class for all these which inherit from it. Therefore, all classes derive attributes and properties from GEOMETRY, depending on the type of feature they represent. A detailed description of all classes can be found in Open GIS specification: *OpenGIS Implementation Specification for Geographic information – Simple Feature Access*.

Data Formats for Spatial Information

MySQL implements – also according to Open GIS specification – two kinds of spatial data formats. All functions called by client applications, operating on spatial data, can use one of them. These are:

- WKT – Well Known Text Format,
- WKB – Well Known Binary Format.

Here are some examples of data in WKT format:

- a point with coordinates (10, 12): POINT(10,12),

- a linestring consisted of four vertices: `LINESTRING(0 0, 10 10, 20 28, 50 65)`,
- a polygon with a linear ring inside: `POLYGON((0 0, 10 0, 10 10, 0 10, 0 0),(5 5, 7 5, 7 7, 5 7, 5 5))`,
- Line and point in one geometry type: `GEOMETRYCOLLECTION(POINT (10 10), LINESTRING(11 12, 15 20))`.

The data represented in WKB format is specially prepared BLOB¹ values. For example: Point with coordinates (1.0,1.0) will be represented as:
010100000000000000000000F03F000000000000F03F

Where the different parts of the data stream specified above in hexadecimal notation, means:

- 01 – byte order (determine whether the most significant bit is at the beginning or end of a stream, affects the order of reading the bytes),
- 01000000 – feature geometry type (point, line polygon etc. 1 to 7),
- 00000000000000F03F – X coordinate (double),
- 00000000000000F03F – Y coordinate (double).

Functions Operating on Spatial Data

Internally, the data of the geometry objects are not stored in any of the above formats. MySQL uses its own format, while WKT and WKB are used to exchange data. Spatial extensions are available through appropriate functions, whose interfaces are described in the OpenGIS specifications. These functions can be divided into:

1) Functions for creating spatially enabled database. They return geometry value of the specified type (eg. POLYGON, LINESTRING, etc.). Available functions are using WKT or WKB format or created for MySQL (not included in the OpenGIS specification) format.. They are primarily used for such tasks as:

- creating spatial data type columns,
- inserting spatial values into database tables,
- selecting spatial values from database,
- conversion between spatial data formats.

2) Functions for analysis of spatial information. They are used for:

- obtaining information about the graphical attributes of the object – e.g. length, the number of vertices, area, the number of objects in the collection, etc.

¹ BLOB – Binary Long Object – binary data type used in relational databases. It is used to store binary data such as media files, pictures etc.

- creating geometry from existing elements – e.g. join, difference, buffer zone, next vertex etc.,
- the analysis of the relationship between objects – e.g. intersection, disjoint, contain, overlap, etc.

These functions can be used in SQL queries. This makes it possible to manipulate spatial data and perform spatial analysis through a commonly known language of structured queries. For example, to insert into the field *geo_kol* in table *geo_tab* value that represents the point with the coordinates (1,1) the following query can be used:

```
INSERT INTO geo_tab(geo_kol) VALUES(GeomFromText('POINT(1,1)'))
```

Where `GeomFromText()` is one of the functions described above, which converts string `POINT(1,1)` in WKT format into a value which can be saved in the database.

Spatial analysis can be performed in the same way, except that a different function and SQL keywords must be used.

User-Defined Procedures and Functions

MySQL ver.5 makes it possible to create user-defined functions and procedures (stored routines). According to the information contained in the *MySQL Reference Manual*, their syntax is compatible with SQL: 2003 standard. Use of the routines increases functionality of the system. After the procedures are created and saved in the system, they can be used as a part of SQL queries, just like functions operating on spatial data, which were described before. Such functionality can be found in commercial systems e.g. Oracle. Routines allow to:

- automate internal processes such as: fields update, replication, performing several operations in one call and other operations on the data in the database,
- enhance the safety of performed operations – the client cannot access tables directly, only through the routines; in this way operations performed on the database are invisible for him.
- enhance performance – single procedure call instead of many consecutive commands to the server.
- improve overall functionality (beyond SQL) – the syntax of the routines is similar to well known programming languages and includes loops, conditions, declaration of variables etc.; SQL commands also can be used.

Implementation of Spatially Enabled Database in Mysql

The database discussed in this paper can be supplied with data from an external data source which is a database from Intergraph MGE-PC GIS system, running in Microstation environment. A special application, called Sipos-export, was created by the author for this purpose. It can convert and upload data into the MySQL database. A short description of Sipos-export can be found in the chapter *The Role of User-Defined Routines in the Process of Data Processing*.

However, in the data conversion process, user defined routines, mentioned above, are used. They were programmed and applied specifically to automate activities related to data conversion and uploading into the server.

The data presented in this work was originally produced, as already mentioned, in the MGE-PC GIS system. It has been moved and transformed from this system by the author, with a specially developed application, as described here. The general scheme of the database after transformation consists of the following tables:

1) feature – a table with information about the feature classes in the system – this table contains following columns:

- fclassname – taken over from MGE-PC feature class name (fname),
- fcode – taken over from MGE-PC feature class code,
- ftype – taken over from MGE-PC and modified feature type – takes the following values: 1 – not present in the MGE-PC – this code is used for graphical elements which are not GIS features (not having identifiers binding them with attributes), 0 – undefined, 1 – point, 2 – line, 3 – area, 4 – centroid, 5 – label,
- category – taken over from MGE-PC category identifier,
- mgetablename – MGE-PC table name in which feature attributes were originally stored (MGE-PC feature table name),
- mgelevel – layer number, to which features of this class were assigned in MGE-PC,
- csid – coordinate system identifier,
- f-geometry-column – column name in the feature table, where geometry attributes are stored;

2) primitive – stores vertex coordinates of individual features (point primitives). Contains columns:

- pid – the identifier of the point primitive,
- X – the X coordinate,
- Y – the Y coordinate,

3) prim-feature – stores connection schemas of vertexes for every single feature. Columns are:

- pid – point primitive identifier from *primitive* table,
- fclassname – feature class name,
- fid – feature identifier,
- elnum – the number of a graphical element as a part of the feature; the numbering proceeds according to the order of writing elements in DGN project file,
- eltype – integer specifying the type of graphical element as a part of the feature (eg. line – 3, polyline – 4, shape – 6, etc.),
- num – the number of a node in the graphical element as a part of the feature; always starts from 1, within the component;

4) <feature table> – a table, with any name, which contains descriptive and graphical data for all features of a given class. A single line of such a table corresponds to a single feature, while a column corresponds to a single attribute. The number of tables in the table depends on the number of classes defined by the user in the system. It may contain the following columns:

- <descriptive attribute> – a column, with any name, which contains a descriptive attribute, eg. name, size, etc.). The table may contain any number of these columns,
- <graphical attributes> – a geometry column (in accordance with OpenGIS) which contains geometric attributes of a feature. There can only be one column of this type. The default name during export is: GEOMETRY_ATT.

The schemas of all tables except feature tables are predetermined, so their creation in the system is not problematic. The construction of a feature table is automatically set during export, based on the information in MGE-PC database.

According to OpenGIS specifications, feature tables contain a column with geometric attributes (feature geometry). The remaining attributes may be of any type and are derived from the original versions of these tables (MGE-PC). An example of database schema is shown on figure 2.

In geodesy points with coordinates obtained by calculations or in a measurement play a pivotal role. It is a basic piece of data needed for the preparation of cartographic document. In this situation, the most logical path in the creation of a GIS system is to (simplified):

- 1) Obtain data (by a measurement, calculation, etc.)
- 2) Feed the system with points,
- 3) Construct features based on these points.

Following this line of reasoning, the proposed way of converting and storing data makes use of two tables: *primitive* and *prim-feature*. The former table stores the points' coordinates – point primitives. They can be obtained from different sources (e.g. calculations, direct measurements, other systems). Features are then constructed on the basis of these coordinates. Each feature

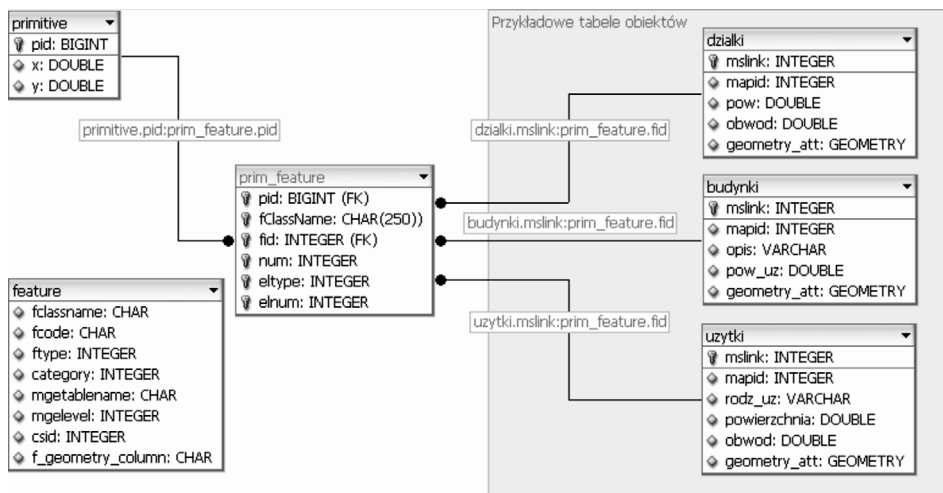


Fig. 2. An example of a MySQL server-side database schema

Source: own work.

has a map of node connections – in this case stored in the the table *prim-feature*. Each node is assigned a point with specific coordinates – point primitive – stored in the table *primitive*. A primitive is assigned to the node by an identifier (PID). Such a format makes it easier to conduct operations on separate points, to use them for calculations, measurements or setting up another system. The conversion of all the coordinates simultaneously is also easier. In this format the connection maps of different features may share the same point primitives. This eliminates the problem of duplicating the same coordinate values for different features. A change in the coordinates of a primitive will change the boundaries of all the features containing the primitive.

The data including point primitives is saved according to the following rules:

- 1) The point coordinates are stored as a separate set – point primitives (table *primitive*).

- 2) Each feature consists of elements. A feature is defined by a pair of identifiers: *nazwa klasy* (class name) and *identyfikator obiektu* (feature identifier). An element of the feature may be a point, line, multiline or area.

- 3) Each element has nodes ordered by their occurrence in the original project file – i.e. in the order they were digitized.

- 4) The coordinates of each node are assigned by the identifier (PID) from the table of primitives (*primitive*).

No matter what the format of graphical data is in the system, it usually has to be converted if it is to be displayed on the computer screen or a printout. As a result, the user can be presented with certain geometrical shapes (lines, polygons, points, etc.). They are built based on the data collected by the system and drawn using appropriate software functions responsible for the visual display. These functions must access the information about the type of the shape to be drawn, the coordinates of the nodes and, additionally, colour and line style. They must, independently of how the feature is described, “construct” geometrical shapes to be displayed, on the basis of the data obtained from, for example, a database. This model of data presentation is analogous to a simple vector model, where each feature is defined separately, including geometry. Thus, even if a program uses a completely different format of storing graphical data, for visualization purposes they will be converted to a format resembling a simple vector model. A simple vector model, despite certain drawbacks (resulting, for example, from node repetition for features sharing a boundary) has undeniable advantages, such as simplicity and display speed. It focuses on those properties of graphical elements, which are important for visual representation, and does not require additional interpretation.

Applications which use a relational database, especially over the Internet, should generate the lowest possible data transfer. A large amount of information sent between clients and the server has a significant impact on efficiency. One way to optimize the cooperation between the program and the database is to reduce the number of inquiries. If the same amount of data can be retrieved or sent to the server using one or many queries, the time necessary for the server to send and process the data will be much shorter in the former case.

Taking this into consideration, I decided to take advantage of the possibilities offered by MySQL and implement in it, in accordance with OpenGIS specification, spatial data types. They are discussed in more detail in the chapter on MySQL server. OpenGIS specification suggests a feature table schema, which, apart from descriptive attributes, contains a column with spatial data type, containing geometric data. Henceforth I will call this table geometric attribute of the feature. In taking this step I focused on simplicity, speed and efficiency, which are particularly important when the information is accessed via the Internet. This is especially true when using the popular SQL, as processing speed might become a problem.

A similar treatment of geometric data (node coordinates and the identifier in one record of the same table) has been proposed elsewhere and referred to as object-oriented topological model (ECKES 2006) or a physical model of a topological database (LONGLEY et al. 2006). The difference is that in the physical model a set of topological rules for different classes of features (for example different buildings cannot be located in the same area, plots cannot

overlap, etc.) is recorded, together with the information on topological errors and areas which have been edited, but not yet corrected with respect to topology. Using this information the system reproduces topological relations among features on the fly, when requested by the user. This kind of formatting is used, for example, in ESRI ArcGIS. It need not involve storing the topology in, for example, the structure of nodes and edges. Consequently, it is not necessary to reconstruct their geometry every time they are being displayed and thus to slow down this operation.

The solution described here uses the functions of MySQL server created by the author, which produce a geometric attribute of the feature based on the information from the database (point primitives and a map of node connections). This attribute is naturally recorded and stored in a spatial data type column, in a specific feature table. Once the feature table is created in this way, a simple SQL query may retrieve both descriptive attributes and feature geometry. The output of the query is a single record containing all the necessary information. This considerably speeds up the loading of data from the server, which is an important issue on the Internet. The application which retrieves the data does not need to “assemble” the feature from point primitives and analyse the connection map, because this operation is only done once after each feature update. This means that the update of the feature geometry causes the geometric attribute needed for visualization to be updated as well. This is the method used in my applet – *Sipos-klient*, The geometric attribute retrieved by the client is not only used for the visual presentation of the feature, but, above all, serves as the interface for the identification of the feature in the database. By clicking on the picture on the computer screen the user retrieves the feature identifier. This gives him access to any data on the selected feature, and the possibility to modify it.

The feature tables contain – in compliance with OpenGIS specification – geometric attribute. The usage of such tables has an additional advantage of interoperability with other systems reading this format.

As can be seen in Figure 3, the table *prim-feature* stores the maps of node connections for all features in the system. This concept of the table *prim-feature* was partly determined by technical problems in MySQL routine implementation. Among others, it is impossible to use a table name in the routine as an input parameter. As a result, the routine can only operate on tables whose names are contained in the routine code as constants. The solution of this problem would offer greater elasticity in constructing database schemas. For example, it would enable the creation of a separate table with point primitives for each feature class. I hope it will be possible in forthcoming editions of MySQL server.

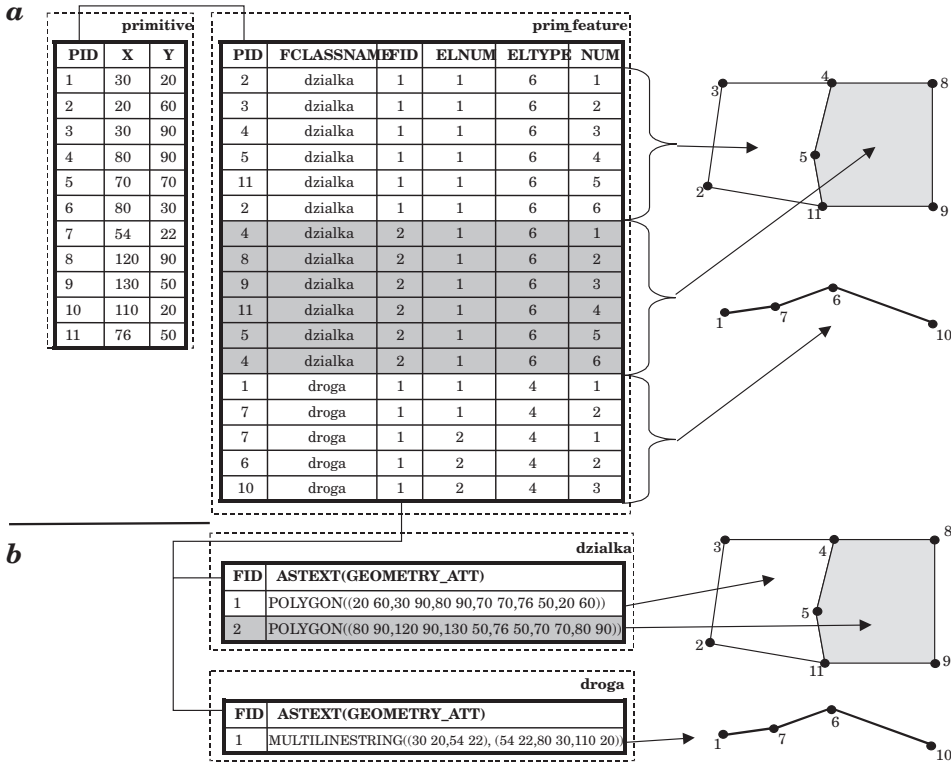


Fig. 3. The format of features' geometric data in database tables: a) – the format of features' geometric data in a relational database table based on point primitives; b) – the format of features' geometric data using spatial data types. The geometric attributes have been recorded in the feature tables in the column GEOMETRY_ATT (only this column and FID identifier are visible in figure) Source: own work.

The Role of User-Defined Routines in the Process of Data Processing

The author of this paper has created several MySQL server routines, which play a rather important part in the process of uploading the data to the server: `pre_proc()`, `post_proc()`, `Repair_primitives()`, as well as function: `MakeGeometry()`.

They were designed to automate and simplify the process of exporting and data processing when working with the system. Once implemented they are an integral part of the database and can be called in the same way as any standard command, function or routine.. Besides, because they are stored on the server, there is an additional possibility to modify what routines do, by editing their

code. Thus, the process may be modified and improved without the necessity to tamper with the structure of the application which exports the data. Naturally, such modifications may only be made by a user with the appropriate authorization in the database management system.

The data is uploaded to the server with a program created just for this purpose – Sipos-eksport. It is a desktop program, written in Object Pascal in Delphi environment. Its role is to read data from the original MGE-PC database, convert it into a text file with SQL commands and export it to the spatially-enabled database on MySQL server, discussed above. The process uses the routines discussed here, which make it possible to create tables, load data, convert it to the appropriate format and finalize the process. An sample content of the data file created to export the data to the server is shown below:

```

budynek.sql
call pre_proc()
INSERT INTO budynek(HSLINK,HAPID,NAZWA,POW) VALUES(1,1,"mieszk",null);
INSERT INTO tmp (fclassname,fid,num,x,y,eltype,elnum) VALUES ("budynek",1,1,770966,877964,4,1), ("budynek",1,2,769225,850078,4,1),
("budynek",1,3,790119,849643,4,1), ("budynek",1,4,791860,879271,4,1), ("budynek",1,5,771837,878399,4,1);
INSERT INTO budynek(HSLINK,HAPID,NAZWA,POW) VALUES(2,1,"gosp",null);
INSERT INTO tmp (fclassname,fid,num,x,y,eltype,elnum) VALUES ("budynek",2,1,765308,828293,4,1), ("budynek",2,2,786201,829600,4,1),
("budynek",2,3,785766,810865,4,1), ("budynek",2,4,766178,809557,4,1), ("budynek",2,5,765308,826550,4,1);
INSERT INTO budynek(HSLINK,HAPID,NAZWA,POW) VALUES(3,1,"bud gosp",null);
INSERT INTO tmp (fclassname,fid,num,x,y,eltype,elnum) VALUES ("budynek",3,1,683184,835938,4,1), ("budynek",3,2,694944,836810,4,1),
("budynek",3,3,697993,809779,4,1), ("budynek",3,4,686668,808253,4,1), ("budynek",3,5,683184,835502,4,1);
INSERT INTO budynek(HSLINK,HAPID,NAZWA,POW) VALUES(4,1,"gosp",null);
INSERT INTO tmp (fclassname,fid,num,x,y,eltype,elnum) VALUES ("budynek",4,1,662059,753274,4,1), ("budynek",4,2,674037,754364,4,1),
("budynek",4,3,674908,719267,4,1), ("budynek",4,4,662930,719267,4,1), ("budynek",4,5,662277,753274,4,1);
call post_proc()
call repair_primitives()
UPDATE budynek SET geometry_att=(SELECT makegeometry(mslink,"budynek")
WHERE mslink IN (SELECT DISTINCT fid FROM prim_feature WHERE fclassname="budynek");

```

Fig. 4. A sample content of a file with SQL queries which exports descriptive and geometric feature attributes

Source: own work.

As shown in Figure 4, procedures are called in the appropriate places before and after the data is loaded by SQL commands. The execution of all calls from the file results in the data being exported to the server in the appropriate format, designed by the author.

The procedures mentioned above, *pre-proc* and *post-proc* perform the following actions:

- *pre_proc* – among others, initializes the export process, creates temporary tables, assigns identifiers.
- *Post_proc* – finalizes the data export process, deletes temporary tables.

The role of the routine *Repair_primitives()* and function *MakeGeometry()* is the conversion of the data after it has been exported to the server.

Repair_primitives() deletes the duplicates of primitives. Duplicates of primitives are defined as those points, for which the coordinates $X_n = X_m$ and $Y_n = Y_m$, while PID identifiers $n \neq PID_m$. Procedure *Repair_primitives()*, first of all, deletes the duplicated records in the table *primitive* so that only one

instance remains. Secondly, it updates the appropriate fields in the table *prim_feature* where PIDs of deleted primitives were located and replaces them with the identifier of the primitive which was not deleted. Duplicates of this kind occur when linear elements meet (the end of one element meets the beginning of another) and when features share boundaries. Procedure *Repair_primitives()* is called directly with: call *Repair_primitives()*.

Function *MakeGeometry()* (Fig. 5) creates and updates geometric attributes of features in the feature table. The function has the following input parameters: feature identifier (*feature_id*) and class name (*fclassname*). The output is a geometric (spatial) type value. The input data on which the function operates is taken from the tables *primitive* and *prim_feature*. Based on the information from these tables the function creates and returns geometric values appropriate for a given feature, using MySQL functions which operate on spatial data types.

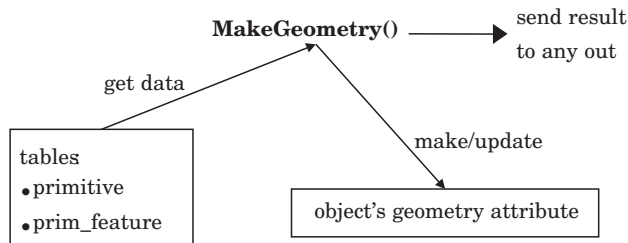


Fig. 5. The role of the function *MakeGeometry()*

Source: own work.

Function *MakeGeometry()* is used as a part of an SQL query, so it can serve a number of purposes, for example to update geometric values in an feature table. An example of a query which performs this task is shown below.

– A query updating geometric attributes of all features of the class *autostrada* in the table *autostrada*:

```

UPDATE autostrada
SET geometry_att=SELECT MakeGeometry(mslink,"autostrada")
WHERE mslink IN
(SELECT DISTINCT fid FROM prim_feature
WHERE fclassname="autostrada");
  
```

Result:

All values of geometric attributes will be generated and inserted into the field *geometry_att* of the table *autostrada*.

When selecting data from a table with spatial data type, geometric attributes are treated in the same way in SQL queries as descriptive attributes. For this reason they can be retrieved together for a feature or a set of features, for example:

```
SELECT mslink,szerokosc,pasy_ruchu,astext(geometry_att) as geometria
FROM autostrada WHERE mslink=3892;
```

Result: shown in table 1.

Table 1

Result of SQL query

| Mslink | szerokosc | Pasy_ruchu | Geometria |
|--------|-----------|------------|--|
| 3892 | 10 | 2 | MULTILINESTRING((81058880 43978312,80650010 43893707,80366165 43881624,80172909 43911833,79949457 43990377,79798476 44068921,79587102 44141423,79492733 44158282),(79492733 44158282,79418003 44171632,79280809 44152701),(79280809 44152701,79073766 44123297,78892588 44093088,78669136 44002461,78439644 43905791,78343016 43875582)) |

Descriptive data is readable immediately after download, independently of the method used. An application able to read and draw an feature based on geometric value is needed to see a visualisation of the geometry. This format can be read, among others, by GRASS – a free GIS system. For the purpose of this paper the author wrote his own application in Java.

Internet Client

I have written the program *Sipos-klient* as an example of a tool for data retrieval from the database discussed in the article. The program can be used to test the basic capabilities of the database. Its functions make it possible to:

- connect to MySQL database,
- retrieve the classes of features available in the database,
- send a query which selects features – attribute analysis,
- display and browse through features form the selected classes, retrieve the values of features' attributes, in a simple way adjust the view of the displayed feature classes and the results of queries (on/off, colour change, scaling, movement).

The addition of other functions to the program *Sipos-klient*, like analytic or editorial functions, would make it useful for specific purposes expected of this kind of software.

Sipos-klient connects to MySQL server using a JDBC driver² for MySQL. It can be used on a desktop computer or over the Internet. Java technology makes it possible to run this program under any operating system with a browser and Java Runtime Environment installed.

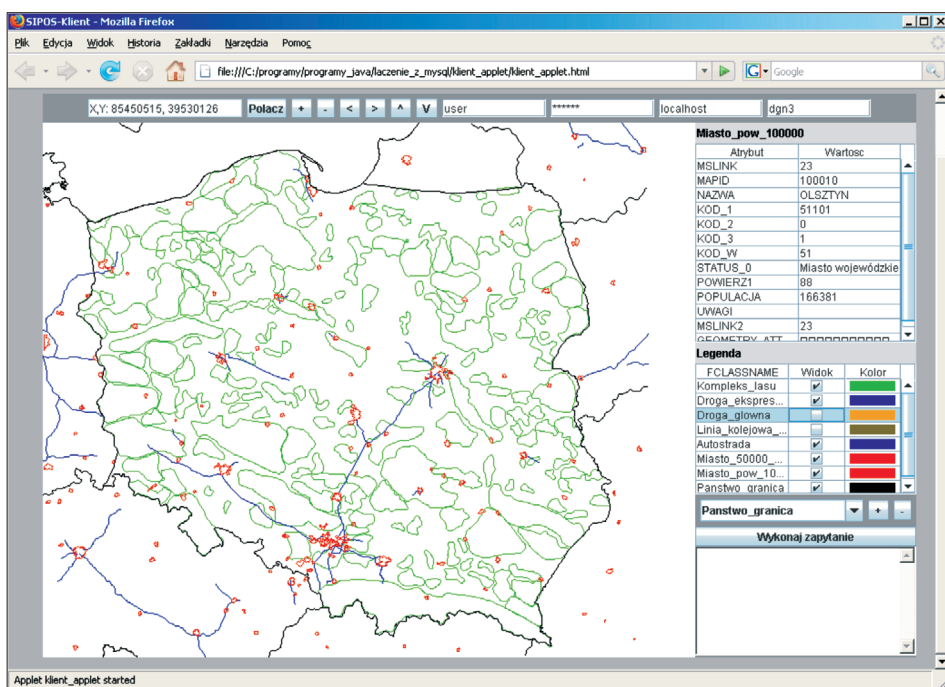


Fig. 6. Sipos-klient. Main window

Source: own work.

Figure 6 shows the interface of *Sipos-klient* run in Firefox browser. The upper part contains navigation buttons for scaling and scrolling the map, as well as editing fields for entering database connection parameters. The left-hand bottom part of the window, which occupies the most space, shows a map consisting of the feature classes retrieved from the database. The right-hand side shows the attributes of a selected feature, the key – a list of the displayed feature classes, a context menu which allows to select a feature class from the database, buttons which add and remove classes from the list and a window for

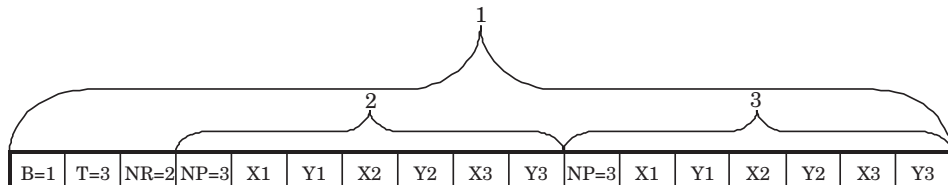
² JDBC – *Java Database Connectivity* – an interface for Java programs, analogous to ODBC. It allows to connect to the database using SQL. In order to work with a Java application a database must have a dedicated driver which uses JDBC interface. For MySQL, *Connector/J* is one of such drivers. It translates JDBC calls into MySQL network protocol.

entering and executing queries for the table with the attributes of the selected feature class.

Sipos-klient uses a database created earlier using *Sipos-eksport*. Feature tables with geometric attributes filled in (field *geometry-att*) and table *feature* are also necessary.

Sipos-klient retrieves geometric attributes of a feature from the database as binary streams in WKB format. OpenGis (ECKES 2006) specification (*OPEN-GIS Implementation Specification 2005*) contains a description of how to implement structures representing geometry in this format. According to this description, each geometry is built out of basic elements, such as points (*Point*) or linear rings (*Linear ring*). Each structure consisting of simpler structures (for example *MultiLinestring*) is built using already defined features. The following is an example of a definition of a structure for geometry of *WKBPolygon* type in C programming language:

```
WKBPolygon {
byte byteOrder;
uint32 wkbType; // 3
uint32 numRings;
LinearRing rings[numRings];
};
```



explanations:

- 1 – WKB Polygon
- 2 – ring 1
- 3 – ring 2

Fig. 7. Feature geometry in WKB representation. Byte order – little-endian³ (B=1), type POLYGON (T=3), contains two elements linear ring (NR=2), each consisting of three points (NP=3).

Source: *OpenGIS Implementation Specification for Geographic information – Simple feature access – Part 1: Common architecture*. <http://www.opengeospatial.org/>.

The definitions discussed above have been used to determine how to represent, build and manage a map composed of geometrical features. Using this information, a model of the classes implemented in *Sipos-klient* has been designed.

³ *Little-endian* byte order means that the least significant byte is first. It is an important piece of information when reading consecutive values in the stream, which determines the order in which bytes are read.

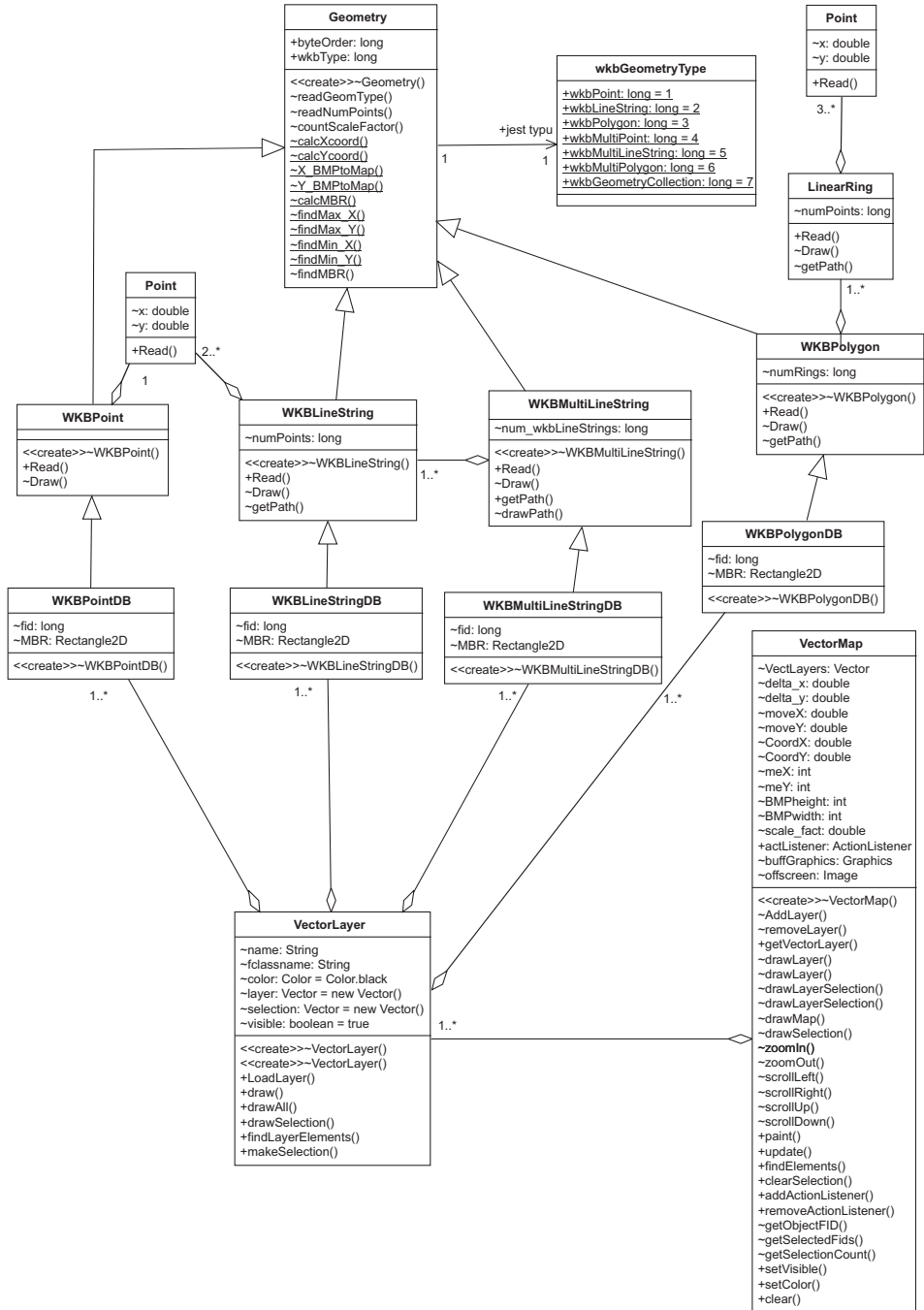


Fig. 8. UML diagram showing classes in Sipos-klient

Source: own work.

The flow chart below (Fig. 8) shows the classes which are the most important for the structure of the inner layer of the program, which operates on geometric features. The chart does not show the relationships with classes used in the user interface. The whole structure may be categorised into two interrelated class areas:

1. Geometric model, with the class *Geometry* as the main element. Classes which represent feature types are derived from it.

2. Vector map, consisting of layers, which in turn are constructed as collections of specific GIS features. Features are assigned to a layer based on a specified criterion. The default criterion is the membership of a specific class. However, the model allows the use of other rules, for example the result of a query which contains features of different classes may be presented as a separate layer.

There is an intermediate layer between the geometric model and the vector map. It connects geometric and descriptive attributes. The layer consists of classes derived from the geometric model classes: *WKBPointDB*, *WKBLines-tringDB*, *WKBMultiLinestringDB*, *WKBPolygonDB*. Features in these classes have an identifier *fid* linking them to a corresponding record in the attribute table. This information is used for the identification of the feature by the user, for example when the user points at the feature on the map and retrieves its descriptive attributes.

Conclusion

The concept of a spatially-enabled database discussed in this paper is based mostly on open source software and open standards. The relational MySQL database management system used here can be used for GIS purposes, as shown by the functionality of spatial extensions, data types, user-defined functions and routines described above. The mechanisms of spatial data processing implemented in MySQL comply with OpenGIS specifications. As a result, so does the created database. This enables interoperability with other databases created in the same standard. It should also be noted that MySQL is available free of charge, which considerably reduces costs.

A spatially-enabled database on a MySQL server makes it possible for its data to be accessible on the Internet. The data is accessible on the condition that MySQL is installed on a computer connected to the Internet, with a public IP address. The data can be accessed with any MySQL client, but it is easier and more efficient to use a special application, such as Sipos-klient. The best solution would be for the data to be made accessible on the Internet via a WWW website. The free Apache or Windows Server 2003 Web Edition may be

used as the HTTP server. It is not the only method of sharing this kind of data however. More complex solutions can also be employed (for example, using so called distributed architecture), which additionally use script languages (for example PHP⁴, Python, VBScript, JScript i in.), application servers (Apache Tomcat⁵, IBM WebSphere Application Server, Oracle Application Server, Windows Server etc.) and web services (a large number of useful web services has been proposed in OGC open specifications). MapServer – an environment for building web applications – can also be used for sharing the data. Access to the data from a spatially-enabled database may also be provided using a desktop client application, e.g. written in Delphi environment, which directly accesses the server without the help of a website.

Free software and open standards are becoming more and more popular not only among individuals and companies, but even governments in Europe and worldwide. It is reasonable to bear this tendency in mind when choosing a commercial product. It is often worthwhile to consider its open source counterparts. It may turn out that despite a smaller number of functions a free alternative will meet the user's expectations. The database proposed here as an answer to a specific problem using open source software and own solutions shows that the goal can be achieved at a lower financial cost.

Translated by ŁUKASZ ARENDARSKI, MICHAŁ BEDNARCZYK

Accepted for print 22.03.2011

References

- AXMARK D., WIDENIUS M. 2007. *MySQL 5.0 Reference Manual*. MySQL AB.
- BANACHOWSKI L. 1998. *Bazy danych Tworzenie aplikacji*. Akademicka Oficyna Wydawnicza PLJ, Warszawa.
- BEDNARCZYK M. 2005. *Oprogramowanie open source na potrzeby systemów informacji przestrzennej na przykładzie systemu zarządzania relacyjną bazą danych MySQL*. Biuletyn Naukowy UWM, 25: 215–222.
- BEDNARCZYK M. 2008. *Zastosowanie systemu zarządzania relacyjną bazą danych MySQL do automatyzacji przetwarzania informacji geograficznej*. Biuletyn Naukowy UWM, 29: 5–15.
- ECKES K. 2006. *Modelowanie rzeczywistości geograficznej w systemach informacji przestrzennej*. Roczniki Geomatyki, IV(2): 43–73.
- GAŹDZICKI J. 2007. *Standardy otwarte w geomatyce*. Roczniki Geomatyki, V(2): 7–11.
- HAMLET D., MAYBEE J. 2003. *Podstawy techniczne inżynierii oprogramowania*. Wydawnictwo Naukowo-Techniczne, Warszawa.
- LONGLEY P.A., GOODCHILD M.F., MAGUIRE D.J., RHIND D.W. 2006. *GIS Teoria i praktyka*. Wydawnictwo Naukowe PWN, Warszawa.

⁴ PHP, an Apache HTTP server and a MySQL database server on a Linux system are a very common Open Source software bundle for a website (so called LAMP solution stack).

⁵ These are J2EE (Java 2 Platform Enterprise Edition) application servers, with Java the programming language. Of these, only IIS as a Microsoft product supports ASP.NET technology (VBScript, JScript languages).

- OpenGIS Implementation Specification for Geographic information – Simple feature access – Part 1. Common architecture.* 2005. OGC (Open Geospatial Consortium), <http://www.opengeospatial.org/>.
- OpenGIS Implementation Specification for Geographic information – Simple feature access – Part 2. SQL option.* 2005. OGC (Open Geospatial Consortium), <http://www.opengeospatial.org/>.
- STONES R., MATTHEW N. 2003. *Bazy danych i MySQL od podstaw.* HELION, Gliwice.
- STARZYŃSKI P. 2004. *Zamówienia publiczne a Open Source – stan prawny.* In: *Budowa społeczeństwa informacyjnego w Polsce i Unii Europejskiej.* Ed. P. Bała. Uniwersytet Mikołaja Kopernika, Toruń, pp. 107–109.

THE ACTIVATION ENERGY OF PRIMARY CRYSTALLIZATION OF Fe₉₅Si₅ METALLIC GLASS

Adam Frączyk

Chair of Functional Materials and Nanotechnology
University of Warmia and Mazury in Olsztyn

Key words: metallic glass, energy activation, crystallization kinetics parameter, DSC.

Abstract

The primary crystallization process of Fe₉₅Si₅ metallic glass was investigated by DSC and X-ray diffraction methods. The crystalline phase α -Fe(Si) was identified during the primary crystallization process. The activation energy of crystallization E_a has been calculated in the frame of two models: Kissinger and Ozawa. The activation energy for primary crystallization of amorphous Fe₉₅Si₅ alloy are determined as 235.2 and 247.3 kJ mol⁻¹ by means of the Kissinger and Ozawa equations, respectively.

ENERGIA AKTYWACJI KRYSZALIZACJI PIERWOTNEJ SZKŁA METALICZNEGO Fe₉₅Si₅

Adam Frączyk

Katedra Materiałów Funkcjonalnych i Nanotechnologii
Uniwersytet Warmińsko-Mazurski w Olsztynie

Słowa kluczowe: szkło metaliczne, energia aktywacji, parametr kinetyki krystalizacji, skaningowa kalorymetria różnicowa.

Abstract

Proces krystalizacji pierwotnej szkła metalicznego Fe₉₅Si₅ badano metodą różnicowej kalorymetrii skaningowej (DSC) oraz dyfraktometrii rentgenowskiej. Zidentyfikowano fazę powstającą podczas pierwszego etapu krystalizacji jako α -Fe(Si). Obliczono energię aktywacji przemiany krystalicznej na podstawie dwóch modeli: Kissingera oraz Ozawy. Energia aktywacji obliczona z równań Kissingera i Ozawy wyniosła odpowiednio 235,2 oraz 247,3 kJ mol⁻¹.

Introduction

The excellent soft magnetic properties of metallic glasses have found use in many industrial applications and new glasses and their properties are continually being explored (LI et al. 2008, SAHINGOZA et al. 2004, NOBUYUKI et al. 2007).

The amorphous alloys are metastable materials. On increase of temperature, such non-crystalline alloys transform into crystalline state in course of time. From the technological application point of view, the thermal stability of the amorphous alloys is of considerable importance.

The thermal stability of metallic glasses is a subject of considerable interest, since the properties of these engineering materials may be significantly changed by the onset of crystallization (LIU et al. 2004, BHATTACHARYA et al. 2009, SANTOS et al. 2001).

The crystallization behaviour of various metallic glasses has been studied using a variety of techniques, such as ferromagnetic resonance, differential scanning calorimetry (DSC), Mössbauer spectroscopy, X ray diffraction, and electrical resistance variations. (RIBEIRO et al. 2004, JAKUBCZYK et al. 2007).

The study of crystallization kinetics in glass-forming liquids has often been limited by the elaborate nature of the experimental procedures that are employed. The increasing use of thermoanalytical techniques such as differential thermal analysis (DTA) or differential scanning calorimetry (DSC) has, however, offered the possibility of obtaining useful data with simple methods.

Many authors for example (RIBEIRO et al. 2004, JAKUBCZYK et al. 2007, MINIĆ et al. 2009, SOLIMAN et al. 2004) characterized the thermal stability and effective activation energies E_a using differential scanning calorimetry (DSC) by isothermal and non-isothermal methods.

The present work concerns studies on activation energy E_a for the $\text{Fe}_{95}\text{Si}_5$ metallic glass in primary crystallization.

Theory

The study of crystallization kinetics of glassy materials can be calculate the one of three kinetic parameters – activation energy E_a . In calorimetric measurements, isothermal and non-isothermal methods can be used. Most methods is based on Johnson-Mehl-Avrami (JMA) equation of isothermal transformation kinetics (MÁLEK 2000):

$$x(t) = 1 - \exp(-Kt^n) \quad (1)$$

where: $x(t)$ is volume fraction transformed after time t , n is Avrami kinetics exponent (the exponent which reflects the nucleation rate and the growth morphology), K is the reaction rate constant. The temperature dependence is usually assigned from Arrhenius equation:

$$K = K_0 \exp\left(\frac{-E_a}{RT}\right) \quad (2)$$

where: E_a is the activation energy for the crystallization reaction, K_0 is the frequency factor and R is the gas constant.

The non-isothermal crystallization, is characterized by a constant heating rate. The relation between the sample temperature T and the heating rate β can be written:

$$T = T_0 + \beta t \quad (3)$$

A popular non-isothermal analysis method developed by KISSINGER (1957) and OZAWA (1970). Their methods is based on JMA theory and logarithmic form of equation 2. The Kissinger and Ozawa models are considered that on the top of crystallization peak DSC the amount of crystallized fraction is $x_p = 0.63$. Using the highest rate of a transformation at maximum peak approximations interpreted in this equations, respectively:

$$\ln\left(\frac{\beta}{T_p^2}\right) = \frac{-E_a}{RT_p} + \ln\left(\frac{K_0 E_a}{R}\right) \quad (4)$$

$$\ln(\beta) = \frac{-E_a}{RT_p} + \ln\left(\frac{K_0 E_a}{R}\right) \quad (5)$$

where: T_p the temperature of a peak, $\beta = dT/dt$ heating rate.

The partial $\ln(K_0 R/E_a)$ and $\ln(K_0 E_a/R)$ in equations 4 and 5 are constant. From the slope and the intercept of the straight line (Eq. 4, 5) it is possible to derive the value of the activation energy E_a and the pre-exponential factor K_0 of the crystallization process, respectively.

Experimental

The amorphous samples were obtained by rapid solidification from the melt using the melt-spinning method. The obtained ribbon was 20 mm wide and 0,03 mm thick, with nominal composition of $\text{Fe}_{95}\text{Si}_5$.

The crystallization process was investigated by differential scanning calorimetry (DSC) in nitrogen atmosphere using a NETZSCH DSC 204 instrument. The sample masses used for DSC measurements were about several milligrams. The samples were heated from 340 K to 840 K using different rates $\beta = 2, 5, 10, 20$ and 30 K min^{-1} .

The structural characterization was carried out by an X-ray diffraction. The sample of amorphous alloy $\text{Fe}_{95}\text{Si}_5$ annealed at different temperature 753 K in a stream of nitrogen during 30 min. The X-ray diffraction measurements were performed on DRON 4.07 diffractometer using $\text{CoK}\alpha$ radiation, over a 2θ angle range of $35 \div 105$ degrees with a step of $0.05 \text{ deg min}^{-1}$. The voltage was set at 31 kV and the current set at 21 mA.

Results and discussion

The kinetics of non-isothermal crystallization of $\text{Fe}_{95}\text{Si}_5$ amorphous alloy was investigated by DSC method. Figure 1 shows DSC curves for $\text{Fe}_{95}\text{Si}_5$ amorphous metallic alloys, obtained at a heating rate of 2, 5, 10, 20 and 30 K min^{-1} . Samples of the alloy present two distinct exothermal peaks, and this behavior is independent of the applied heating rate, suggesting a crystallization process with two distinct exothermal reactions. When the heating rate increases, the position of both peaks was shifted to the higher temperatures.

Figure 2 presents XRD pattern for the sample of $\text{Fe}_{95}\text{Si}_5$ alloy annealed at 753 K temperature during 30 min. On the basis X-ray diffraction analysis after crystallization (see Fig. 2) the $\text{Fe}_{95}\text{Si}_5$ metallic glass primary crystallizes into phase the $bcc\text{-}\alpha\text{-Fe(Si)}$ of lattice constant $a = 2.867 \text{ \AA}$. It corresponds to literature data about kinetic crystallization of Fe-Si-X amorphous alloys for example (LI et al. 2008, SAHINGOZA et al. 2004, JAKUBCZYK et al. 2007, RIBEIRO et al. 2009).

The activation energy E_a of primary crystallization of metallic glass $\text{Fe}_{95}\text{Si}_5$ has been calculated by Kissinger and Ozawa method. For this purpose, the plots $\ln(\beta/T_p^2)$ vs. $10^3/T_p$ (Fig. 3) and $\ln(\beta)$ vs. $10^3/T_p$ (Fig. 4) are plotted for the present metallic glass.

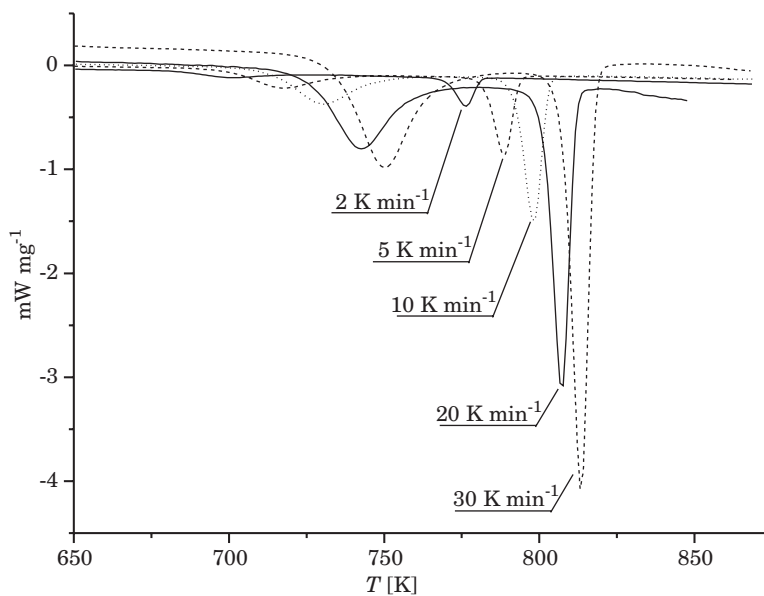


Fig. 1. DSC curves of $\text{Fe}_{95}\text{Si}_5$ for several heating rates showing the primary crystallization process (first peak) and secondary crystallization (second peak)

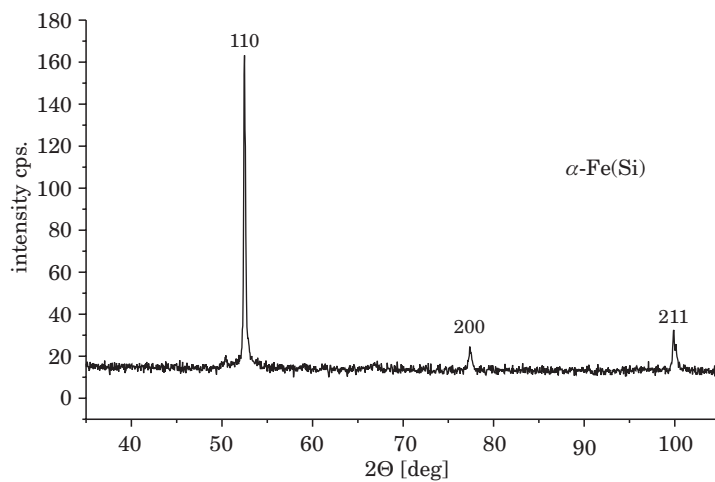


Fig. 2. X-Ray diffractogram of the $\text{Fe}_{95}\text{Si}_5$ metallic glass annealed at 753 K during 30 min

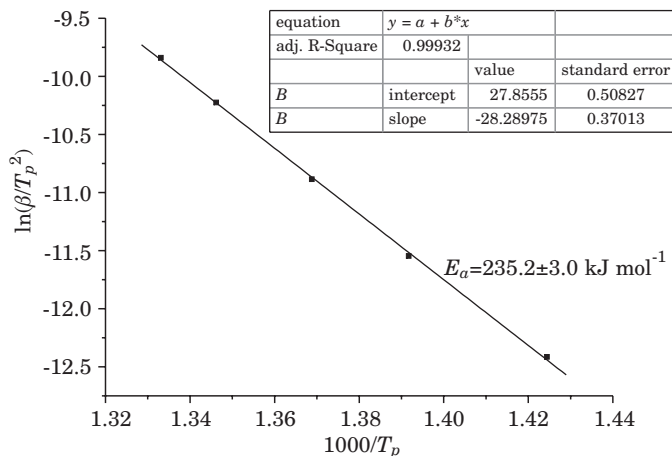


Fig. 3. Kissinger plot for determination of the activation energy E_a from a set of DSC scans with different heating rates (2, 5, 10, 20 and 30 K min⁻¹). In the case of the Fe-Si alloy. This analysis was performed for first observed exothermal reaction from DSC

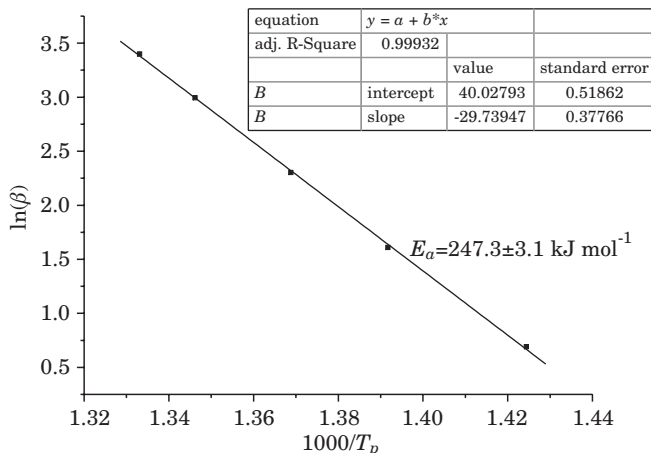


Fig. 4. Ozawa plot for determination of the activation energy E_a from a set of DSC scans with different heating rates (2, 5, 10, 20 and 30 K min⁻¹). In the case of the Fe-Si alloy. This analysis was performed for first observed exothermal reaction from DSC

From the slope ($-E_a/R$) of the line activation energy E_a of an amorphous alloy can be obtained. A best fit for the results was calculated by the least-square method. The arithmetic mean as well as the standard deviation were calculated for the activation energies.

The primary crystallization parameters are presented in Table 1.

Table 1

Primary crystallization parameters of Fe₉₅Si₅

| Heating rate β [K min ⁻¹] | 2 | 5 | 10 | 20 | 30 |
|---|---|-------|-------|-------|-------|
| Temperature max. peak T_p [K] | 702.1 | 718.6 | 730.6 | 742.9 | 750.2 |
| Enthalpy phases transformation [J g ⁻¹] | 32.78 | 43.61 | 41.95 | 42.54 | 41.42 |
| Energy activation E_a (by Kissinger equation) [kJ mol ⁻¹] | 235.2 ± 3.0 | | | | |
| Energy activation E_a (by Ozawa equation) [kJ mol ⁻¹] | 247.3 ± 3.1 | | | | |
| Phasecubic | α -Fe(Si) (Im3m) $a = 2.856 \text{ \AA}$ | | | | |

The activation energy E_a is one of the most important kinetic parameters for the crystallization of an amorphous alloy.

The values of the kinetic parameters determined according to the Kissinger method are some higher than ones determined by applying the Ozawa method, but the differences between the values determined by the two methods are under 6%. Similar results received authors (MINIĆ et al. 2009, WANG 2003) when they studied crystallization kinetics of Fe_{89.8}Ni_{1.5}Si_{5.2}B₃C_{0.5} and Zr₇₀Cu₂₀Ni₁₀ metallic glasses.

Conclusions

The activation energies connected with the first peak temperature in the continuous heating DSC curves of the amorphous Fe₉₅Si₅ alloy have been calculated using different methods. These are determined as 235,1 and 247,2 kJ mol⁻¹ when using the Kissinger and Ozawa equations, respectively. The Ozawa equation gives the largest value of activation energy.

To compare the activation energy of different amorphous alloys, the same equation or model should be utilized.

Translated by AUTHOR

Accepted for print 22.03.2011

References

- BHATTACHARYA S., LASS E.A., POON S.J., SHIFLET G.J. 2009. *High thermal stability of soft magnetic (Fe,Co)-Mo-B-C-P-Si metallic glasses*. Journal of Alloys and Compounds, 488: 79–83.
- JAKUBCZYK E., KRAJCZYK A., JAKUBCZYK M. 2007. *Crystallization of amorphous Fe₇₈Si₅B₁₃ alloy*. Journal of Physics: Conference Series, 79.
- KISSINGER H. E. 1957. *Reaction kinetics in differential thermal analysis*. Analytical Chemistry, 29: 1702–1706.

- LI H.X., JUNG H.Y., YI S. 2008. *Glass forming ability and magnetic properties of bulk metallic glasses $Fe_{68.7-x}Co_{7.0}Si_{3.3}B_{5.5}P_{8.7}Cr_{2.3}Mo_{2.5}Al_{2.0}Co_x$ ($x = 0-10$)*. Journal of Magnetism and Magnetic Materials, 320: 241–245.
- LIU D.Y., SUN W.S., WANG A.M., ZHANG H.F., HU Z.Q. 2004. *Preparation, thermal stability, and magnetic properties of Fe–Co–Zr–Mo–W–B bulk metallic glass*. Journal of Alloys and Compounds, 370: 249–253.
- MÁLEK J. 2000. *Kinetic analysis of crystallization processes in amorphous materials*. Thermochemica Acta, 355: 239–253.
- MINIĆ D.M., GAVRILOVIĆ A., ANGERER P., MINIĆ D.G., MARIČIĆ A. 2009. *Thermal stability and crystallization of $Fe_{89.8}Ni_{1.9}Si_{5.2}B_{3}C_{0.5}$ amorphous alloy*. Journal of Alloys and Compounds, 482: 502–507.
- NOBUYUKI N., KENJI A., AKIHISA I. 2007. *Novel applications of bulk metallic glass for industrial products*. Journal of Non-Crystalline Solids, 353: 3615–3621.
- OZAWA T. 1970. *Kinetic analysis of derivative curves in thermal analysis*. Journal of Thermal Analysis, 2: 301–324.
- RIBEIRO R. M., SANTOS D. S., BIASI R. S. 2004. *Crystallization kinetics of the $(Fe_{50}Co_{50})_{73.5}Ag_{1}Nb_{9}Si_{13.5}B_{9}$ amorphous alloy*. Journal of Alloys and Compounds, 363: 232–235.
- RIBEIRO R.M., BIASI R.S., SANTOS D.R., SANTOS D.S. 2009. *Nanocrystallization of Fe-based amorphous metallic alloys studied by non-isothermal and isothermal techniques*. Journal of Alloys and Compounds, 483: 495–498.
- SAHINGOZA R., EROLA M., GIBBS M.R.J. 2004. *Observation of changing of magnetic properties and microstructure of metallic glass $Fe_{78}Si_{9}B_{13}$ with annealing*. Journal of Magnetism and Magnetic Materials, 271: 74–78.
- SANTOS D.R., SANTOS D.S. 2001. *Crystallization Kinetics of Fe–B Based Amorphous Alloys Studied in-situ using X-rays Diffraction and Differential Scanning Calorimetry*, Materials Research, 4(1): 47–51.
- SOLIMAN A.A., AL-HENITI S., AL-HAJRY A., AL-ASSIRI M., AL-BARAKATI G. 2004. *Crystallization kinetics of melt-spun $Fe_{83}B_{17}$ metallic glass*. Thermochemica Acta, 413: 57–62.
- WANG H.R., GAO Y.L., YE Y. F., MIN G.H., CHEN Y., TENG X.Y. 2003. *Crystallization kinetics of an amorphous Zr–Cu–Ni alloy: calculation of the activation energy*. Journal of Alloys and Compounds, 353: 200–206.

**THE EFFECT OF THE SURFACE LAYER
OF A PLOWSHARE CHISEL ON PLOWSHARE WEAR
IN MEDIUM LOAM***

Jerzy Napiórkowski, Karol Kołakowski

Department of Vehicle and Machine Design and Operation
University of Warmia and Mazury in Olsztyn

Key words: surface layer, wear, plowshare chisel, medium loam, niobium carbide.

A b s t r a c t

The effect of the surface layer of a plowshare chisel on plowshare wear in medium loam was studied under laboratory conditions. The hardness, percentage composition of chemical elements, including transition metals, and microstructure characteristics of the surface layer were determined. The obtained results suggest that niobium and chromium content and the microstructure of the surface layer significantly affect the intensity of plowshare wear.

**WPLYW RODZAJU WARSTWY WIERZCHNIEJ DŁUTA LEMIESZA PŁUŻNEGO
NA ZUŻYCIE W GLINIE ŚREDNIEJ**

Jerzy Napiórkowski, Karol Kołakowski

Katedra Budowy, Eksploatacji Pojazdów i Maszyn
Uniwersytet Warmińsko-Mazurski w Olsztynie

Słowa kluczowe: warstwa wierzchnia, proces zużycia, dłuto lemiesza, glina średnia, węglík niobu.

A b s t r a k t

Przedstawiono wyniki badań nad wpływem warstwy wierzchniej dłuta lemiesza płużnego na przebieg zużywania w glinie średniej w warunkach laboratoryjnych. Warstwy wierzchnie scharakteryzowano twardością, procentowym udziałem poszczególnych pierwiastków, w tym metali przejściowych, oraz charakterystyką mikrostruktury. Na podstawie przeprowadzonych badań stwierdzono istotny wpływ zawartości niobu, chromu oraz mikrostruktury warstwy wierzchniej na intensywność zużywania.

* Research was conducted under a grant Nr NN504087238

Introduction

The properties of working elements are one of the three principal factors affecting the wear intensity of soil engaging implements. Resistance to wear in the soil is determined by the hardness, plasticity, microstructure, microstructure stability and crystalline anisotropy of the surface layer. The above properties are optimized through the selection of the appropriate chemical composition, including the size, shape and distribution of carbide grains (RUTKOWSKI, STOBIEŃSKI 2007). NAPIÓRKOWSKI (2005) demonstrated that the presence of selected elements which make up the working element intensifies hydrogen absorption (e.g. sulfur), while other elements inhibit the process (e.g. manganese, silicon, carbon). The cited author noted that materials with a high content of C+Cr (45%) and boron (2.7%) were characterized by the highest resistance to wear. The crumbling of hard carbide particles out of the matrix can be inhibited through the use of compounds with a higher content of transition metals and amphoteric elements.

The highest wear intensity is noted in working elements of plowing implements, in particular plowshares, leading to interruptions in tillage operations and increasing process costs. The above problem prompts tool suppliers to search for new structural solutions (e.g. plowshares with chisels) and materials with increased resistance to wear.

Pad welding is one of the methods applied to increase the resistance of working elements. JANKAUSKAS et al. (2008) compared the wear of original and pad welded plowshares in a sugar beet harvester. The authors investigated pad welds with a low carbon and chromium content, pad welds with a high carbon and chromium content, pad welds with a high carbon, chromium, silicon and boron content as well as pad welds with a high carbon, chromium, niobium, molybdenum, tungsten and boron content. The results of their experiment indicate that the wear intensity of standard plowshare material was six-fold higher than that of pad welds containing Fe-C-Cr-Nb-Mo-W-B. It should be noted, however, that the grain size distribution of the processed soil and the chemical composition of the plowshare were not given in the cited study.

The aim of this study is to compare the wear intensity of surfaces faced with iron-based pad welds with a high content of C + Cr and transition metals and plowshare chisels coated with boron steel.

Materials and Methods

The experimental material comprised the surface layers of Kverneland plowshare chisels and chisel surfaces pad welded with materials that increase tilling equipment's resistance to wear (Tab. 1). The investigated plowshare

chisels were made of fine-grained boron steel treated with heat induction. Detailed information concerning the chemical composition of boron steel applied in Kverneland chisels could not be obtained, therefore, it was assumed that its composition is similar to that of boron steel used by other chisel suppliers in the world (Tab. 2).

Table 1

Chemical composition of padded welds [%]

| Element | Abrador 64 | EStelMn60 | EStelMoNb60 |
|---------|------------|-----------|-------------|
| C | 7.0 | 4.40 | 5.11 |
| Mn | 1.73 | 4.82 | 1.02 |
| Si | 0.38 | 1.68 | 1.46 |
| Cr | 24.20 | 29.60 | 21.90 |
| Mo | 0.11 | 0.04 | 7.00 |
| Ni | 0.12 | 0.30 | 0.06 |
| Al | 0.04 | 0.03 | 0.05 |
| Cu | 0.08 | 0.09 | 0.09 |
| P | 0.03 | 0.05 | 0.02 |
| S | 0.01 | 0.01 | 0.02 |
| B | – | 0.03 | – |
| W | – | 0.05 | 2.00 |
| V | 0.06 | – | 1.10 |
| Ti | – | – | 0.03 |
| Nb | 7.00 | – | 7.00 |

Table 2

Characteristics of boron steel used in working elements of soil engaging implements

| Steel type | Chemical composition [%] | | | | | | | |
|-----------------------|--------------------------|------|------|------|------|------|------|-------|
| | C | Si | Mn | P | S | Cr | Ti | B |
| ThyssenKrupp Tbl Plus | 0.35 | 0.25 | 1.30 | 0.04 | 0.03 | 0.14 | 0.03 | 0.003 |
| Ovako 27MnB4 | 0.27 | 0.30 | 1.20 | 0.03 | 0.03 | 0.20 | – | 0.004 |
| Rautaruukki B27 | 0.27 | 0.25 | 1.20 | 0.03 | 0.02 | 0.30 | – | 0.002 |

The hardness of the investigated surface layers was measured with the HMu 10 hardness tester in accordance with standard PN-EN ISO 6507. Microscopic evaluations were carried out using the Neophot 52 microscope with standard and reversed lenses under 50x to 2000x magnification. Surface layers were observed under the TESLA BS340 scanning electron microscope coupled with the TESLA NL-2001A microanalyzer.

A total of 20 samples were prepared, including five samples of every material type. The samples were overlaid using the following low-hydrogen, heavy coated electrodes:

- Abradur 64,
- EStelMn60,
- EStelMoNb60.

Prior to pad welding, traces of corrosion, paint and impurities were removed from the chisels. Additional materials were overlaid in accordance with the manufacturer's requirements at the Laboratory of the Department of Vehicle and Machine Design and Operation. Layers with the thickness of 2.5 mm – 3.0 mm were placed on a rectangular prism cut out from a Kverneland chisel, measuring 30 × 25 × 10 mm. After pad welding, the samples were ground.

The samples were tested in a wear testing machine with the involvement of a "rotating pan method" (Fig. 1). The abrasive substance was natural soil whose grain size distribution was determined as medium silty loam by Bouyoucose-Casagrande's aerometric method modified by Prószyński in accordance with standard BN-78/9180-11 (Tab. 3). Soil moisture was kept constant at approximately 11%. Soil pH(KCl) was 6.19 (slightly acidic).

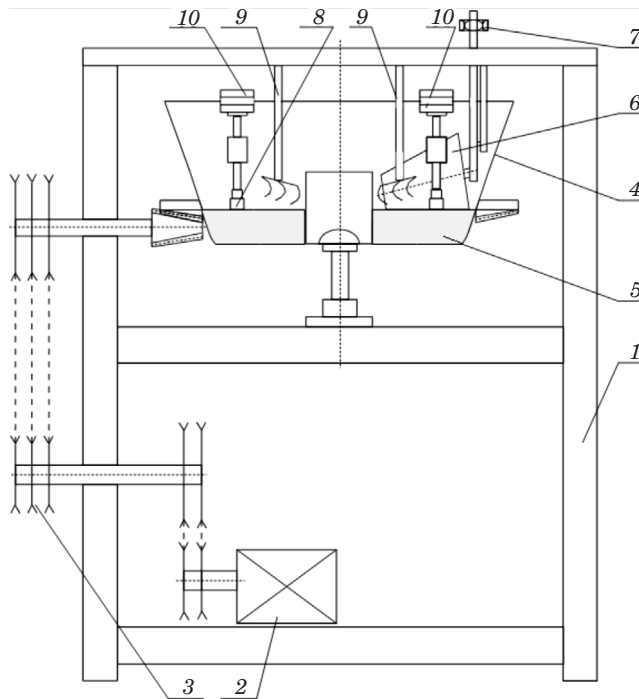


Fig. 1. Test stand for testing wear resistance in soil: 1 – frame, 2 – engine, 3 – belt transmission, 4 – pan, 5 – soil, 6 – crushing rollers, 7 – roller clamp, 8 – sample holder, 9 – loosening forks, 10 – sample weights

Table 3

Grain size distribution in soil

| Grain size groups | Sand | | | Silt | | Clay | | |
|--|-------------------|----------|----------|----------|----------------|-----------------|------------------|--------|
| | 1.0–0.5 | 0.5–0.25 | 0.25–0.1 | 0.1–0.05 | 0.05– –0.02 | 0.02– –0.005 | 0.005– –0.002 | <0.002 |
| Fraction content [%] | 5 | 8 | 21 | 8 | 20 | 16 | 11 | 11 |
| | 34 | | | 28 | | 38 | | |
| Classification as per BN-78/9180-11 | medium silty loam | | | | | | | |

Results and Discussion

The surface layer padded with the Abradur 64 electrode (Table 4) was characterized by the highest hardness and the lowest hardness range, indicating relatively even distribution of chromium and niobium carbides throughout the surface layer (Fig. 2). According to RUTKOWSKI and STOBIERSKI (2009), when a small quantity of chromium carbide is added, microstructures with a niobium and chromium carbide matrix may be single-phase structures containing only solid chromium carbide solution in the matrix carbide, or two-phase structures containing Cr_{23}C_6 as well as Cr_7C_3 .

Table 4

Results of hardness measurements

| Series | Average hardness HV10 | Standard deviation HV10 | Confidence interval boundaries $\alpha = 0.05$ HV10 | Range HV10 |
|------------------|--------------------------|----------------------------|---|------------|
| Kverneland steel | 597.56 | 14.54 | 586.59 ÷ 608.52 | 48 |
| EStelMoNb60 | 723.89 | 61.00 | 677.88 ÷ 769.90 | 161 |
| Abradur 64 | 760.56 | 28.50 | 739.06 ÷ 769.90 | 77 |
| EStelMn60 | 678.67 | 44.69 | 644.96 ÷ 712.37 | 130 |

The second highest hardness value was reported for the EStelMoNb60 padded weld which was characterized by highly irregular distribution of numerous Mo_2C , VC and TiC carbides (Fig. 3). The microstructure of the EstelMn60 weld (Fig. 4) comprised primary carbides with diverse thickness and length and $[\alpha + (\text{Fe}, \text{Cr})_7\text{C}_3]$ eutectic. The lowest hardness range was observed in respect of boron steel. The reference microstructure of boron steel is presented in Figure 5.

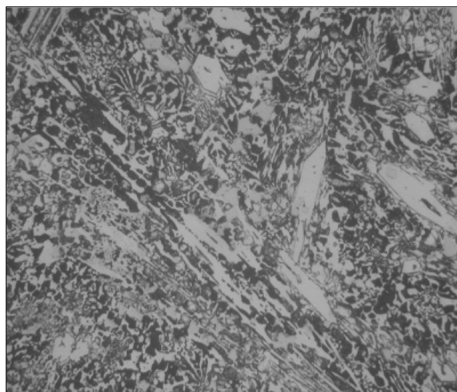


Fig. 2. Microstructure of Abradur 64 padded weld

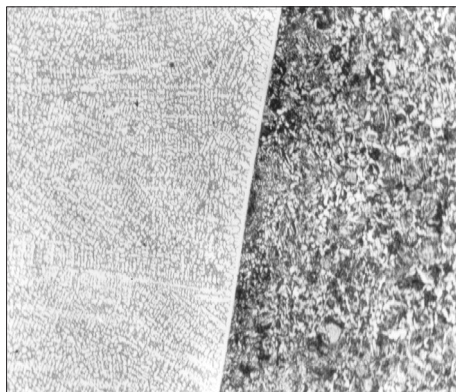


Fig. 3. Microstructure of EStelMoNb60 padded weld

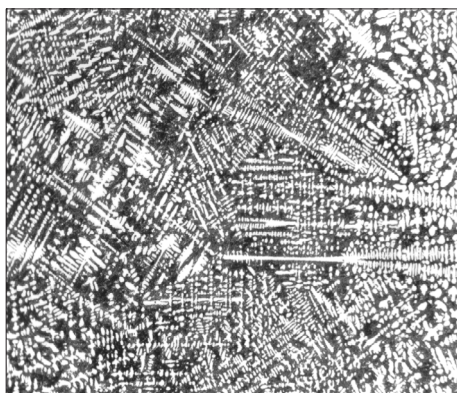


Fig. 4. Microstructure of EStelMn60 padded weld

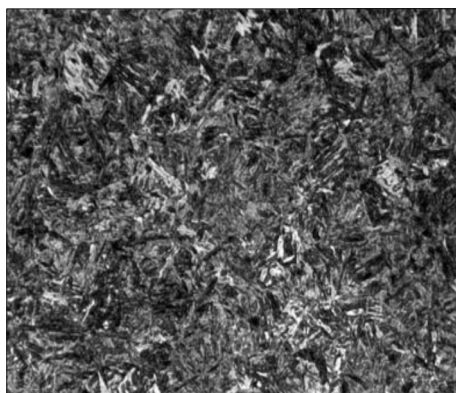


Fig. 5. Microstructure of boron steel
Source: ŁABĘCKI et al. (2007)

In the studied group of structural materials, surface layers containing niobium, transition metal of group VB in the periodic table, were characterized by the highest resistance to wear (Fig. 6). Niobium carbides were marked by significant structural variation, thus supporting the production of ceramic matrix composites (CMC). Structural variations in niobium carbides NbC (hardness of 1800 HV) limits the solubility of chromium carbides in the network carbide, thus supporting the synthesis of $\text{NbC}_{0.95}\text{-Cr}_{23}\text{C}_6$ composites (RUTKOWSKI, STOBIEŃSKI 2009). The resulting structure significantly reinforces the surface layer whose resistance to wear increases with its C and Cr content.

The wear intensity of pad welded surface layers was more than 21.3- (Abradur 64) to 3.5-fold (EStelMn 60) lower than that of Kverneland boron steel (Fig. 7).

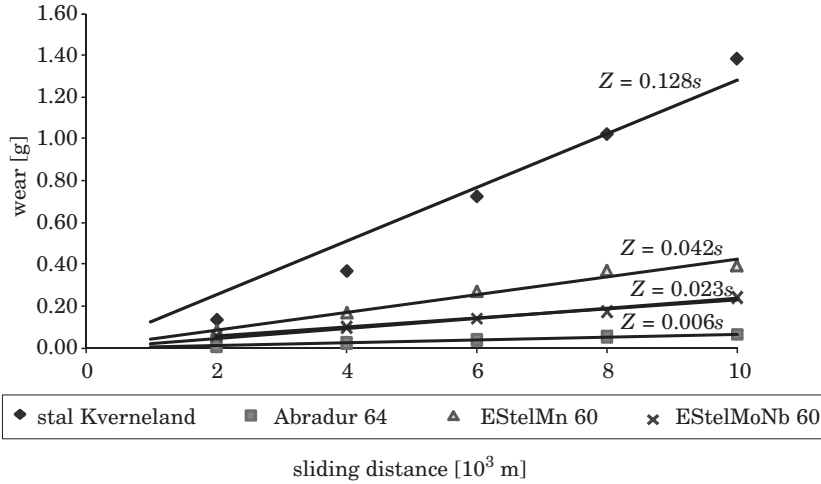


Fig. 6. Wear of padding welds as a function of sliding distance

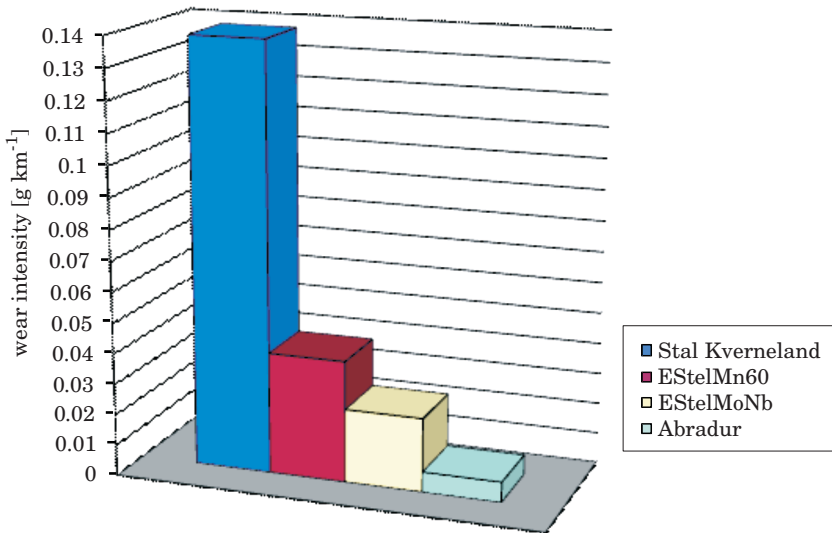


Fig. 7. Wear intensity of padded welds in medium silty loam

Conclusions

The pad welding technology supports the selection of surface layer properties that best match working process requirements. In comparison with boron steel, iron-based welds are characterized by significantly higher resistance to wear in the soil environment. The highest resistance to wear in medium silty

loam was reported for surfaces padded with the Abradur 64 electrode with weld hardness of 760 HV10. The average wear of Kverneland boron steel was more than 20-fold higher in comparison with Abradur 64 welds. Wear intensity in medium silty loam decreases with a rise in the niobium and chromium content of welds, thus contributing to the formation of surface layers that are highly resistant to wear. The wear intensity of a surface layer is determined by its structural homogeneity and the range of surface hardness.

Translated by ALEKSANDRA POPRAWKA

Accepted for print 21.03.2011

References

- JANKAUSKAS V., KREIVAITIS R., STONKUS D., ANDRIUŠIS A. 2008. *Research of strengthening plough parts by welding*. *Mechanika*, 1(69): 80–84.
- ŁABECKI M., GOŚCIAŃSKI M., KAPCIŃSKA D., PIROWSKI Z. 2007. *Badania tribologiczne, wytrzymałościowe i strukturalne wybranych materiałów stosowanych na elementy maszyn rolniczych pracujące w glebie*. *Journal of Research and Applications in Agricultural Engineering*, 52(2): 68–77.
- NAPIÓRKOWSKI J. 2005. *Zużyciowe oddziaływanie gleby na elementy robocze narzędzi rolniczych*. *Inżynieria Rolnicza*, 17.
- RUTKOWSKI P., STOBIERSKI L. 2009. *Ewolucja mikrostruktury tworzyw kompozytowych z węglików metali przejściowych*. *Materiały Ceramiczne*, 2(61): 140–145.

**WORK INDICATORS TEST FOR PROTOTYPE
JOHN DEERE 6830 AGRICULTURAL TRACTOR
FUELED WITH PURE VEGETABLE OIL**

Piotr Pasyniuk¹, Wojciech Golimowski²

¹ Institute of Technology and Life Sciences, Department in Warsaw

² Institute of Technology and Life Sciences, Department in Poznan

Key words: diesel fuel, pure plant oil fuel, tractor engine power, fuel consumption.

A b s t r a c t

The paper summarizes results of tests of John Deere agricultural tractor type 6830 fueled with pure raps oil. The measurements were performed using an electro-magnetic brake connected to the tractor with a power transfer shaft (WOM). Specification of the engine fueled with pure raps oil was drawn up during the tests and it was compared with the engine fueled with diesel. The main conclusions include identification of a power drop of the engine fueled with the raps oil by an average of 10% in comparison with the same engine fueled with diesel and increase of fuel consumption per kWh by 15%. The identified drop of power had no impact of work efficiency including power consuming agricultural works.

**BADANIA WSKAŹNIKÓW PRACY PROTOTYPOWEGO SILNIKA CIĄGNIKA
ROLNICZEGO JOHN DEER 6830 ZASILANEGO NIEPRZETWORZONYM
OLEJEM ROŚLINNYM**

Piotr Pasyniuk¹, Wojciech Golimowski²

¹ Instytut Technologiczno-Przyrodniczy w Falentach, Oddział w Warszawie

² Instytut Technologiczno-Przyrodniczy w Falentach, Oddział w Poznaniu

Sł o w a k l u c z o w e: olej napędowy, czysty olej roślinny, moc ciągnika, zużycie paliwa.

A b s t r a k t

W artykule podsumowano wynik badań ciągnika rolniczego marki John Deer typu 6830 zasilanego czystym olejem rzepakowym. Pomiar prowadzono z wykorzystaniem hamulca elektromagnetycznego podłączonego do ciągnika przez wałek odbioru mocy (WOM). W trakcie badań sporządzono zewnętrzną charakterystykę silnika zasilanego czystym olejem roślinnym i w celu

porównania – olejem napędowym. Zauważono spadek mocy silnika zasilanego olejem roślinnym średnio o 10% w stosunku do tego samego silnika zasilanego olejem napędowym oraz zwiększone o 15% jednostkowe zużycie paliwa w przeliczeniu na kWh. Zarejestrowany spadek mocy nie miał wpływu na efektywność wykonywanej pracy także podczas wykonywania energochłonnych prac polowych.

List of units

M_o – torque [Nm]

N_e – effective power [kW]

G – fuel consumption [kg h⁻¹]

g_e – fuel consumption per unit [g kWh⁻¹]

Introduction

In the twentieth century crude oil has become a strategic resource for the whole global economy. The first diesel engine was developed in line 1890s. It revolutionized the world and diminished importance of steam engines. Initially it was fueled with raps oil. Fast development of crude oil extraction and its processing resulted in replacement of raps oil with diesel produced from crude oil. The first major energy crisis took place in 1970s. It caused increase of prices of diesel and undermined fuel supply. The crisis triggered research for alternative fuel for common use in internal combustion diesel engines. The idea of use of raps oil as an alternative source of fuel for diesel engines was reconsidered. Characteristics of raps oil, however, significantly differs from parameters of diesel. Therefore simple replacement of crude-oil derivative fuel with raps oil in commonly used engines is impossible, mainly due to the significantly higher viscosity of this liquid. Tests of six different diesel engines indicated that engines with direct fuel injection cannot be fueled with raps oil due to high growth of deposits in a combustion chamber (HEMMERLEIN et. al. 1991). Similar results were presented by VELLGUTH (1983) who observed residues in injector nozzles which stopped engines after just 50 working hours. In 1964 Klaus Elsbett developed an engine with hearth combustion chamber adjusted to combustion of raps oil (BOCHEŃSKI 2003). The solution, however, cannot be applied to ready engines since the adjustment of a finished engine would require significant structural changes.

Rape oil, in comparison with diesel, is characterized by high viscosity with an impact on distribution of an oil spray in a combustion chamber. Fuel and air mix is not fully combusted in a cylinder chamber and produces residues. Viscosity of raps oil drops rapidly with increase of temperature and at 70oC it is similar to viscosity of diesel oil. This property of raps oil was used to test an agricultural tractor equipped with a double tank installation (BOCHEŃSKI 2008). Results of operating tests indicated that it was a good solution.

It, however, has some significant disadvantages. Firstly, the vehicle is equipped with two independent fuel tanks. Secondly, diesel has to be used to start up the engine and operate it until coolant is heated to a high temperature (DZIENISZEWSKI 2006). Comparison of parameters of rapeseed oil and diesel oil clearly indicates that a rapeseed oil engine would have less power. Research performed by Polish scientists indicated that application of rapeseed oil resulted in a power drop of approximately 10–20% combined with an increase of fuel consumption per unit by approximately 15–25%. (ZBŁOCKI 1990, LOTKO 1995, SZLACHTA 2002).

The company John Deere, a global manufacturer of agricultural machines, produced a prototype agricultural tractor adjusted for combustion of pure rapeseed oil based on structural changes developed by a team of engineers of the company Vereinigte Werkstätten Pflanzenöntechnologie GbR (VWP), Germany. Changes related only to the engine accessories and presented them in Figure 1.

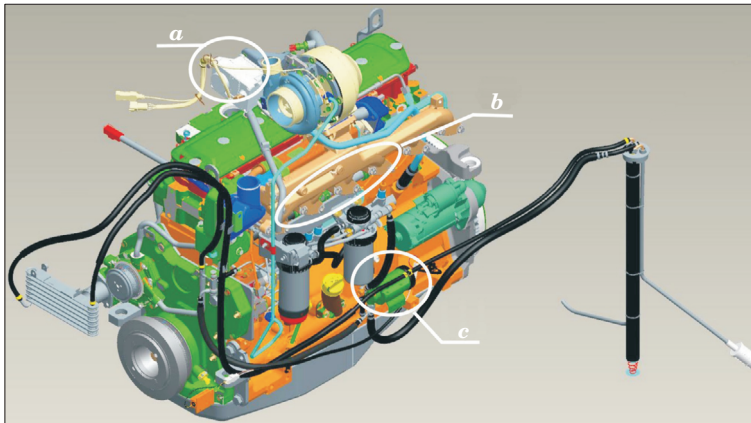


Fig. 1. Major changes in the gear motor. Software engine control computer (a) has been change, was used fuel heater combined with the injectors (b) and increased power of the fuel pump (c)

Sixteen tractors were prepared for tests. They are operated in farms in Austria, France, Germany and Poland. Tests are co-funded by the European Union under the project TREN/FP7/219004/2ndVegOil.

Test Object and Description of the Test Site

The tests were designed to compare parameters of an engine fueled with rapeseed oil and diesel. The test tractor was one time fueled with diesel to compare its power distribution and fuel consumption.

The tests were conducted on John Deere 6830 agricultural tractor equipped with six cylinder engine with turbocharger generating power of 102 kW (140 KM). Introduced changes allowed the tractor to be fully fueled with raps oil even when it was started in low temperature. Prior to the tests the tractor worked for 300 mth. Technical specification of the engine was based on operating manual presented in Table 1.

Table 1

Basic parameters of the tested engine

| | |
|--|---|
| Engine type | 6068HL481 |
| Max. engine power in accordance with 97/68/EC | 103 kW |
| Intelligent power management (momentary power) | 121 kW |
| Max. torque | 620 Nm at 1 400 rpm |
| Number of cylinders | 6 |
| Cylinder diameter / piston travel | 106.5 mm/127 mm |
| Displacement | 6790 cm ³ |
| Nominal revolution | 2100 rpm |
| Range of operating revolutions | 1300–2100 rpm |
| Size and type of injection system | PowerTech, 4 Valves |
| Air intake system | Turbocharger with active air cooling system |
| Fuel injection system | High-pressure “CommonRail” |
| Combustion chamber | Swirl chamber |

The tests were conducted in the Institute’s branch in Poznań in Autumn 2009 in good weather and the average ambient temperature of 18°C. The tractor was prepared one day prior to the actual tests. Fuel meter was connected to a fuel installation at the main fuel tank. The fuel meter consisted of a strain scales connected to the control system. Scales measurement cylinder with the capacity of approximately 1.2 dm³ was fueled through a solenoid valve from a tank with the capacity of 10 dm³ located above the scales. In addition, a return fuel line from the engine was connected to the scales.

A mobile engine brake PT 301 MES was connected through the power transmission shaft (WOM). It is a dynamometric device mounted on a stable frame structure which can be easily disassembled and transported. It is equipped with an independent control system and PC output used to register measurement signals. A shaft (WOM) socket located at the back of the brake. It was used to connect the agricultural tractor through a telescopic shaft. The device records two parameters: torque on the shaft between the tractor and two electromagnetic brakes and the shaft rotation speed. The above data is uploaded to software which draws a curve showing relationship between torque and power, and the engine speed. Test station is presented on Figure 2.



Fig. 2. Test station

Test Methodology

The test started with heating up of the engine to the operating temperature. During the measurements the engine coolant temperature was maintained between 79 and 83°C. At the same time data necessary for calculations was uploaded to the PC connected to the brake. Data about coupling between the engine and WOM was entered which for the tractor amounted to 2000:1000. Other information included air temperature, atmospheric pressure and WOM revolution setting at the output. The tractor was tested at the speed of 1000 rpm.

The first test was conducted using raps oil. The tractor's operator turned on the power transfer shaft and set the maximal engine speed at 2250 rpm. A potentiometer controlling the brake was used to set a point when the engine speed started to drop and then the first measurement point was recorded at 2200 rpm. Subsequent points were recorded every 50 rpm until the engine reached 1200 rpm.

The range of measured engine speed reflected the full power potential of the engine. During the second test the engine was fueled with summer diesel purchased in a gas station located in the vicinity of the test site. The measurement was conducted in accordance with the same methodology as applied to the raps oil.

Test Results

The following table presents results measured and calculated by PC connected to the brake, as well as readings from the fuel meter.

Table 2

Parameters of the engine of the tested agricultural tractor

| Engine speed [rpm] | Diesel test | | | Raps oil test | | |
|-----------------------|---------------|---------------|------------------------------|---------------|---------------|------------------------------|
| | M_o [Nm] | N_e [kW] | G [kg h ⁻¹] | M_o [Nm] | N_e [kW] | G [kg h ⁻¹] |
| 2200 | 214 | 50.5 | 16.33 | 188 | 43.8 | 17.72 |
| 2150 | 363 | 83.2 | 21.76 | 302 | 68.9 | 21.58 |
| 2100 | 389 | 86.6 | 22.26 | 317 | 70.5 | 22.23 |
| 2050 | 413 | 90.2 | 22.54 | 337 | 73.6 | 22.14 |
| 2000 | 442 | 94.0 | 23.56 | 368 | 78.0 | 23.45 |
| 1950 | 460 | 95.7 | 23.12 | 394 | 81.6 | 23.85 |
| 1900 | 484 | 97.9 | 23.46 | 420 | 84.5 | 24.38 |
| 1850 | 504 | 99.3 | 23.80 | 438 | 86.2 | 24.34 |
| 1800 | 526 | 100.5 | 23.85 | 455 | 87.2 | 24.55 |
| 1750 | 544 | 101.4 | 23.80 | 477 | 88.8 | 25.2 |
| 1700 | 563 | 101.9 | 24.30 | 497 | 89.9 | 25.18 |
| 1650 | 579 | 101.3 | 24.32 | 505 | 90.5 | 25.47 |
| 1600 | 584 | 99.6 | 24.17 | 516 | 87.6 | 24.82 |
| 1550 | 577 | 94.6 | 22.90 | 512 | 84.6 | 23.96 |
| 1500 | 581 | 92.5 | 22.01 | 514 | 82.0 | 22.62 |
| 1450 | 582 | 89.6 | 21.39 | 514 | 79.4 | 21.64 |
| 1400 | 574 | 84.3 | 19.50 | 504 | 75.2 | 19.80 |
| 1350 | 572 | 81.7 | 18.19 | 494 | 70.7 | 19.10 |
| 1300 | 572 | 78.8 | 17.66 | 494 | 68.5 | 18.00 |
| 1250 | 566 | 74.8 | 17.07 | 492 | 65.3 | 17.30 |
| 1200 | 566 | 72.2 | 16.32 | 498 | 61.7 | 16.51 |

The speed range of 2200–1200 rpm fully reflected distribution of power and torque of the tested engine. The maximal power generated by the tested engine fueled by diesel and raps oil amounted to 101.9 kW and 90.5 kW, respectively. Obtained test results allowed us to draw a curve reflecting distribution of tested parameters and perform a comparative analysis of various types of fuel. The following drawing presents distribution of the tractor's power in relation to torque for raps oil and diesel.

The above numbers shows, that the maximal and minimal power and torque values are observed at the same crankshaft speed for both fuel type. For the tested engine the optimal speed at which torque and power curves cross, amounts to 1700 rpm. The difference between generated power is stable through the whole range of speed and amounts to approximately 10%. Tests performed by HEMMERLEIN and KORTE (1991) indicated that the power drop

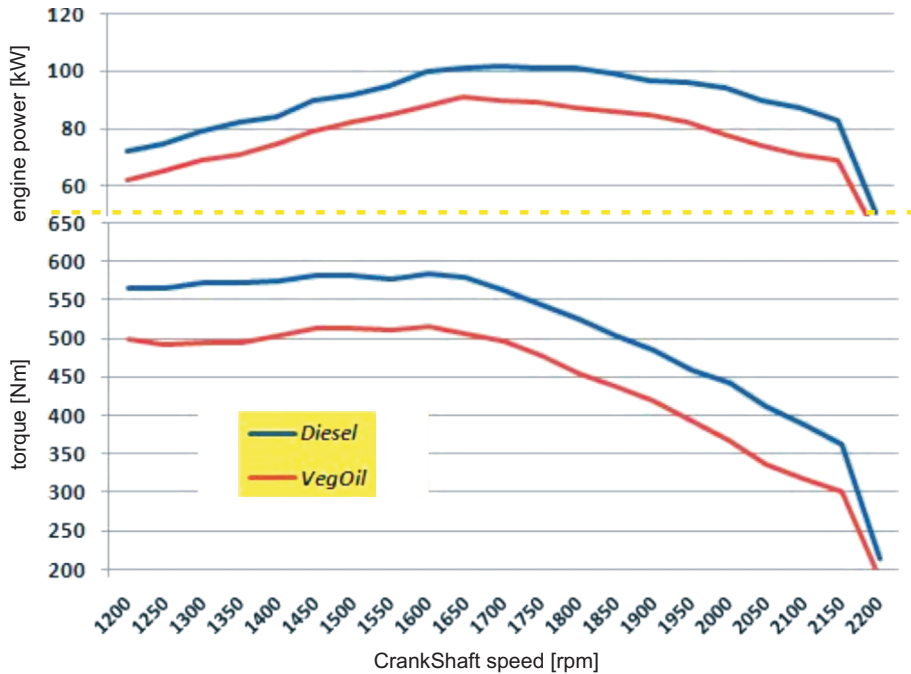


Fig. 3. Relation between torque and power of the tested engine

for the tested engine with direct injection generating power of 40 kW amounted to just 2%. It ought to be noted, however, that the tested engine was damaged after 155 hours of work. Tests performed in Lublin University of Technology on a high-speed engine with direct injection and a vortex combustion chamber confirmed the power drop of 10% (KIERSKI, STRZEŚLY 1994). Power consumption curves for both tests were drawn based on fuel consumption and power data (Fig. 4).

The tests indicate that consumption of raps oil per hour is comparable to diesel. There was a slight difference at the engine speed of 1500–2000 rpm. Raps oil is on average 12% more dense than diesel and its calorific value is by 17% lower (MATYSCHOK 2001). Consequently, these properties have an impact on volume of consumed fuel. Raps oil consumption per kWh is on average by 15% higher than consumption of diesel. It is related to the fact that the tractor fueled by raps oil generated on average 10% less power. In addition, a slight raps oil consumption per hour also has an impact on the parameter.

Comparison of differences of power generated by the tested tractor and fuel consumption per unit with results of other Polish tests which achieved 10–20% power drop and 15–25% increase of fuel consumption leads to the conclusion

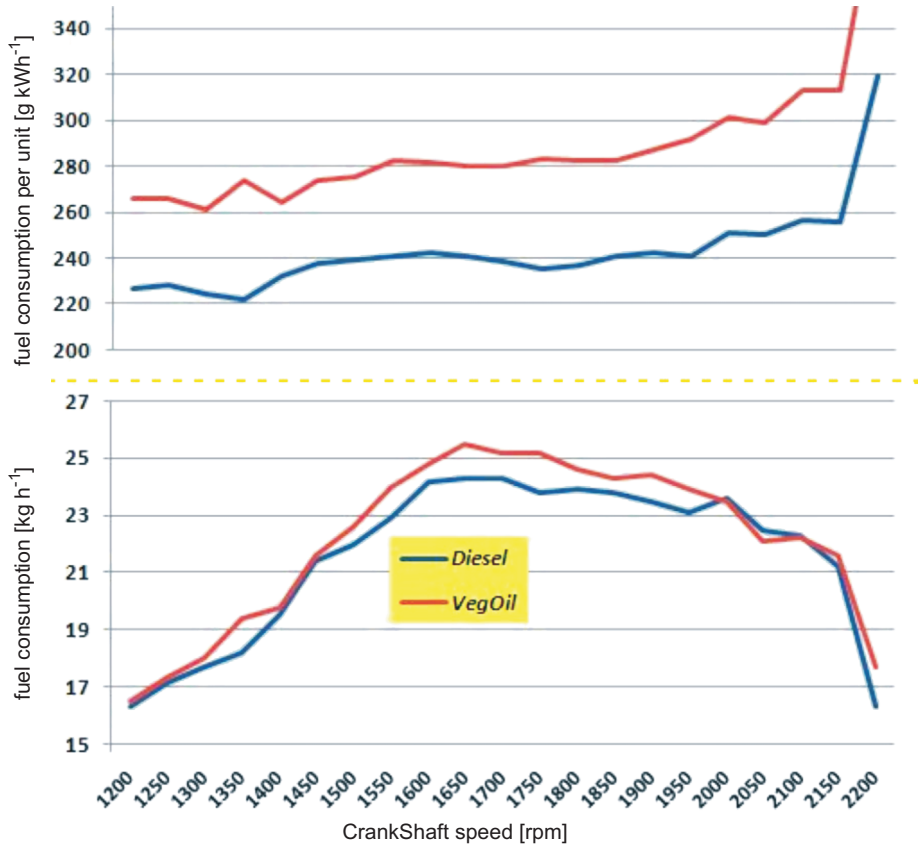


Fig. 4. Fuel consumption per hour and unit

that the tested tractor fueled with raps oil could be classified at the lowest edge of the difference brackets.

Conclusions

1. Innovative structural solutions introduced by the company John Deere allow for use of the tractor fueled with pure raps oil. In addition, there was no problem with starting up of the tractor in low temperature.

2. Performed tests indicated power drop of 10%. In comparison with earlier tests which identified 10–20% power drops, the achieved result ought to be deemed as good.

3. Considering 10% power drop and little change of power consumption per hour, raps oil consumption per unit is by 15% higher than diesel consumption.

In theory, a tractor fueled with rapeseed oil would consume 15% more fuel than an engine fueled with diesel.

Translated by MICHAŁ IWANCUK

Accepted for print 7.10.2010

References

- BOCHEŃSKI C.I. 2003. *Biodiesel paliwo rolnicze*. Wydawnictwo SGGW, Warszawa.
- BOCHEŃSKI C., KIRYLUK J. 2008. *Prace badawcze Pronaru*. Pronar, 4(7).
- DZIENISZEWSKI G. 2006. *Analiza możliwości zasilania silnika diesla surowym olejem roślinnym*. Inżynieria Rolnicza, 12.
- HEMMERLEIN N., KORTE V., RICHTER H., SCHROEDER G., 1991. *Performance, exhaust emissions and durability of modern diesel engines running on rapeseed oil*. SAE Technical Papers Series, 91 0848.
- LOTKO W. 1995. *Zasilanie silników spalinowych paliwami alternatywnymi*. Wydawnictwo Instytutu Technologii Eksploatacji, Radom.
- KIERSKI Z., SZCZĘSNY P. 1994. *Badania silnika wysokoprężnego S-4002 zasilanego biopaliwem na bazie oleju rzepakowego*. Journal of KONES, 94.
- MATYSCHOK H. 2001. *Odnawialne, oparte na olejach roślinnych, alternatywne paliwa dla silników wysokoprężnych*. Chemik, 3.
- SZLACHTA Z. 2002. *Zasilanie silników wysokoprężnych paliwami rzepakowymi*. Wydawnictwo Komunikacji i Łączności, Warszawa.
- VELLGUTH G. 1983. *Performance of vegetable oils and their monoesters as fuels for diesel engines*. SAE Transactions, 83 1358.
- ZABŁOCKI M. 1990. *Olej rzepakowy jako paliwo do silników wysokoprężnych*. Teza Komisji Naukowo-Problemovej PAN, Oddział w Krakowie 2.

**THE USE OF FRICTION PARAMETERS
IN EVALUATING THE TECHNICAL CONDITION
OF ROLLING BEARINGS BY THE QUASI-DYNAMIC
METHOD***

Arkadiusz Rychlik, Jerzy Napiórkowski

Department of Vehicle and Machine Design and Operation
University of Warmia and Mazury in Olsztyn

Key words: rolling bearing, technical condition, friction parameters, quasi-dynamic method.

Abstract

This paper evaluates the technical condition of rolling bearings by the quasi-dynamic method where a physical pendulum was used as an investigative tool. Friction characteristics as attributes of the diagnostic signal were distinguished to support an evaluation of the technical condition of rolling bearings. The coefficient of friction under oscillating motion was identified as a generalized diagnostic parameter in evaluations of the technical condition of ball bearings.

**ANALIZA WYKORZYSTANIA PARAMETRÓW TARCIA W OCENIE
STANU TECHNICZNEGO ŁOŻYSK TOCZYNYCH METODĄ QUASI-DYNAMICZNA**

Arkadiusz Rychlik, Jerzy Napiórkowski

Katedra Budowy, Eksploatacji Pojazdów i Maszyn
Uniwersytet Warmińsko-Mazurski w Olsztynie

Słowa kluczowe: łożyska toczne, stan techniczny, parametry procesów tarcia, metoda quasi-dynamiczna.

Abstract

Przedstawiono metodę identyfikacji stanu technicznego łożysk tocznych metodą quasi-dynamiczną, w której jako narzędzie badawcze zastosowano wahadło fizyczne. Wyróżniono parametry procesów tarcia jako cechy sygnału diagnostycznego umożliwiającego ocenę stanu technicznego łożysk tocznych. Wskazano na współczynnik tarcia w ruchu oscylacyjnym jako uogólniony parametr diagnostyczny w ocenie stanu technicznego łożysk kulkowych.

* Research was conducted under a grant No NN504087238.

Introduction

Rolling bearings are among the most frequently replaced components during a machine's life. In standard practice, the technical condition of bearings is evaluated subjectively, and as a result, nearly 34% of rolling bearings are prematurely scrapped (DWOJAK, RZEPIELA 2003). In the majority of cases, the above is due to the absence of generally available methods for a quick and reliable identification of the technical condition of bearings in the verification process. The need to optimize machine operating costs and environmental protection requirements call for new methods that support the identification of the actual state of rolling bearings before they are classified as fit for repair or replacement.

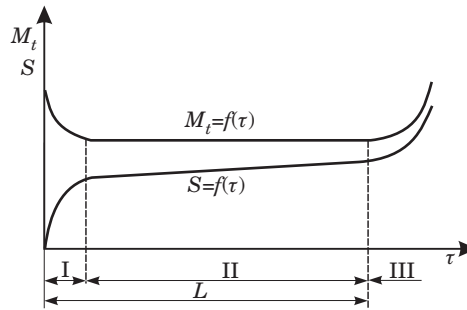
The nominal operating parameters of a bearing assembly can be reinstated by replacing or repairing the bearing. Subject to the required servicing effort, the cost of repairing a damaged bearing is equivalent to 50–90% of the price of a brand-new bearing (ROGER 2004).

A number of methods have been proposed for diagnosing the technical condition of rolling bearings of varied complexity and localizing the site of damage in the assembly:

- organoleptic method (*Łożyska toczne* 2005, *Poradnik obsługi...* 1994);
- evaluation of radial clearance, axial clearance and bearing misalignment (*Łożyska toczne* 2005, *Poradnik obsługi...* 1994);
- physical and chemical analyses of bearing lubricant (*Łożyska toczne* 2004, *Poradnik obsługi...* 1994);
- determination of the coefficient of friction (CAPANIDANIS, CZARNY 2003);
- coasting method (BIELAWSKI 2003).

The main problem in evaluating the condition of bearings is the determination of boundary values of the diagnostic signal which support unambiguous identification of the degree of wear. Most of the existing methods for identifying the condition of rolling bearings rely on their geometric characteristics rather than usable properties which generate vast quantities of practical information.

The above approach has been described by STYP-REKOWSKI (2001) who investigated the use of diagnostic signals in analyses of the technical condition of special-purpose rolling bearings. The results of the cited study indicate that the moment of friction is a robust measure of the degree of wear. An increase in the moment of friction to the value referenced for brand-new, broken-in bearings was proposed as the boundary value of the diagnostic signal. The life cycle curve of rolling bearings was shown to have a bathtub shape where the moment of friction is a function of its curvature $M_i = f(\tau)$ – Fig. 1.



$M_t = f(\tau)$ – moment of friction at constant rotational speed, $S = f(\tau)$ – intensity of wear symptom, I – degressive increase in wearing symptom (breaking-in), II – constant level or minor increase, III – progressive increase in wear symptom, L – service life of a hypothetical rolling bearing

Fig. 1. Life cycle curve of a rolling bearing as a function of time

Source: STYPIŃ-REKOWSKI (2001).

Friction power which is a measure of wear intensity in bearing assemblies of a combustion engine was proposed as the diagnostic signal by BIELAWSKI (2003). Friction power is identified during engine run-up and run-down in terms of mechanical efficiency and/or the product of the moment of friction and the rotational speed of the engine's crankshaft.

The objective of this study was to investigate the option of using friction parameters as diagnostic signals for evaluating the technical condition of ball bearings by the quasi-dynamic method.

Materials and Methods

The quasi-dynamic evaluation of the technical condition of rolling bearings relied on the identification of the characteristics of a physical pendulum's oscillating motion. Changes in the pendulum's angular velocity were analyzed at known energy required to displace the pendulum from its equilibrium position. Initial angular displacement α was adopted as a measure of displacement from equilibrium in accordance with the mathematical model proposed by RYCHLIK (2008). Signals were analyzed in a test stand (Fig. 2) comprising a base (1) and a physical pendulum (2). The examined bearing (3) was placed in the housing of the pendulum machine, and it was mounted in a self-centering clamp to immobilize the bearing's inner raceway relative to its outer raceway. The angular velocity of the bearing which carried the load of the pendulum ($m = 1.67$ kg) was measured using the CF-110 (4) photo-optical sensor and the KSD-400 measurement analyzer (5).

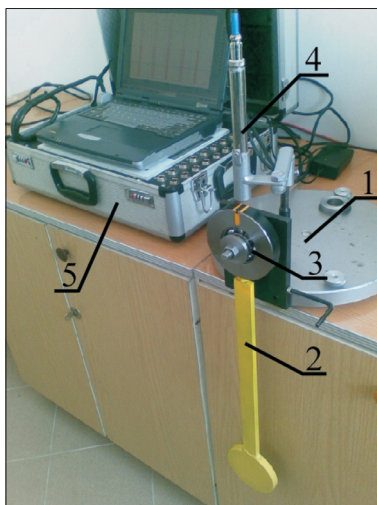


Fig. 2. Test stand for identifying the technical condition of rolling bearings by the quasi-dynamic method (described in the text)

Diagnostic signal parameters required for the assessment of the bearing's technical parameters were measured only during the pendulum's clockwise return to equilibrium. The pendulum's movement was measured in only one direction to avoid static and dynamic calibration during bearing replacement.

The results of previous studies (RYCHLIK 2008) indicate that the above method can be applied to inspect the condition of single-row ball bearings which are characterized by an absence of sealants or lubricants, normal clearance and an absence of ring misalignment. The pendulum's aerodynamic drag and the bearing's mass were not taken into account. Diagnostic signal parameters were identified at the lowest position of the pendulum.

Selected parameters of diagnostic signals for evaluating the usability and the quality of the signal conveying information about the technical condition of bearings are presented in Table 1.

The initial identification of the signal relied on a statistical analysis of the observed angular velocity values of the pendulum and the examined bearing's outer ring. The results of the analysis suggested that in the tested environment, angular velocity was a stationary and a repeatable signal.

Results and Discussion

The experimental material comprised single-row, unsealed rolling bearings. Five brand-new CX 6305 rolling bearings and five bearings with various

Table 1
Parameters of diagnostic signals describing the technical condition of rolling bearings

| Diagnostic signal parameter | Symbol | Formula | Remarks |
|--|-----------------------------|---|---|
| Period of swing | T [s] | – | |
| Number of swings | i | – | the number of times the pendulum swings through its lowest position |
| Coefficient of friction under oscillating motion | μ_o | $\mu_o = \frac{720 \cdot mg \cdot e \cdot (1 - \cos \alpha)}{\pi \cdot i \cdot \alpha \cdot m \cdot (D + d)}$ | – |
| Viscotic damping coefficient | C_w [Nm s ⁻¹] | $C_w = \frac{mg \cdot e \cdot \sin \alpha - I_o \cdot \varepsilon}{\omega}$ | coefficient defined in angular motion |
| Moment of friction | M_t [Nm] | $M_t = I_o \cdot \alpha = I_o \cdot \frac{\omega_1 - \omega_2}{\Delta t}$ | – |
| Coefficient of rolling friction | f_t [m] | $f_t = \frac{M_t}{mg}$ | indicates the condition of the surface of bearing elements |
| Friction power | W_t [Wat] | $W_t = M_t \cdot \alpha$ | generalized mechanical efficiency of a bearing |

where: α – initial angular displacement; e – distance between the pendulum's center of gravity and the pivoting point; mg – pendulum's gravity force; D , d – bearing's outer and inner diameter, respectively; I_o – pendulum's mass moment of inertia relative to the pivoting point; ω_1 , ω_2 – pendulum's angular velocity at the lowest position for two successive swings.

Source: own study based on KOWAL (2003), RYCHLIK (2008)

wear symptoms, up to 89 million revolutions at the nominal load torque, were used. The investigated parameters were measured for each bearing in five replications.

The base of the test stand was leveled, and the pendulum with the bearing were mounted in a self-centering clamp. Changes in the pendulum's angular velocity were registered using a photo-optical speed sensor and a signal recorder.

The pendulum was displaced from its equilibrium position by angle α , and changes in the period of swing between two mark points on the pendulum machine were registered. The mark points supported the identification of the pendulum's angular velocity at its lowest position which corresponds to its highest angular velocity. The time of the pendulum's swing between mark points was measured only in the clockwise direction (right to left).

The obtained results suggest that angular velocity of the bearing's outer raceway increased with a rise in the period of swing, and that a higher degree of bearing wear was accompanied by lower angular velocity. The above did not apply to brand-new bearings. The time course of angular velocity of outer raceways in bearings marked by a higher degree of wear, determined at the lowest position of the pendulum, is presented in Figure 3.

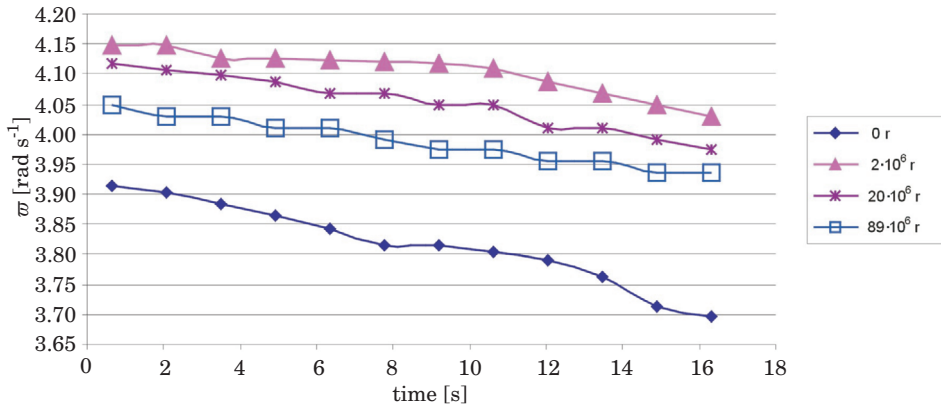


Fig. 3. Time course of angular velocity of bearings 6305 marked by different degree of wear

The angular velocity (ω) and angular acceleration (ε) of the pendulum for brand-new bearings as a function of: period of swing (t), number of swings (i) and the angle of displacement (α) at the lowest position of the pendulum, are presented in Figure 4.

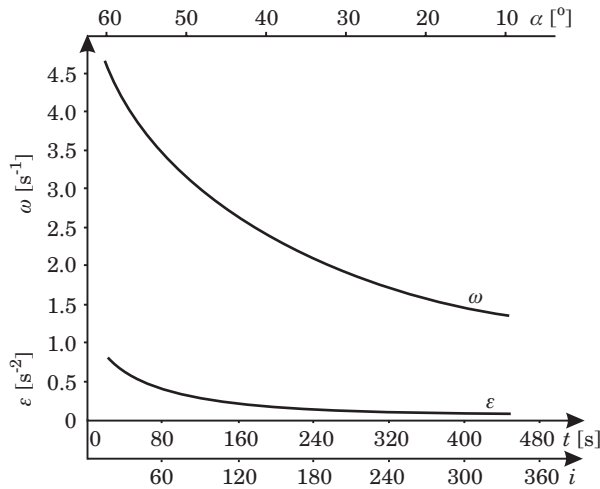


Fig. 4. Time course of angular velocity and angular acceleration of the outer raceway of bearing 6305, subject to the period of swing, the number of swings and initial angular displacement

Figure 5 illustrates changes in friction power W_i and the moment of friction M_i of brand-new bearings as a function of the period of swing at the lowest position of the pendulum.

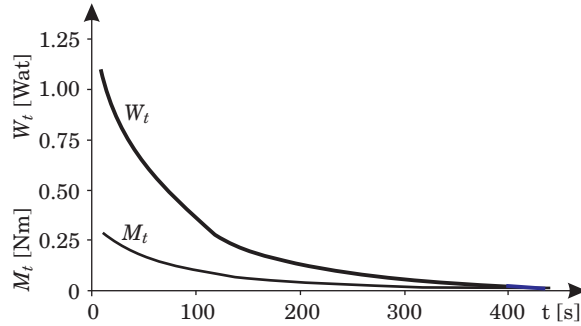


Fig. 5. Time course of friction power (W_t) and the moment of friction (M_t) of bearing 6305

The results of the experiment supported the determination of the values of diagnostic signal parameters for five brand-new bearings at the lowest position of the pendulum. The resulting values are presented in Table 2.

Table 2

Values of diagnostic signal parameters for bearing 6305

| Diagnostic signal parameter | Symbol | Average value | Standard deviation |
|--|--------------|---------------|--------------------|
| Period of swing | T [s] | 454.6 | 2.88 |
| Number of swings | i | 320.2 | 1.788 |
| Coefficient of friction under oscillating motion | μ_o | 0.01218 | 0.00011 |
| Viscotic damping coefficient | C_w [Nm/s] | 0.063 | 0.00408 |
| Moment of friction | M_t (Nm) | 0.278 | 0.01095 |
| Coefficient of rolling resistance | f_t [m] | 0.0134 | 0.00612 |
| Friction power | W_t [Wat] | 1.034 | 0.04560 |

The value of the coefficient of friction under oscillating motion μ_o is significantly higher than the referenced value stated by the manufacturer. The coefficient of friction for an unsealed CX rolling ball bearing is $\mu = 0.0010 \div 0.0015$ (Łożyska toczne 2005), and for an SKF bearing – $\mu = 0.0015$ (Poradnik obsługi... 1994).

The differences in the referenced values of μ and the values noted in this study could be attributed to the industrial practice of stating friction coefficients for broken-in bearings for different bearing load values and standard lubrication (elastohydrodynamic lubrication). For this reason, the values of μ indicated by manufacturer are only reference values. Frictional resistance is determined mainly by contact pressures between the balls and the raceway

and micro-spins in contact zones resulting from elastic strain of the raceway and the balls. Therefore, the value of the friction coefficient will be determined by the bearing's rotational speed and load (KRZEMIŃSKI-FREDA 1989).

The obtained results indicate that every selected signal parameter carries diagnostic information for evaluating the technical condition of rolling bearings. The results of previous experiments suggest that the coefficient of friction under oscillating motion is a generalized parameter of a rolling bearing's diagnostic signal. The values of the coefficient of friction may be compared with the referenced values for brand-new bearings or with historical values.

The moment of friction, the coefficient of rolling resistance or friction power during bearing operation are identified as reliable indicators of the degree of wear of a bearing assembly.

Conclusions

The results of this experiment lead to the following conclusions:

- The quasi-dynamic method supports a relatively simple evaluation of the technical condition of rolling bearings at different stages of their life cycle.
- The coefficient of friction under oscillating motion is a generalized parameter of a rolling bearing's diagnostic signal. The values of the coefficient of friction may be compared with the values referenced for brand-new bearings by the supplier.
- The use of the coefficient of rolling friction, the moment of friction and friction power is justified when boundary values that unanimously describe the bearing's technical condition are determined.
- In further studies aiming to improve the techniques for identifying the condition of rolling bearings with the use of the quasi-dynamic method, the presented diagnostic signal parameters should be analyzed as a function of the degree of bearing wear.

Translated by ALEKSANDRA POPRAWKA

Accepted for print 21.02.2011

References

- BIELAWSKI P. 2003. *Diagnostowanie maszyn z wykorzystaniem mocy tarcia*. Diagnostyka, 29: 15–20.
- CAPANIDIS D., CZARNY A. 2003. *Stanowisko dydaktyczne do wyznaczania oporów ruchu łożysk stożkowych*. Zeszyty naukowe, 8: 135–140.
- CONYERS J. 2004. *Lekcja z uszkodzenia łożyska*. Utrzymanie Ruchu, Marzec.
- DWOJAK J. RZEPIELA M. 2003. *Diagnostyka i obsługa techniczna łożysk tocznych*. Biuro Gamma, Warszawa.

-
- KOWAL A. 2003. *Opory ruchu w mechanizmach maszyn górniczych*. Monografia. Wydawnictwo Politechniki Śląskiej. Gliwice.
- Łożyska toczne*. 2005. Katalog produktów CX-LO/PL/2.01/07.2005. Delta Marketing Sp.z o.o.
- KRZEMIŃSKI-FREDA H. 1989. *Łożyska toczne*. Państwowe Wydawnictwo Naukowe, Warszawa.
- ROGER L. 2004. *Naprawa łożyska tocznego jako alternatywa jego wymiany*. Utrzymanie Ruchu, Maj.
- RYCHLIK A. 2008. *Diagnostyka łożysk tocznych metodą quasi-dynamiczną*. Diagnostyka, 4(48): 113–118.
- Poradnik obsługi technicznej łożysk*. 1994. SKF, Warszawa.
- STYP-REKOWSKI M. 2001. *Diagnozowanie specjalnych łożysk tocznych*. Diagnostyka, 25: 65–71.

Reviewers

Jarosław Bosa, Grzegorz Dzieniszewski, Jarosław Frączek,
Marek Grochowski, Elżbieta Kusińska, Zygmunt Owsiak,
Wojciech Pachelski, Mykhaylo Pashechko, Michał Styp-Rekowski,
Ewa Wachowicz, Bogdan Wolski